Review



# β/γ-Crystallins, Redox Chemistry, and Melatonin: The Regulation of Phase Separation in Cataractogenesis

Doris Loh * and Russel J. Reiter *

Posted Date: 6 October 2025

doi: 10.20944/preprints202510.0392.v1

Keywords: Melatonin indole ring; crystallins; phase separation; critical solution temperature; disulfide bond; glutathione; Greek key motif; van der Waals forces; hydrophobic effect; adenosine triphosphate

 doi:10.20944/preprints202510.0392.v1



*Review*

# β/γ-Crystallins, Redox Chemistry, and Melatonin: The Regulation of Phase Separation in Cataractogenesis

**Doris Loh [1,*] and Russel J. Reiter [2,*]**

[1] Independent Researcher, Marble Falls, TX 78654-4065, USA

[2] Department of Cellular and Structural Biology, UT Health San Antonio, San Antonio, TX 78229, USA

* Correspondence: lohdoris23@gmail.com (D.L.); reiter@uthscsa.edu (R.J.R.)

**Abstract**

A high concentration of soluble crystallins in the eye lenses ensures transparency and maintains vision acuity. Evolution selected special amino acids that promote high refractive power in crystallins. Due to the aromaticity and the hydrophobic, redox-sensitive natures of these residues, they are mostly buried in the core of crystallins. This not only maintains the stability and folding of crystallins, but also protects the residues from hydrophobic interactions that cause protein unfolding, phase separation, and aggregation. Stress responses including the formation of disulfide bonds, S-glutathionylation, deamidation, and domain swapping can cause structural frustration and conformational changes that expose these buried residues. The indole ring of melatonin is attached to two unique side groups that support the scavenging of multiple reactive oxygen species via the formation of potent metabolites in the free radical scavenging cascade. The amphiphilic nature of melatonin allows binding to water molecules via hydrogen bonding and hydrophobic residues via van der Waals forces and other noncovalent hydrophobic interactions. When the indole of melatonin stacks with the adenosine moiety of ATP, their combined dipole moments can significantly increase the strength of van der Waals forces, hydrogen bond, and π-cation interactions. This allows melatonin to effectively shield exposed hydrophobic residues from the hydrophobic effect, preventing hydrophobic collapse and molecular crowding that can cause phase separation and aggregation. The ability of melatonin to change its conformation, enabled by its flexible side chain with rotatable bonds, further amplifies its potential in the regulation of phase separation via enhanced protein interactions. Melatonin may be the ideal candidate that maintains crystallin redox balance to prevent irreversible phase separation and aggregation in cataractogenesis.

**Keywords:** melatonin indole ring; crystallins; phase separation; critical solution temperature; disulfide bond; glutathione; Greek key motif; van der Waals forces; hydrophobic effect; adenosine triphosphate

## 1. Introduction

The high concentration of transparent, multifunctional, refractive crystallin proteins in the eye lens not only ensures transparency and flexibility of the lens but also generates a high refractive power that promotes vision acuity [1,2]. Cataractogenesis in humans is inevitable during the natural aging process. The formation of cataracts results in the loss of optical acuity, contrast sensitivity, and uncorrected refractive error, all of which can contribute to blindness and vision impairment in adults aged 50 years and older [3,4]. A systematic review and meta-analysis of 137 global and regional population studies published between 2000 to 2020 on blindness (presenting visual acuity <3/60) and severe vision impairment (presenting visual acuity < 6/18, ≥ 3/60) reported that in 2020, 17.1 and 83.48 million people ≥ 50 years (95% UI) were blind or exhibited severe vision impairment due to cataracts, respectively [5]. It is estimated that the burdens of cataracts associated with health and economic

 doi:10.20944/preprints202510.0392.v1



consequences will continue to rise as a result of the increasing global aging population [6]. The aberrant aggregation of lens crystallin proteins is believed to be the major cause of cataracts [1,7,8].

During the lifetime of lens maturation and aging, the lens epithelial cells elongate and differentiate into new fiber cells devoid of nuclei and mitochondria that overlay existing ones, where oldest fibers are located at the center of the lens [9]. As a result of the lack of turnover of lens fiber cells, long-lived $\alpha$, $\beta$ and $\gamma$-crystallins must be able to maintain soluble, functional conformations throughout the lifetime of the organism [1,10]. In order to focus light onto the retina to transmit a sharp, clear image, the lens must maintain transparency and a high refractive power. The refractive index gradient, which increases from the periphery to the nucleus of the lens, allows precise control of image acuity [11]. The nucleus of vertebrate lenses consists mainly of extremely soluble $\gamma$-crystallins. The high refractive index increment of $\gamma$-crystallins is the result of a unique combination of aromatic and sulfur-containing amino acids that exhibit high polarizability and refractive index increment, including tryptophan (Trp), phenylalanine (Phe), tyrosine (Tyr), histidine (His), cysteine (Cys), arginine (Arg), and methionine (Met). Whereas, many species of fish with increased requirement for refractive power due to their optically ineffective cornea under water have totally eliminated amino acids with low refractivity such as alanine, lysine, and/or threonine from their lens $\gamma$-crystallins [12]. Accordingly, the non-uniform distribution of $\gamma$-crystallins, responsible for the maintenance of this refractive index gradient, differs from species to species. In the mammalian lens, the difference in concentration gradient is approximately 100-250 mg/mL between the cortex (200-350 mg/mL) and the nucleus (400-450 mg/mL) [13,14]. Whereas, the $\gamma$-crystallin concentration in fish often exceeds 850 mg/mL, with peak values at ~1,120 mg/mL to support the acute refractive power requirements in aquatic environments [15–17]. Aging, exogenous and endogenous stress can cause the irreversible aggregation of $\beta/\gamma$-crystallins. Changes in protein conformation causes deviations in the structural order and precise packing of lens crystallins that alter the refractive index gradient, scattering light, causing opacity, and the eventual formation of cataracts [1,18].

This review will examine relevant molecular interactions and biochemical modulations that result in irreversible phase separation and aggregation of $\beta/\gamma$-crystallins. Importantly, the antioxidant-dependent and -independent mechanisms employed by melatonin in the regulation of $\beta/\gamma$-crystallin redox chemistry, phase separation, as well as the attenuation of irreversible aggregates responsible for the formation of cataracts will be thoroughly investigated (Figure 1).

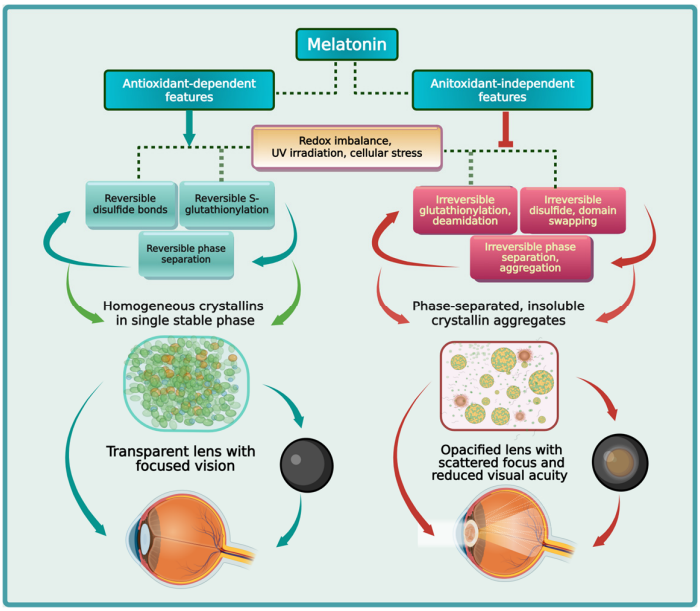


**Figure 1.** Schematic illustration of the antioxidant-dependent and antioxidant-independent features of melatonin in the maintenance of lens transparency by preventing irreversible crystallin phase separation and aggregation.

 doi:10.20944/preprints202510.0392.v1



## 2. Cold Cataracts: The Epitome of β/γ-Crystallin Phase Separation

Phase separation is understood to be an evolutionarily conserved, thermodynamic process that is fundamental for maintaining biological processes in all living organisms [19,20]. In biological systems, phase separation describes a physical phenomenon where a homogeneous mixture separates into two or more distinct, inhomogeneous phases [21]. The spontaneous self-assembly of these micron-scale, membraneless biomolecular condensates (BCs) enable the reversible compartmentalization of specific proteins and nucleic acids. In essence, phase separation creates versatile microenvironments that facilitate energy-efficient biochemical reactions and the organization of cellular information to ensure cellular function and survival under physiological and stressful conditions [22–24]. The multivalent molecular interactions that drive phase separation include hydrogen bonding, electrostatic interactions, and hydrophobic interactions [25]; while π-π stacking and other weak, non-covalent interactions can contribute to binding affinity and enhance the overall multivalency to promote phase separation [26,27]. Importantly, the intrinsically disordered regions (IDRs) and low complexity domains (LCDs) of proteins are easily affected by changes in temperature, ion concentration, and pH. Subsequent alterations in the solubility, interactions, and overall behavior of IDPs and LCDs as a result of these changes can dynamically affect their ability to activate or modulate BC formation and dissolution [28–31].

Cold cataracts—experimentally defined by Zigman and Lerman in 1965—is a reversible, stress response mechanism that employs phase separation of crystallin proteins to protect the lens during cold exposure [32,33]. When exposed to cold temperatures, eye lenses of mammals, including pigs (4 °C) [34], cows (11.7 °C) [35], rats (25 °C–4 °C) [36], and hibernating ground squirrels (4 °C) [37], turn opaque but become transparent again upon rewarming. It is possible that controlled phase-separation of crystallin proteins effectively prevents the irreversible aggregation or misfolding of proteins that could occur in extreme cold. Conceivably, the formation of cold cataracts safeguards the optical properties of the lens until the ambient temperature rises again [34]. In contrast, lenses of cold-blooded fish can withstand temperatures 10 to 40 °C lower than those for mammals [38]; while lenses of unique cold-adapted species such as the *Dissostichus mawsoni* Antarctic toothfish can retain transparency between -1.9 °C to -12 °C [39].

During the formation of reversible cold cataracts, the high concentration of γ-crystallins in the nucleus and cortex of mammalian lens phase separate into distinct, dense protein-rich and dilute protein-poor phases. This reduces the refractive power of the lens, resulting in light-scattering and opacity that are commonly observed in nuclear cataracts that develop during aging of the lens [34]. Since phase separation, and not protein unfolding, is largely responsible for the opacity in lenses exposed to cold temperatures, the study of cold cataracts becomes relevant for understanding how aberrant phase separation of crystallins can promote the formation of irreversible cataracts. Unlike cold-blooded, ectothermic animals, warm-blooded mammals maintain stable core body temperatures via thermoregulation [40]. Consequently, even when the external temperature is significantly reduced, in vivo mammalian lenses under homeostatic conditions can be maintained at temperatures where crystallins remain miscible and transparent. Conversely, cold cataracts in lenses of hibernators develop when their core body temperatures drop dramatically, often to below 0 °C [41]. Nevertheless, stress from endogenous and exogenous sources, biochemical modulation, and post-translational modifications (PTMs) can modify the redox chemistry of β/γ-crystallin proteins. This changes the critical solution temperatures of proteins and leads to aberrant phase separation that matures into irreversible cataract-forming aggregates.

### *2.1. Phase Separation of β/γ-Crystallins is Dependent Upon Critical Solution Temperatures*

Reversible cold cataracts are formed when the lens temperature falls below that at which β/γ-crystallins in the lens precipitates from a single miscible phase into distinct, dense and dilute phases. Since the lens nucleus contains a relatively higher proportion of γ-crystallin, when phase separation of this crystallin is triggered, lens opacity and cloudiness quickly develops [42]. Similar to many

 doi:10.20944/preprints202510.0392.v1



proteins, γ-crystallins undergo reversible phase separation when temperatures fall below system-specific upper critical solution temperature (UCST) [43,44]. Conversely, various RNAs and polymers with lower critical solution temperature (LCST) will transition from one-phase regimes into two-phase regimes when the temperature is increased above the LCST [45,46] (Figure 2).

The lens of pigs (4 °C) [34], cows (11.7 °C) [35], rats (25 °C–4 °C) [36], and hibernating ground squirrels (4 °C) [37] exhibit classic UCST behavior, where nucleus and cortical γ-crystallins reversibly phase separate into protein-rich and protein-poor phases upon exposure to temperatures below their respective UCSTs (identified in brackets). Upon rewarming, the lenses become transparent again when the two-phase regimes revert back into a single phase as the temperature of the lenses rise above the UCSTs. The lenses of Antarctic toothfish *D. mawsoni* contain a high level of γS-crystallins with very low UCSTs that can prevent phase separation as low as −12 °C. This confers extreme cold tolerance and high refractive index gradient to the cold-adapted fish [47].

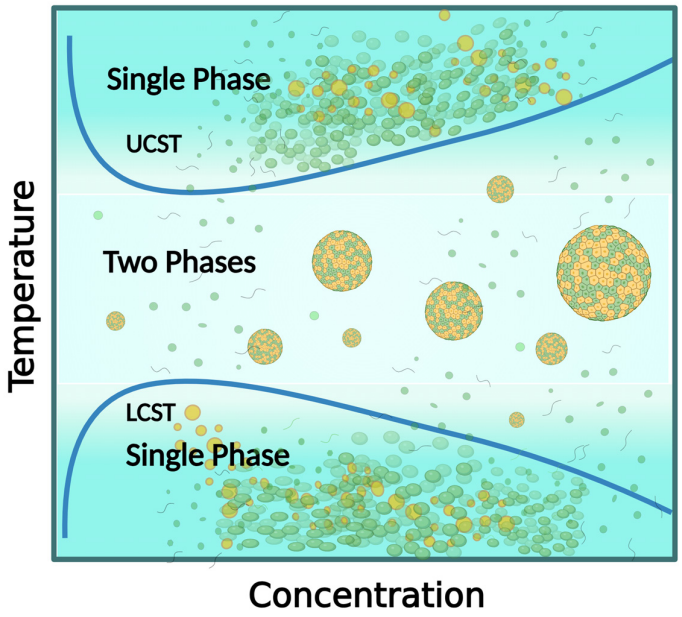


**Figure 2.** Illustration of reversible phase separation when critical solution temperature is breached. Upper Critical Solution Temperature (UCST): Proteins with UCST behavior will phase separate when temperature falls below their UCST. Conversely, proteins with LCST behavior will phase separate when temperature rises above their LCST. When temperature is reverted back to the single-phase level, droplets formed via phase separation will disassemble.

### *2.2. The Irreversible Aggregation of Crystallins by Sodium Selenite*

Sodium selenite (Na2SeO3) is an inorganic salt comprising sodium and selenite ions in a 2:1 ratio. In excess, sodium selenite supplementation can induce oxidative stress that causes acute toxicity [48,49]. In rodent studies, sodium selenite can change the UCST of lens proteins, causing rapid lens opacification. Since its first reported use in 1978, this chemical compound is preferred in the study of cold cataracts as it can provide reproducible results in the investigation of biochemical and molecular processes that may be responsible for cataractogenesis [50–52]. An acute overdose of sodium selenite (3.8 mg/kg body weight) injected into 14 day old suckling rats can cause irreversible, dense nuclear cataracts after 6 days [53]. Intriguingly, on the second day post-treatment, lenses of 10 day-old rat pups treated with 1.5 mg/kg body weight sodium selenite remained clear above 26.5 °C but developed irreversible nuclear cataracts in 3-4 days. Conversely, lenses from control non-treated pups increased opacity when temperature dropped below 32 °C [54]. At the time, it was unclear how sodium selenite could lower the phase separation temperature ($T_{ph}$) initially, but then cause a

 doi:10.20944/preprints202510.0392.v1



dramatic increase of $T_{ph}$ to above physiological temperature to induce dense opacification of the lens, causing irreversible nuclear cataracts [55]

Under normal conditions, the $T_{ph}$ of animal lenses vary according to the age of the cell. $T_{ph}$ may actually decrease to values below body temperature as the animal ages, possibly due to relocalization and differential expression and accumulation of γ-crystallins [56–58]. It is worth noting that the γS-crystallin (γS), a highly conserved protein in animal and human eyes [59], has been observed to exhibit an extremely low UCST that allows it to withstand phase separation at temperatures as low as −28 °C under experimental conditions [60]. In calf lenses, increasing the amount of γS can suppress phase separation of γ-crystallins in solution by lowering the mixture's phase separation temperature [61]. Notwithstanding, experimental results demonstrate that exposure to intense ionizing irradiation or oxidative stress can elevate the $T_{ph}$ of γ-crystallins in the rabbit and bovine eye lenses, respectively, to cause opacification and the generation of irreversible cataracts [62,63]

Compared to normal controls, much higher levels of reactive oxygen species (ROS) levels and lipid peroxidation products were detected in Wistar rats treated with sodium selenite [64,65]. Sodium selenite, in excess, creates oxidative stress resulting in biochemical and biomolecular changes that alters $T_{ph}$ of lens crystallins to cause phase separation. The subsequent reduction of adenosine triphosphate (ATP) and glutathione (GSH) [54,55,66,67], the increased formation of irreversible disulfide bonds [68] from glutathionylation [69] and deamidation [70] results in the exposure of hydrophobic residues leading to dehydration and hydrophobic collapse of protein shells [2,71–73]. In the crowded molecular environment of the lens [74,75] these forces all converge to promote the elevation of $T_{ph}$ and the subsequent pathological, irreversible aggregation of crystallin proteins. Consequently, increasing temperatures to as high as 50 °C was totally ineffective in reversing crystallin aggregation formed after day 5 as a result of $T_{ph}$ elevation from sodium selenite treatment [53] (Figure 3).

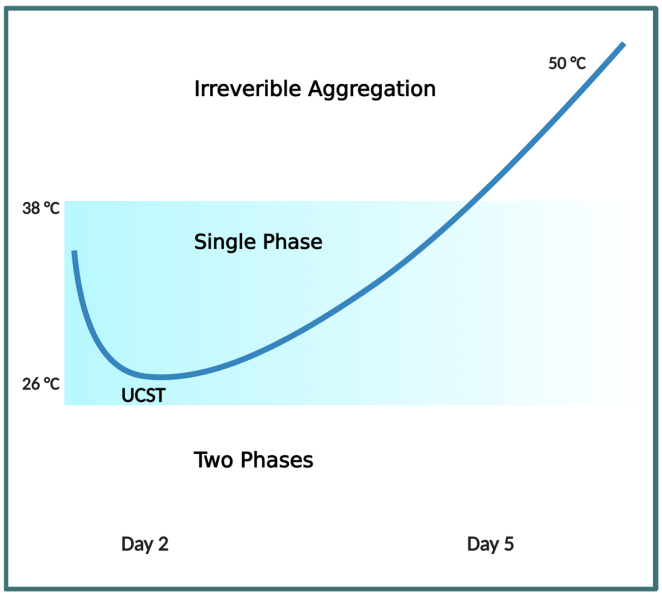


**Figure 3.** Sodium selenite treatment induces changes in UCST to cause rapid onset of nuclear cataracts by Day 5. Irreversible protein aggregation is observed when the UCST was elevated to >40 °C by sodium selenite. This represents a deviation from the standard single to two phase regimes in phase separation studies. Clark and Steele (1992) described this phenomenon as a transition from reversible LLPS (UCST) to irreversible aggregation, with abnormal turbidity observed at physiological 37 °C.

While many small molecules—including phase separation inhibitors—have emerged in the relentless search for viable candidates to attenuate cataractogenesis [53,65,67,76–83], perhaps none has been more enduring than melatonin. Since 1994, melatonin has been intensively and extensively

 doi:10.20944/preprints202510.0392.v1



tested in experiments investigating the formation of cataracts under a wide variety of conditions that involve oxidative stress, cold stress, heat stress, metabolic stress, mitochondrial dysfunction, as well as exposure to cytotoxic UVB and ionizing gamma radiation [84–90]. Please refer to Table 1 for details of study designs and results (studies arranged in chronological order). Conclusions from these reports invariably showed that melatonin can prevent and attenuate the formation of cataracts due to its widely acclaimed function as a scavenger of ROS and free radicals.

**Table 1.** In vivo and in vitro studies testing the effectiveness of melatonin against stressors that can cause irreversible phase separation of crystallins to promote cataractogenesis.

| Melatonin Dosage / Duration | Study Design | Results | Ref. |
|---|---|---|---|
| 4 mg/kg BW melatonin via IP injection daily x 15 days, starting on postnatal day 2. | Rat pups were treated with IP injections of buthionine sulfoximine (BSO) (3 mmol/kg BW) daily x 3 starting postnatal day 2 to induce cataract formation. | Melatonin treatment reduced cataract formation by 93.3% (1/15) and more than doubled the level of GSH* (wet weight) in the lens of rat pups on postnatal day 9. | [84] |
| 4 mg/kg BW melatonin via IP injection daily x 7 or 15 days, starting on postnatal day 2. | Rat pups were treated with IP injections of buthionine sulfoximine (BSO) (3 mmol/kg BW) daily x 3 starting postnatal day 2 to induce cataract formation. | Melatonin treatment prevented accumulation of lipid peroxidation (MDA, 4-HDA) in lens and major organs, resulting in a 72% reduction in cataract formation compared to controls. | [85] |
| 5 mg/kg BW melatonin via IP injection daily x 10 days, with first dose 30 mins before irradiation on day 1. | Adult female SD rat cranium, exposed to a single 5 Gy ionizing gamma radiation to damage eye lens, causing cataract formation. | Melatonin treatment produced a significant 3-fold reduction in cataract development (9/10 versus 3/10); MDA in MEL + IR group was similar to control, whereas SOD and GSH-Px* mean levels were actually higher than control group levels. | [86] |
| 10 mg/kg melatonin via IP* injection daily x 7, starting on postpartum day 8, 2 days before sodium selenite injection, until day 15. | SD* rat pups administered with subcutaneous sodium selenite injections (30 nmol/g BW*) on postnatal day 10 to induce formation of senile nuclear cataract. | Melatonin exerted anticataract activity by preventing (2/7) and lowering (5/7) nuclear opacity in pup lenses, protecting lens and serum antioxidants (GSH*, SOD*, CAT*), and reducing markers of protein oxidation (PC*) and lipid peroxidation (MDA*) compared to controls. | [87] |
| Single STZ* (50 mg/kg BW*) IP injection in healthy, adult SD male rats to induce diabetes. | 5 mg/kg BW melatonin daily x 8 wks via gavage, 1 wk after STZ* administration. | Melatonin treatment produced statistically-significant prevention in the onset of nuclear cataracts compared to diabetic controls, while lowering mortality rate by ~30% (47% versus 33%) and reducing glucose and HbA1c levels significantly. | [88] |
| 200 mM melatonin (5 µl/eye, total 232 µg) injected subconjunctivally 5 min before UVB irradiation, every other day for 9 weeks. | In vivo UVB-induced ARC* using 6-wk-old male SD* rats exposed to 312 nm UVB at 5 W/m2 output for 30 min every other day for 9 weeks. | Melatonin treatment significantly inhibited ferroptosis and lipid peroxidation, reducing lens turbidity compared to development of C3N0P1 grade cataracts (LOCS III*) in 85% of UVB exposed rats (51/60) in a SIRT6-dependent manner. | [89] |
| 250 µM** melatonin applied to tested cell lines before UVB irradiation | In vitro human lens epithelial cells B-3, SRA01/04, and human embryonic kidney HEK-293 T cells exposed to 312 nm UVB at 5 W/m$^2$ output, achieving 500 J/m$^2$ | Melatonin application suppressed lipid peroxidation and ferroptosis by marked elevation of antioxidant gene expression, preventing shriveling of mitochondria and restoring normal features. | [89] |
| 200–1200 µM melatonin | Purified, recombinant human αB-crystallin protein at 15 µM concentration exposed to 66°C temperature to induce precipitation/aggregation with and without preincubation at 4°C. | Melatonin binds to αB-crystallin, reducing aggregation from 66°C exposure dose-dependently; 800 µM melatonin achieved best aggregation suppression when proteins | [90] |

 doi:10.20944/preprints202510.0392.v1



| | |
|---|---|
| | were preincubated for 24 h at 4℃ to induce phase separation. |

*Abbreviations: ARC, age-related cataracts; SD, Sprague–Dawley; LOCS III, Lens Opacities Classification System III; IP, intraperitoneal; BW, body weight; GSH, glutathione; SOD, superoxide dismutase; CAT, catalase; MDA, malondialdehyde; PC, protein carbonyl; 4-HDA, 4-hydroxyalkenals; STZ, streptozotocin; GSH-Px, glutathione peroxidase. ** Unpublished dose. Note: Adapted from the preprint version "Melatonin, ATP, and Cataracts: The Two Faces of Crystallin Phase Separation" by Loh D, Reiter RJ. Qeios. doi:10.32388/D09YND. CC BY 4.0.

## 3. The Significance of Melatonin and its Indole Ring in Crystallin Redox Chemistry

Ubiquitously synthesized by all tested living organisms in the three major domains of life—Archaea, Eukarya, and Bacteria [91,92]—the highly evolutionary conserved, pleiotropic melatonin (N-acetyl-5-methoxytryptamine) molecule [93] contains a heterocyclic aromatic indole ring ($C_8H_7N$) comprising a six-membered benzene ring fused with a five-membered nitrogenous pyrrole ring (Figure 4). The structure of the benzene six-carbon, hexagonal ring confers stability to the entire indole structure [94]. There are a total of 10 π-electrons in indoles. 8 of these electrons are from the double bonds within the fused benzene and pyrrole rings, and 2 additional electrons are from the lone pair on the nitrogen atom. These delocalized π-electrons in the indole molecular orbital system enhance the chemical reactivity of indoles and facilitate electrophilic substitution reactions, making indoles excellent electron donors [95–97]. Melatonin is regarded as an effective electron donor and scavenger of an extensive range of both oxygen- and nitrogen-based reactants [98–100] partly due to the reactivity of its indole. However, the attachment of the methoxy group ($-OCH_3$) to the 5th carbon and the N-acetyl-2-aminoethyl group to the 3rd carbon of the indole ring in melatonin [101] sets it completely apart from other antioxidants and indoles (Figure 4).

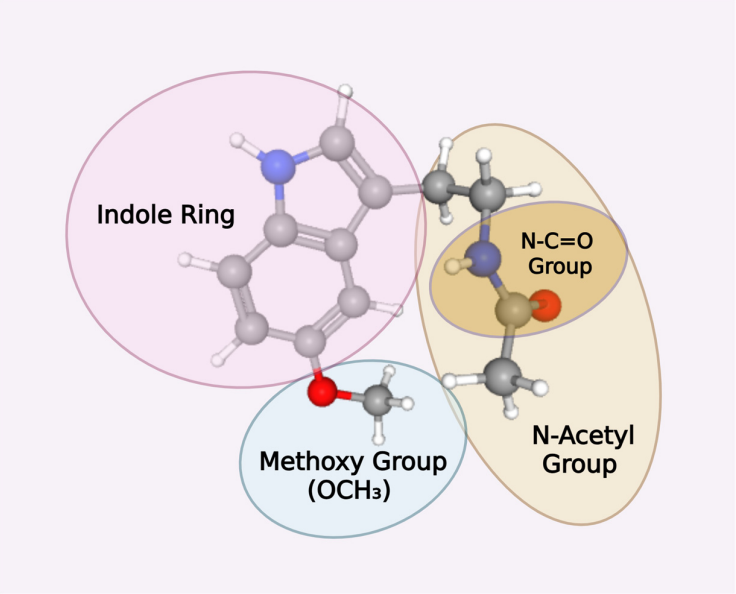


**Figure 4.** Melatonin Indole Ring and Side Groups—The indole ring in melatonin [102]] serves as the core scaffold, with its pyrrole moiety (particularly the C3 position) being highly susceptible to electrophilic attack by radicals due to its high electron density and resonance stability. This initiates the cascade through radical addition or hydroxylation at C3, forming intermediates like the melatonyl cation radical or cyclic 3-hydroxymelatonin (c3OHM), which then continue scavenging additional radicals such as hydroxyl ($OH^{\bullet}$) or peroxyl speciesMelatonin amide group—The N-C=O functional group, part of the N-acetyl group, is located on the N-acetyl-2-aminoethyl side chain attached to the 3rd carbon of the indole ring in melatonin. Specifically, it is within the acetyl portion ($CH_3$-C=O) bonded to the nitrogen of the aminoethyl group (-NH-$CH_2$-$CH_2$-). The N-acetyl

 doi:10.20944/preprints202510.0392.v1



side chain, with its N-C=O amide functionality, contributes by facilitating the formation of stable cyclic structures (e.g., in cyclic 3-OHM) and enabling further metabolic transformations. The 5-methoxy group (-$OCH_3$) acts as an electron-donating substituent that enhances the indole ring's reactivity, lowering the activation energy for free radical interactions and stabilizing radical intermediates. This group is retained in key metabolites like N1-acetyl-N2-formyl-5-methoxykynuramine (AFMK) and N1-acetyl-5-methoxykynuramine (AMK), which form via pyrrole ring cleavage and continue the scavenging process by donating electrons to species like nitric oxide ($NO^{\bullet}$) or peroxynitrite ($ONOO^-$). Colors for atoms: Gray: Carbon © White: Hydrogen (H) Red: Oxygen (O) Blue: Nitrogen (N).

### *3.1. The Free Radical Scavenging Cascade Sets Melatonin Apart from Other Antioxidants*

Unlike classic antioxidants—including GSH, ascorbic acid, and vitamin E—that are continuously regenerated/recycled, melatonin is a terminal antioxidant that is not regenerated/recycled. Instead, melatonin's unique free radical scavenging cascade reaction supports the scavenging of multiple ROS via the successive formation of metabolites that retain potent or even superior antioxidant properties, promoting a chain-like detoxification process [103]. The indole ring is regarded as a privileged scaffold, where its core serves as a versatile, foundational structure that allows for diverse chemical modifications that enhances its intrinsic functions [104,105]. The melatonin scavenging cascade induces structural changes to its indole ring, and even minor substitutions can have a large influence on the resulting interactions. Metabolites of melatonin can acquire distinct properties and functions after interacting with ROS and free radicals in animals and plants [106–110].

During the formation of the melatonin metabolites N1-acetyl-N2-formyl-5-methoxykynuramine (AFMK) and N1-acetyl-5-methoxykynuramine (AMK), melatonin can scavenge up to 10 ROS and reactive nitrogen species (RNS) molecules [111,112]. The N-acetyl group containing the N-C=O functionality is retained in AFMK as the N1-acetyl group. While the 5-methoxy group is also retained, a new N-formyl group at the N2 position is formed as the result of the transformation of the pyrrole ring during oxidative cleavage. Alterations in the structure and biochemical reactivity of the melatonin indole scaffold in the kynurenic AMK and AMFK may account for their enhanced antioxidant activities [113–116]. Even though 6-hydroxymelatonin (6-OHM) is the major melatonin metabolite in rats and mice ([117,118], due to the high specific requirement for ocular antioxidant protection [119], intraperitoneal administration of melatonin at 40 mg/kg body weight significantly elevated the formation of AFMK in the rat retina as a result of oxidation by hydrogen peroxide [120]. Statistically significant experiments showed that human lens epithelial cells (HLECs) exposed to 100 μM hydrogen peroxide but pretreated with melatonin, dose-dependently decreased the oxidative stress-induced apoptosis ratio in HLECs [121].

The attachment of the methoxy group and the N-acetyl-2-aminoethyl group not only enhances the antioxidant and radical scavenging effects of the electron-donating delocalized π-cloud, but also may promote melatonin's ability to regulate crystallin phase separation. Enhanced π-π interactions and hydrogen bonding with other aromatic systems—including the adenosine moiety in ATP and aromatic residues in crystallins—can increase protein solubility and reduce hydrophobic aggregation from aberrant phase separation. The ability to regulate BC dynamics may explain why melatonin readily elevates transcription and expression of antioxidant enzymes associated with glutathione in animals and plants [115,122–135]. The ability of melatonin to elevate the expression of glucose-6-phosphate dehydrogenase (G6PD) and increase the $NADPH/NADP^+$ ratio is paramount for maintaining GSH in the reduced state [134–136]. GSH concentration in the lens is reduced in the nucleus, with no evidence, to date, of its ability to cross membranes [137]. Melatonin is believed to be synthesized mainly in the mitochondria of possibly all cells and organs in living organisms [138]. Ocular production of melatonin has been identified in the lens [139–141], the retina [142], and the retinal pigment epithelium [143]. Even though the lens nucleus is devoid of mitochondria, melatonin is able to reach the nucleus efficiently to protect crystallins. Melatonin exhibits high membrane permeability, enabling it to readily cross cell membranes in all subcellular locations. Melatonin is

 doi:10.20944/preprints202510.0392.v1



estimated to equilibrate across the plasma membrane in approximately 3.5 seconds, with a membrane permeability of around 1.7 μm/s [144,145]. This may be one of the reasons why melatonin treatment exerted impressive anticataract effects, especially in the nucleus, in experiments employing chemicals that alters redox chemistry in crystallins by depleting GSH (Table 1).

### *3.2. The Relevance of Maintaining a Balanced Lens Redox Environment in the Prevention of Phase Separation and Aggregation*

The toxic, soluble sodium selenite must be reduced by living organisms into the nontoxic, insoluble elemental selenium that is an essential micronutrient required in vital biological functions [146,147]. In eukaryotes, selenite is generally reduced to elemental selenium via enzymatic pathways that involve GSH, thioredoxins, and various NADPH-dependent reductases, often linked to oxidative stress and energy production [148]. Unreduced sodium selenite or even supranutritional levels of selenium > 1 μM are pro-oxidants that elevate ROS. At low physiological levels, ROS are important pleiotropic molecules that regulate important redox signaling events in cells [149]. Whereas, at high concentrations, ROS can exert detrimental effects that cause an extensive variety of pathologies [150]. The catalysis of selenite produces metabolites that elevate oxidative stress [151–153]. Excess ROS from sodium selenite results in mitochondrial dysfunction, endoplasmic reticulum stress,DNA damage, and the suppression of Nrf2/Keap1 dependent antioxidant protection that exacerbate the production of ROS [154–156]. Therefore, the dramatic depletion of GSH by ≥ 60% within the first 24 h in the lens cortex of rat pups treated with sodium selenite is not unexpected [67,157].

Nonetheless, the subsequent rapid onset of both cortical and nuclear opacity requires elucidation of the multifaceted effects of Cys redox chemistry in crystallins. Afterall, the 60% decrease in ATP level in cold cataract lenses is a direct result of sodium selenite inhibition of ATP synthesis by modulating the redox chemistry of thiols in the $F_1F_0$-ATPase [67,158]. The redox chemistry of thiols in crystallin Cys residues [159] is directly affected by the concentration of surrounding GSH. The formation of disulfide bonds and glutathionylation can contribute to changes in phase separation behavior of crystallins. Therefore, the ability of melatonin to scavenge ROS and elevate GSH production are the most obvious reasons for its success in reversing cataractogenesis under different experimental contexts (Table 1). Accordingly, the depletion of GSH in the lens merely reflects the observable tip of the redox iceberg in lens crystallins. Ultimately, redox chemistry affects phase separation and aggregation of β/γ crystallins that can result in light scattering, lens opacity, and the formation of reversible/irreversible cataracts.

## 4. The Redox Chemistry of Glutathione, β/γ Crystallins, and Disulfide Bonds: Location and Composition Determines the Outcome of Phase Separation and Aggregation in the Lens

In humans, GSH is a potent, effective antioxidant due to its high cellular concentration (between 0.1 to 10 mM) and low standard redox potential (-240 mV) [160–162]. Importantly, GSH homeostasis is rigorously maintained by the effective recycling of reduced and oxidized GSH (GSSG). The interconversion of the GSH and GSSG redox pair is facilitated by the addition or loss of electrons. The active site of this redox reaction is located in the sulfhydryl (or thiol) group comprising a sulfur atom bonded to a hydrogen atom (-SH). -SH donates electrons in redox reactions to neutralize free radicals and ROS. The oxidation of -SH forms disulfide bonds, creating oxidized glutathione (GSSG) [163]. GSSG can be recycled back into its reduced form, GSH, by the enzyme glutathione reductase (GR), using nicotinamide adenine dinucleotide phosphate (NADPH) as an electron donor. The successful continuation of this recycling process protects cells from oxidative stress via redox buffering that regulates cell signaling processes [161,164–166]. In an oxidative environment, a higher concentration of GSSG can oxidize reactive thiols in Cys residues to form mixed disulfide bonds in mitochondria complex I, elevating superoxide production [167]. This results in the inactivation of

 doi:10.20944/preprints202510.0392.v1



complex I that leads to significantly depressed ATP production [168,169]. In mitochondria, selenite forms protein adducts that oxidize free thiol groups in GSH or Cys residues to form seleno-disulfide bonds. This results in increased ATP hydrolysis and inhibition of ATP synthesis [158]. The oxidation of free thiol groups by selenite to form disulfide bonds and intermediate seleno-sulfur compounds is one of the main molecular mechanisms affecting crystallin redox chemistry responsible for the rapid onset of nuclear cataracts [170–172].

### *4.1. Disulfide Bonds are Tunable Levers of Phase Separation*

Oxidative stress in the lens due to ineffective antioxidant response is believed to be a major cause for cataractogenesis [173,174]. Lens β/γ crystallins contain Cys residues that can be directly oxidized by sodium selenite and other endogenous oxidants [158,175,176]. This oxidative reaction creates covalent bonds between the thiol (−SH) groups of two Cys residues within the same (intramolecular) or different (intermolecular) protein polypeptides [177]. The removal of hydrogen atoms and electrons from −SH results in a new sulfur-sulfur covalent bond, known as the disulfide bond (−S–S−) that is traditionally associated with increased protein stability by 'locking' the protein in its folded state to suppress unfolding. The location and number of Cys residues in a protein can affect the phase transition temperature and the viscoelastic properties of the condensates. Under oxidizing conditions, disulfide bonds can act as tunable levers in regulating protein phase separation, with the ability to drive the formation of liquid condensates and to be reversibly switched on and off by redox chemistry. Variations in the protein's Cys composition is directly associated with changes in the viscoelastic behavior of phase-separated condensates [178].The formation of intermolecular disulfide bonds is critical for activating the phase separation of RIG-1. This process leads to the compartmentalization of the signalsome, which is requisite for immune signaling [179].

Recent advances, however, reveal that the location of disulfide bonds in the protein structure determines whether mechanical stability is increased or decreased [180]. The location of disulfide bonds in crystallins, the geographic distribution of crystallins with different composition and conformation of sulfur and aromatic residues [181], and the differential location of GSH in the lens may explain why sodium selenite-induced nuclear cataracts within 3–5 days were irreversible; whereas cortical cataracts that developed 15–30 days post-injection were reversed within a few months [182]. More importantly, the adequate presence of melatonin in all these locations may determine whether pathological progression towards cataractogenesis can be attenuated.

### *4.2. Location and Aging Determine the Differential Glutathione Concentration in the Lens*

The abundance of GSH in the young human lens creates a highly reducing environment that naturally resists the formation of cataracts. Cataract formation and aging can lower GSH concentration in the lens by > 50% [183,184]. De novo glutathione (GSH) synthesis in the lens, primarily in the epithelial and outer cortical layers [185], is the primary source of high GSH concentration in the anterior and posterior lens cortex. Even though GR in the lens is capable of regenerating GSSG, the lens nucleus is incapable of synthesizing GSH and must obtain its supply from the epithelium and cortex [186]. Both the vitreous humor and aqueous humor of LEGSKO transgenic mice, incapable of de novo GSH synthesis in the lens, have been demonstrated to supply GSH to the lens via passive high-flux transport and active carrier-mediated absorption, respectively [187]. Even though the existence of a concentration gradient that supports the diffusion of GSH into the nucleus via gap junctions mediated by connexins is widely accepted [188], the precise transport mechanisms of GSH in the lens require further elucidation [189].

Maintaining homeostasis of GSH in the lens becomes paramount, especially when the lens nucleus is particularly vulnerable to oxidative stress due to low availability and activity of the GSH redox cycle in this location [190]. In the rat lens, even though the duration of light (12 h day/12 h dark) and dark (24 h dark) cycles modulated the time-of-day expression patterns of clock and redox genes that regulate GSH homeostasis, GSH levels remained constant [191]. However, results obtained from matrix-assisted laser desorption/ionisation (MALDI) FT -ICR imaging mass spectrometry (IMS)

 doi:10.20944/preprints202510.0392.v1



studies that mapped the regional changes in GSH in the human lens showed not only a regional difference, but also a significant age-dependent decline. The difference in GSH between the cortex and nucleus in young 34 year old lenses was 24.3%. Despite a 27% decline in GHS in the cortex, 74 year old lenses showed a dramatic 70.3% difference in GSH between the cortex and nucleus [192].

Sodium selenite cold cataract experiments were usually conducted on young rodent pups. Due to the relatively higher GSH content in the epithelium and cortex, the reversal of opacity in the cortex is not unexpected [182]. Since GSH levels in the young rat lens are comparatively much higher than those in older lenses [193], the rapid onset and irreversible formation of nuclear cataracts in young rat lenses implies other mechanisms are critically involved.

### *4.3. The Differential Location of Crystallins Determines Refractive Index and Susceptibility to Aggregation*

γ-Crystallins are the smallest of the three crystallins—α, β and γ—in the vertebrate lens. They are the main structural proteins responsible for maintaining the high refractive index necessary for vision acuity together with α- and β-crystallins [194]. The oligomeric α-crystallin that makes up ~40% of lens proteins contains two subunits belonging to the small heat shock protein family [195,196]. In addition to maintaining the refractive index with γ-crystallins, α-crystallin behaves like a chaperone that helps prevent pathological aggregation of crystallins [195]. Its function as a chaperone is dependent and enhanced upon temperature-induced structural changes that expose hydrophobic surfaces achieved at temperatures of 30℃ and above [197,198]. Entropically-driven hydrophobic contacts [199] allow α-crystallins to access newly-exposed hydrophobic sites of unfolding protein targets. Thus, hydrophobicity of α-crystallin can be considered as a major determinant of the effectiveness of its chaperone-like activity [200]. α-crystallins are largely absent in the nucleus of older human lenses [201]. The lack of cellular turnover in the lens nucleus [202,203] implies the extremely high concentration of γ-crystallins in the nucleus must be able to maintain solubility, stability, and transparency over the entire lifespan of the organism. For long-lived chordates including humans, achieving kinetic stability that can resist protein unfolding and aggregation in the lens nucleus becomes highly relevant.

#### 4.3.1. The Greek Key Motif Maintains High Refractive Index, Kinetic and Structural Stability in β/γ-crystallins

The β/γ-crystallin superfamily are evolutionarily conserved proteins found in all three major kingdoms of life [204,205]. The proteins in this superfamily share a structural motif where the single polypeptide chain of the β- and γ-crystallin folds into two distinct domains—an N-terminal and a C-terminal domain—with each domain composed of two Greek key motifs. These two domains are linked together to form the complete protein structure [206]. The Greek key motif, named for its resemblance to ancient Greek pottery designs, consists of four beta (β) strands arranged in an antiparallel, interlocking pattern that resembles a geometric Greek key. The first and fourth β-strands are connected by a longer loop to form a closed, compact structure. Greek key motifs promote protein stability in folded domains [206–208] (Figure 5).

The unique composition of amino acids in the Greek key motif of β/γ-crystallins contribute to the high solubility, transparency, and refractive index of vertebrate lenses through dense packing and specialized non-covalent interactions. The inherent stability from the stable globular structures formed as a result of the Greek motif effectively prevents proteins from unfolding under physiological conditions [208,209]. These domains are hydrophobic and rich in aromatic Tyr and Phe residues that contribute to high refractive index increments due to their polarizable aromatic side chains with π-electron systems that can facilitate interact with light, leading to a greater change in refractive index for a given concentration change [12,210].

 doi:10.20944/preprints202510.0392.v1



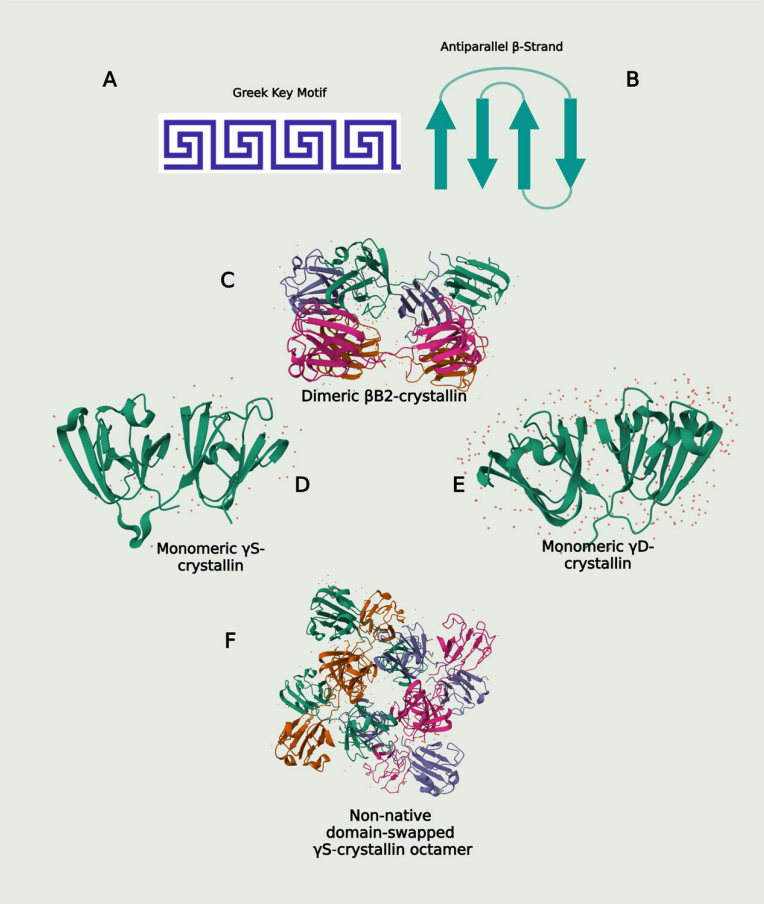


**Figure 5.** Illustrations of the Greek Key Motif and Structures of β/γ-crystallins (A) The Greek key motif is a common supersecondary protein structure composed of four antiparallel β-strands that are folded into a twisted β-sandwich, resembling the decorative patterns on Greek vases. (B) The Greek key motif contains β-hairpins within its structure; the motif itself is formed by three connected beta-strands joined by hairpins, followed by a fourth strand connected by a longer loop, all arranged in an antiparallel fashion. (C) The dimeric βB2-crystallin (PDB 9D1V) is formed when two β-crystallin monomers are linked by chemical bonds to form a stable two-subunit complex. Dimerization is essential for the structural integrity and stability of β-crystallins. After dimerization, oligomerization follows when dimers themselves add to each other to create complex, higher-order structures of two to eight units often observed in the β-crystallin family. (D) γS-crystallin structure with a long, flexible linker. E) γD-crystallin structure with a shorter, more rigid linker. (F) The mouse γS-crystallin L-16 octamer (PDB 7RJ0) is induced upon exposure to mild-stress. Non-native disulfides from oxidative stress result in strained domain swapping that oligomerizes a distorted octamer ring associated with partial intermolecular disulfides. The partial unfolding of the asymmetrical octamer structure is prone to additional aggregation [211].

### 4.3.2. The Interactions Between Aromatic and Sulfur Residues in Greek Key Motifs Contribute to Lens Thermal Stability, Structural Integrity, and Transparency

Aromatic rings in Tyr and Phe are evolutionarily conserved to enhance protein folding [212,213]. The maintenance of nucleus γ-crystallins in the folded state is essential for their solubility because a lower level of exposed protein surface area reduces the energetic cost of solvation, and allows for efficient hydration by water molecules that forms a stabilizing hydration shell around the protein [214,215]. Conversely, unfolded crystallins present a much larger surface area and a higher entropic cost for the solvent, leading to aggregation and a decrease in solubility [216], scattering light and reducing transparency. Furthermore, Tyr and Phe in β/γ-crystallins form tyrosine corners and

 doi:10.20944/preprints202510.0392.v1



aromatic pairs that are essential for maintaining their structural integrity and thermal stability [217–220].

Hydrophobic sulfur-containing Cys and Met residues are buried together with Tyr and Phe in the hydrophobic core of β/γ crystallins. The interaction between the Met side chain and aromatic rings of Tyr and Phe greatly strengthen the three-dimensional structural stability of the β/γ crystallin Greek key motif. The "3-bridge clusters" of the methionine-aromatic motif involve interactions between the sulfur atom and the methylene and methyl groups of Met, and the π-systems of the aromatic residues [221–223]. Additionally, Met can lower oxidative damage by acting as an antioxidant [224–226]. Under oxidizing conditions, Cys residues with their reactive thiol (-SH) groups form covalent disulfide bonds that stabilize protein structures by creating a strong bond via a shared electron pair. The sulfur atoms of the disulfide bond act as electron donors from their lone pairs (n) into the antibonding π* orbital of neighboring carbonyl groups that are electron acceptors. Disulfide n→ π* interactions not only lower the p $K_a$ value of the N-terminal Cys residue of the motif to increase stability and nucleophilic reactivity, but also promote the formation of hyperstable β-strands in Greek key motifs [227–229].

Although this β/γ-crystallin fold is responsible for maintaining lens stability and transparency [208], compared to γD-crystallins, βB- and γS-crytallins are thermodynamically and kinetically less stable. The domain pairing interfaces of β-crystallins are dynamic and prone to subunit exchanges, rendering βB2 the least thermodynamically stable among β/γcrystallins [230,231]. Unfolding kinetic experiments conducted at 18 °C (to minimize denaturing effects) on wild-type (WT) γD- and γS-crystallins revealed that the kinetic stability of γDwt crystallins was superior to that of the γSwt. Under an ideal environment, the initial unfolding step—first kinetic transition ($k_{u1}$)—and half life ($t_{1/2}$) of 19 years of γDWT was significantly higher when compared to the 1.6 years (extrapolated values) for γSWT. While the difference in second kinetic transition ($k_{u2}$) between γDwt and γSwt were 129 and 2 days, respectively [232].

These results suggest that relative differences in structure and amino acid variations between γSwt and γDwt contribute to the overall thermodynamic and kinetic stability of the proteins. Despite sharing the common feature of a bilobed arrangement of four Greek key motifs, variations in amino acid side-chain interactions at the hydrophobic interfaces of Greek key motifs can greatly influence the stability and packing of crystallins [206,209,233]. Accordingly, once the initial unfolding barrier is breached, further denaturation can proceed rapidly, albeit at different rates, explaining why the onset of nuclear opacity in cold cataracts can happen within days. The differential protein structure of β/γ-crystallins can directly influence their domain-swapping behaviors, resulting in variations in thermodynamic stability and protein aggregation [209,234].

#### 4.3.3. Domain Swapping and Hydrophobic Interactions: Trading Protein Aggregation for Increased Thermodynamic Stability

Monomeric crystallins in the β/γ-crystallin superfamily all contain the same number of Greek key motifs—four arranged into a double Greek key structure. βB crystallins contain a longer and more flexible linker sequence connecting the N- and C-terminal domains, whereas γD-crystallins have shorter and more rigid linkers. The longer, more flexible linker peptide in βB crystallin monomers promotes the ready exchange of N- and C-terminal domains with the same domain from an adjacent crystallin, leading to the formation of stable, native dimeric and multimeric assemblies characteristic of βB crystallins [207,208,235–238]. Similarly, the relatively longer length and flexible structure of γS-crystallin linker, compared to γD-crystallins, results in differences in protein structures and interactions [209,239,240] (Figure 5). Under stressful conditions including low pH and excess ROS, monomeric γS-crystallin can produce intermediates that undergo domain swapping, forming strained dimers that are partially unfolded and prone to aggregation [211].

Domain swapping involves exchanging intramolecular contacts that stabilize a monomer for intermolecular contacts that stabilize an oligomer [241,242]. However, oligomer formation is entropically disfavored due to reduced translational and rotational freedom compared to monomers

 doi:10.20944/preprints202510.0392.v1



[243–245]. To maintain thermodynamic stability, the entropy loss—often due to the ordering of water molecules in the solvation shell of the oligomeric complex—must be offset by a favorable enthalpy gain [245,246]. Thermodynamic stability is determined by the Gibbs free energy change (ΔG), where a negative ΔG indicates a spontaneous process. This is defined by the equation:

$$\Delta G = \Delta H - T\Delta S$$

Under stress, oligomers formed via non-native domain swapping must remain thermodynamically stable by offsetting entropic loss with enthalpic gains [247,248]. γD-crystallins undergo non-native disulfide bonding and domain swapping, forming non-native dimers stabilized by intermolecular hydrophobic contacts and hydrogen bonds at domain-swapped interfaces. The exposure of hydrophobic residues, via the extrusion of the N-terminal β-hairpin, allows formerly buried hydrophobic regions to interact with complementary surfaces on other molecules [249]. This hydrophobic effect lowers the system's free energy by excluding water molecules from non-polar surfaces, while the negative enthalpy change from new hydrogen bonds or van der Waals (vdW) contacts at swapped interfaces further stabilizes the oligomer [247,250,251]. Despite this stabilization, the cost of maintaining monomeric γD- and γS-crystallins under stress is the formation of pathological aggregates that result in opacity over time [211,234,249,252–256].

### *4.4. Cysteines in β/γ-crystallins: Beyond the Role of Phase Separation Redox Rheostats*

Redox-sensitive Cys residues in β/γ-crystallins form native, intramolecular covalent disulfide bonds that stabilize protein structures under physiological conditions. These disulfide bonds act as tunable redox levers that activate or terminate phase separation of crystallins [178]. Within the β/γ-crystallin superfamily, monomeric γD crystallins in the lens nucleus contain the highest level of Cys that are buried deep within the hydrophobic core. Of the four major amino acids in γD-crystallins that contribute to refractive index increment, Cys has the highest molar residue refractivity (cm3) at 48.58 > Tyr (44.34) > Phe (42.21) > Met (34.45) [257]. In order to maintain sharp visual focus, the concentration gradient of crystallins in the lens nucleus is the highest. When amino acids that have a higher refractive index increment, such as Cys, are selected, the same lens refractive index can be achieved with a lower concentration of crystallins [2]. This suggests that Cys is not only a significant contributor to the high refractive power of γD-crystallins in the lens nucleus, but also reduces molecular crowding that can elevate critical solution temperature that activates phase separation and aggregation [72].

#### 4.4.1. Exposed Cys in β/γ-crystallins Form Non-Native Disulfides Under Oxidizing Conditions

In general, buried Cys are less likely to form native disulfides than those that are exposed. Due to the large sulfur atom that facilitates displacement of its valence electrons, exposed Cys is highly polarizable [258]. Consequently, the enhanced interaction with proteins and charged molecules in the vicinity increases local protein concentration and reduces diffusion. Accordingly, exposed Cys that act as nucleophilic redox switches can promote phase separation by forming reversible disulfide cross-links and lowering the local concentration threshold [178,259]. Ultimately, under physiological conditions, reversible phase separation are protective processes. Due to a lack of cellular turnover and limited access to GSH in the lens nucleus, Cys residues in γD-crystallins are mostly buried in the hydrophobic cores of the proteins. Oxidizing conditions can cause the formation of non-native, internal disulfide bonds that pair Cys residues that normally do not form covalent bonds in their native, functional conformation [260]. Native disulfides are specific Cys-Cys bonds present in the folded protein under physiological conditions and evolutionarily selected to maintain structure. βB-crystallins have a highly conserved disulfidome that functions to stabilize their dimeric interfaces [261]. Conversely, non-native disulfides can disrupt the native fold by locking non-functional confirmations. Non-native disulfides in γD-crystallins lock the N-terminal domain in a partially unfolded, aggregation-prone intermediate state that may be irreversible under oxidizing conditions

 doi:10.20944/preprints202510.0392.v1



[249]. Since disulfides can only be reversed by GSH and thioredoxins, the fate of most of these non-native disulfides in nuclear γD-crystallins likely follows the inevitable path of aggregation and cataractogenesis [68,224,249,261,262].

#### 4.4.2. Exposed Cys in γD-Crystallins Prevents Nucleation in Phase Separation

γD-crystallins have a total of six Cys residues [68]. Native exposed Cys in γD-crystallins are rare and exceptions are often justified by considerable advantages. Consider the evolutionary trade-off for the single, unpaired, most solvent-exposed Cys residue (29%) [263] in human γD-crystallins at position 110 (Cys110), which is also referred to as Cys111 due to minor differences in sequence numbering conventions. The exposed Cys110 has been demonstrated to prevent nucleation and suppress crystallization upon phase separation of the γD-crystallin [264]. It is possible that exposed Cys110, with a less-structured protein hydration shell, releases fewer water molecules into the bulk solution during phase separation. The higher negative entropy of crystallization is thermodynamically unfavorable, leading to the suppression of nucleation in phase separation [265,266]. Accordingly, when Cys110 is replaced by Met, the surface entropy is greatly reduced. With increased hydrophobicity and structuring of water molecules on the surfaces, the exposed Met that replaced Cys110 in γD-crystallins rapidly nucleated and crystallized, forming aggregates that can result in opacity of the lens [264]. Conversely, in an oxidizing environment, the exposed Cys110 readily formed intermolecular disulfide bonds resulting in dimers that elevated UCST of γD-crystallins to cause phase separation and aggregation [263]. This exposed γD Cys110 was even reported to form native disulfide bonds under physiological conditions in tested human lenses [267].

In essence, the native exposed Cys acts as a redox sentinel that can prevent nucleation and further aggregation when phase separation is triggered. However, the sentinel is sacrificed under pathological oxidizing conditions when the disulfide bonds cannot be reversed. One can imagine that this trade-off was a calculated risk that outweighed the major challenge of macromolecular crowding-induced phase separation versus the potential of excess, unneutralized oxidative stress in the nucleus. Under most physiological conditions, this evolutionary bet should generate favorable outcomes, especially in younger lenses. Conversely, due to cellular turnover, higher mitochondrial respiration, and active glutathione synthesis and activity, the outer regions of the lens face a different redox environment. In this region, the ability of βB and γS crystallins to form native and non-native disulfides, which result in domain swapping and domain pairing, presents unique opportunities and challenges in the lens outer regions.

### *4.5. The Lens Redox Environment Dictates the Fate of Non-Native Disulfide Bonds in β/γ-Crystallins*

Cys in most γ-crystallins must undergo prior conformational changes that expose the Cys residue before disulfide bonds are formed. In the nucleus, Cys in γD-crystallins are mostly buried in the core, with only one that is exposed in its native state. Conversely, βB- and γS-crystallins in the outer cortex regions of the lens have fewer Cys residues, but they are exposed and readily form disulfide bonds. Unlike γS-crystallins, βB-crystallins exhibit native, conserved disulfide bonds [261]. Most native disulfide bonds formed in the lenses of young healthy humans and mice are intramolecular, shifting to multimeric intermolecular disulfides in older lenses with lower levels of GSH. Compared to wild types, Cys 83 and Cys130 in γS of young LEGSKO mice (with reduced lens GSH synthesis knocked out) formed four- to 12-fold more disulfides, respectively [261]. It would appear that the selective oxidation of Cys residues in crystallins and the formation of non-native disulfides is highly dependent upon the accessibility of the Cys and the redox environment of the crystallins. The lens nucleus contains less GSH than the outer regions. Accordingly, γD-crystallins bury their Cys, whereas βB- and γS-crystallins contain a higher number of exposed Cys to act as redox sentinels that can help balance temporary elevations of ROS [68,233,262].

 doi:10.20944/preprints202510.0392.v1



4.5.1. Structural Frustration from Disulfides Eventually Results in Aggregation

In the early stages of oxidative stress, S-glutathionylation of a Cys residue covalently bonds a glutathionyl moiety from GSSG, forming a disulfide bond that releases a GSH molecule. This is a highly effective, reversible protective mechanism that prevents the formation of irreversible disulfide crosslinks in crystallins under oxidizing conditions. The formation of the protein-GSH adduct (Pr−SSG) quickly stops the Cys thiol from undergoing further, irreversible oxidation [283,289,292,293]. Intermolecular disulfide bonds are usually associated with increased stability of proteins in folded states [294]. Quantitative dynamics investigating intermolecular disulfides in a peroxiredoxin revealed extensive structural frustration and conformational fluctuations occurring over microseconds (μs). The disulfide bonds induced structural strain that disrupted the stable fold of the protein. The increased μs dynamics enhance disorder, raising conformational entropy and exposing hydrophobic patches [295,296]. This lowers the free energy barrier for phase separation, shifting the UCST higher to cause phase separation and aggregation [297]. Since structural frustration can drive domain swapping, it becomes clear why non-native intermolecular disulfides under oxidizing environments result in domain swapping that eventually leads to aggregation [248,298,299].

4.5.2. Transferring “Redox Hot Potatotes”: Playing Musical Chair with Protein Aggregation

The level of GSH is lower in the lens nucleus [192]. Under oxidizing environments, higher GSSG oxidizes Cys in yD-crystallins, forming disulfides that are not reversed due to lack of GSH [176,300]. In order to remain amorphous, WT yD crystallins transfer the disulfides to neighboring variants with non-native exposed Cys residues and lower kinetic stability. This redox reaction produces fully reduced, soluble WT yD crystallins and variants with non-native disulfide bonds that lock the molecules in intermediate states, exposing hydrophobic contacts prone to aggregation [68,249,301]. S-glutathionylation of crystallins is ultimately a reversible PTM that closely reflects the redox environment. In the lens outer regions, yS dimers can be reversed when the GSH content returns to normal levels [69,286,287]. Conversely, in the GSH-poor regions of the lens nucleus, yD-crystallins can only play musical chair with protein aggregation, shuffling the “redox hot potatoes” to kinetically less stable variants while remaining soluble [68,302].

4.5.3. Irreversible Deamidation Decreases Stability and Increases Aggregation of β/γ-Crystallins

The differences in the number of native exposed Cys in β/γ-crystallins may also determine whether the irreversible spontaneous PTM deamidation can compromise the integrity and stability of the crystallins, causing phase separation and aggregation of crystallins. Deamidation is a physiological, nonenzymatic process that involves a nucleophilic attack on the side-chain amide group, hydrolyzing asparagine (Asn) and glutamine (Gln) residues into their acidic forms [303]. Thiols in exposed Cys are reactive nucleophiles that can exacerbate deamidation in nearby Asn/Glu residues, or contribute to non-native disulfide bond formation [267,304]. It is not surprising that the deamidation of Asn to Asp in yD-crystallins did not produce any meaningful changes in structure or stability that would produce protein aggregation [305]. Conversely, yS- and βB-crystallins all harbor native exposed Cys. Consequently, deamidation was associated with substantial alterations in stability and aggregation propensity of yS-crystallins [70,306–310]] and βB-crystallins [311–314].

Deamidation changes the surface charge and hydrophobicity of crystallins by converting neutral Asn and Glu residues to negatively charged aspartic acid (Asp) and glutamic acid (Glu). The change in charge exposes buried aromatic hydrophobic residues Tyr and Phe that impact structure, function, and interactions with other molecules that lead to the formation of insoluble aggregates [306,308,311,315–318]. Deamidation can prevent $\alpha$-crystallins from effectively engaging deamidated βB- and yS-crystallins to prevent insoluble aggregation [311,315,316,319]. When crystallins in the lens are deamidated, the exposure of buried hydrophobic residues promotes protein aggregation. Deamidated human γS-crystallins exhibited exposed hydrophobic cores that downshifted the

 doi:10.20944/preprints202510.0392.v1



isoelectric point, increasing phase separation via the hydrophobic effect that was exacerbated by the high molecular crowding in the lens [308]. The rapid unfolding of hydrophobic residues can be mitigated by small molecules that compete with the hydrophobic surfaces and protect crystallins from further oxidation and denaturing [320]. Melatonin, an endogenous molecule, engages in hydrogen bonds, π-π stacking, and other non-covalent hydrophobic interactions to stabilize lens crystallins, reducing hydrophobic-driven aggregation and inhibiting pathological phase separation under oxidative and stressful conditions.

## 5. Melatonin: The Multifaceted Regulation of Crystallin Phase Separation and Protein Aggregation in Crystallins

Under oxidizing conditions, the exposure of buried aromatic residues including Tyr and Phe in β/γ crystallins promotes hydrophobic attractive forces that drive aggregation by minimizing water contact. The expulsion of the stable, organized water molecules as a result of hydrophobic clustering increases entropy that favors phase separation and aggregation [43,63,271,321–323]. The inclusion of Tyr and Phe in β/γ crystallins not only strengthens the three-dimensional structural stability of the β-hairpins in Greek key motifs [324], but also elevates the refractive index increment. However, when these aromatic 'sticky' residues are exposed, their hydrophobic interactions elevates the hydrophobic effect that can significantly influence phase separation and aggregation. The nonpolar aromatic ring of Phe and the polar hydroxyl group of Tyr contribute to a large range of attractive forces including vdW forces, hydrogen bonds, and hydrophobic interactions that promote the formation of BCs [325–327]. When deamidation decreases the ability of α-crystallins chaperones to bind to exposed hydrophobic residues [328,329], lens crystallins rely on small molecules such as melatonin and ATP to help prevent phase separation and aggregation.

### *5.1. Melatonin Prevents Phase Separation and Aggregation via Van der Waals Forces, Hydrogen Bonds, and Hydrophobic Interactions*

The aromatic rings in Phe and Tyr exhibit an electrostatic potential with a negatively charged center and a positively charged periphery that create dipoles. Dipoles allow aromatic residues to participate effectively in weak vdW π–π interactions and strong, noncovalent π-cation/π-alkyl interactions involving a π-system and positively charged cations and the non-polar electron cloud of an alkyl group, respectively [330–335]. vdW forces contribute to phase separation by inducing short-range, temporary fluctuations in electron distributions, creating instantaneous dipoles that induce complementary dipoles in neighboring molecules. These weak, non-specific interactions—primarily London dispersion forces and, to a lesser extent, dipole-dipole interactions—stabilize the aggregated state, particularly in proteins with exposed aromatic residues. Additionally, π-π stacking, a specialized vdW interaction between aromatic rings, plays a prominent role in such proteins, enhancing phase separation alongside the dominant hydrophobic effect [336–338]. In folded proteins, these molecular forces allow proteins to maintain stability by exploring different conformations and binding interactions. In exposed, unfolded proteins, the same molecular forces can contribute to protein phase separation and aggregation [337].

#### 5.1.1. The Promotion and Inhibition of Phase Separation by Van der Waals Forces: The Dynamic Relationships Between Entropy, Enthalpy, and the Hydrophobic Effect

Both phase separation and protein folding are driven by the hydrophobic effect ($\Delta S > 0$) that represents a significant increase in the entropy ($\Delta S$) of the water molecules surrounding the protein. Proteins bury their non-polar residues in the core to reduce solvent-exposure in the surface area. This displaces water molecules from ordered structures around the nonpolar surface, allowing these water molecules to become more disordered and free, which increases the overall entropy of the system [339,340]. Similar to protein folding, phase separation is also entropy-driven ($\Delta S > 0$), with entropic gains from the release of structured water around exposed hydrophobic residues. In both cases, the

 doi:10.20944/preprints202510.0392.v1



ordered structures of proteins (folded protein or phase-separated condensates) minimize their contact with water, leading to more disorder in the solvent. This increases overall entropy leading to higher stability and lower Gibbs free energy ($\Delta G = \Delta H - T\Delta S$). In the folded state, the gains in enthalpy ($\Delta H < 0$) from vdW forces, reflecting the energy released when aromatic residues align in the folded state, can stabilize the folded conformation, preventing unfolding and phase separation [73,341–343].

The hydrophobic effect, supported by vdW forces, drives exposed hydrophobic cores towards phase separation and aggregation [338,344,345]. However, when the vdW interactions involve hydrophilic molecules, including melatonin and ATP, the resulting protein-water or protein-hydrophilic interactions modulate protein hydration. This action disrupts protein-protein clustering via weak but stabilizing non-covalent forces (e.g., π-π stacking) and hydrogen bonds that shield exposed hydrophobic patches, thereby inhibiting phase separation and aggregation. Protein surface hydrophilicity, hydrogen bonding, and dynamic polarization fluctuations at interfaces are forces that modulate phase separation [346–349]. Melatonin has been observed to interact with Phe, Tyr, and Cys and other amino acid residues in different proteins and enzymes, lipids and cholesterol in membrane bilayers, tau fibrils and Aβ42 protofibrils, and even the SARS-CoV-2 virus. Melatonin binds to its molecular targets via π–π, π-alkyl, π-sigma, hydrogen bond, and other hydrophobic interactions to induce different effects, including the regulation of phase separation [350–357]. Please see Table 2 for additional details on methodologies and results observed in studies, listed in chronological order.

**Table 2.** Melatonin binds to molecular targets via vdW forces, hydrogen bonds, and non-covalent hydrophobic interactions under different contexts.

| Methodology | Results | Ref. |
|---|---|---|
| In silico molecular docking and protein-molecule interaction simulation analysis. | Computational docking analysis was used to predict melatonin direct molecular interactions with the catalytic groove of FUNDC1 via vdW forces (PHE A:108, ASP A:19, PRO A:32, ILE A:34, VAL A:33), conventional hydrogen bond (LEU A:53), carbon hydrogen bond (PHE A:52), π-cation (LYS A:51), and π-alkyl (ILE A:23). These interactions validate the in vitro functional observations on the suppression of FUNDCI signaling in mitochondria by melatonin.. | [350] |
| Microsecond all-atom molecular dynamics (MD) simulations. | Melatonin engages in strong π-π stacking interactions, cation–π interactions, and hydrogen bonds that destabilize structural components and intermediates of tau fibril assembly. | [351] |
| MD simulations, umbrella sampling, radial distribution function analysis, hydrogen bond analysis, and density profile analysis. | Melatonin formed hydrogen bonds with water and lipid headgroups and engaged in van der Waals (vdW) interactions with the dimyristoylphosphatidylcholine (DMPC) bilayer. These interactions help stabilize melatonin in its membrane-bound state that facilitates its biological functions. | [352] |
| All atom MD simulations (GROMACS 5.1.4). Post simulation analysis include Molecular Mechanics-Poisson–Boltzmann Surface Area, Secondary Structure Analysis (DSSP), Salt Bridge and Contact Number Analysis, and Probability Density Function and Potential of Mean Force Analysis. | Melatonin destabilized Aβ42 protofibrils through strong π–π stacking interactions with N-terminal and central residues (perpendicular with F4, Y10, F19; herringbone with H14, F19) and disrupted hydrophobic cores across central and C-terminal regions via hydrophobic and additional π–π interactions. | [353] |
| Density functional theory (DFT), time-dependent DFT, and molecular docking simulations. | Melatonin engages in conventional and carbon hydrogen bonding, π–π (T-shaped), π-alkyl, and π-sigma interactions with the SARS-CoV-2 virus. | [354] |
| MD simulations, umbrella sampling, RDF analysis, hydrogen | Melatonin interacted with lipids in DMPC-cholesterol membranes via hydrogen bonds (with water and lipid headgroups), hydrophobic interactions (indole ring with lipid tails and cholesterol), inferred vdW interactions (via CHARMM36m's | ]355[ |

 doi:10.20944/preprints202510.0392.v1



| | | |
|---|---|---|
| bond analysis, density profile analysis, and orientation analysis. | Lennard-Jones potentials, supporting bilayer partitioning), and minor electrostatic interactions. | |
| Isothermal titration calorimetry, UV-vis absorption spectroscopy, Fourier transform infrared (FT-IR) spectroscopy, and circular dichroism (CD). | Thermodynamic analysis revealed melatonin interacts with human serum albumin via hydrogen bonds and vdW forces, a process characterized by favorable enthalpy and unfavorable entropy. | [356] |
| Genetic Optimization for Ligand Docking (GOLD), X-Ray Crystallography, Isothermal Titration Calorimetry, and Kinetic Inhibition Assays. | During inhibitory interactions with the oxidized E-FAD form of human quinone reductase 2 enzyme, the hydrophobic methoxy group of melatonin made close vdW contact with Phe106 (4 A°); Phe 106, Phe126, Phe178, Tyr 67, and Cys 121 exhibited hydrophobic interactions with the indole ring; the nitrogen side chain of melatonin formed a hydrogen bond with Asn161 via a relay through a water molecule; and the parallel stacking of the indole moiety with FAD involved π-π and vdW contributions. | [357] |

#### 5.1.2. Melatonin Binds with Exposed Hydrophobic Residues to Prevent Phase Separation and Aggregation

The amphiphilic nature of melatonin's indole ring allows it to participate in both hydrophobic and hydrophilic interactions, including vdW forces, hydrophobic interactions, and hydrogen bonds [104]. The bulk of the indole system is inherently hydrophobic due to its nonpolar structure, consisting of carbon and hydrogen atoms in fused aromatic rings. Notwithstanding, the hydrogen atom on the ring's nitrogen is capable of forming hydrogen bonds that contribute to hydrophilic interactions. The electrostatic potential of indoles, with negatively charged centers and positively charged peripheries, creates dipoles that facilitate π-π and other vdW interactions [358,359]. Car-Parrinello Molecular Dynamics (CPMD) simulations revealed that melatonin forms hydrogen bonds with water, characterized by significant mean resident times, a finding confirmed by Helmholtz free energy calculations. At least one water molecule coordinates with the oxygen (O) of the methoxy group, the N–H hydrogen (H) of the indole ring, and the N-acetyl group. Furthermore, the simulations showed that two hydrogen atoms from two separate water molecules remained associated with the N-acetyl O for a duration exceeding the simulation time, indicating a highly stable hydration at that site [360].

When melatonin binds to exposed hydrophobic residues in crystallins via vdW interactions, its ability to form hydrogen bonds with water may stabilize these residues, thereby preventing hydrophobic collapse [73] and mitigating phase separation and aggregation driven by the hydrophobic effect [297,361]. Computational studies confirmed by experimental observations showed melatonin employed different molecular interactions to suppress FUN14 domain-containing 1 (FUNDC1) mitochondrial signaling by binding to the catalytic groove in FUNDC1. The binding region spanned the N-terminal cytosolic region (exposed), particularly overlapping with or adjacent to the LC3-Interacting Region (LIR) of FUNDC1. The binding site is mostly an exposed, hydrophobic pocket stabilized by specific aromatic and electrostatic contacts. This allows melatonin to engage in vdW forces with PHE A:108, ASP A:19, PRO A:32, ILE A:34, and VAL A:33; a conventional hydrogen bond with LEU A:53; a carbon-hydrogen bond with PHE A:52; and π-cation and π-alkyl interactions with LYS A:51 and ILE A:23, respectively [350]. The stabilization of phase-separated condensates facilitated by FUNDC1 is integral to its ability to regulate mitophagy [362,363]. By suppressing FUNDC1 phase separation, melatonin alleviated hyperglycemia-induced mitochondrial fragmentation, a process linked to dysregulated mitophagy under stress [350,364].

In the study of neurodegenerative diseases, the formation of tau [365–369] and amyloid-beta (Aβ) fibrils [370–372] via phase separation is well-documented. The increased formation of amyloid fibrils in lens crystallins is associated with cataractogenesis [373–378]. Molecular dynamics (MD) simulations and computational analyses revealed that melatonin can destabilize tau structural components and prevent tau fibril assembly via strong π–π stacking interactions, cation–π interactions, and the formation of hydrogen bonds [351]. Similarly, the binding of melatonin to the

 doi:10.20944/preprints202510.0392.v1



N-terminal and central residues of Aβ42 protofibrils via strong π–π stacking interactions caused destabilization. Melatonin also disrupted Aβ42 hydrophobic cores across the central and C-terminal regions via hydrophobic and additional π–π interactions [353]. The disruption and destabilization of Aβ fibrils can suppress further pathological aggregation that contributes to diseases including neurodegeneration and cataractogenesis. The unique amphiphilic features of melatonin and its indole ring are essential for understanding the wide range of molecular mechanisms employed by melatonin to prevent irreversible redox reactions leading to the phase separation of crystallins and cataractogenesis under different contexts (Table 1).

### *5.2. The Synergy Between Melatonin and the Hydrophilic ATP Prevents Phase Separation and Aggregation of Crystallins*

The aromatic purine ring of the adenosine moiety in ATP also engages in π-π, π-cation, and hydrogen bonding interactions [379]. The hydrophilic, triphosphate moiety of ATP is surrounded by 3–4 layers of hypermobile water molecules [380]. The amphiphilic adenosine purine ring in ATP participates in vdW forces, π-π stacking, and π-cation interactions with hydrophobic amino acids. The combined effect of the adenosine moiety and the triphosphate moiety enables the regulation of condensate phase separation behavior in a biphasic manner [381–386]. At lower concentrations (5-10 mM), ATP can induce phase separation and aggregation [387–391]. Conversely, ATP can dissolve BCs and prevent aggregation at higher concentrations [392–395].

The concentration of ATP in the mammalian lenses obtained from experimental studies is around 3 mM [396]; while the calculated molarity of intracellular ATP in human noncataractous lenses is 4.1 mM in the cortex and 1.3 mM in the nucleus, devoid of mitochondria [397]. In the human lens, about 70% of ATP is derived from anaerobic glycolysis [398]. The levels of ATP required to dissolve condensates is usually > 5 mM [395]. In vitro studies demonstrated that at 5 mM concentrations, ATP antagonized the crowding-induced destabilization of human γS-crystallins—found primarily in the outer regions of the lens where ATP concentration is higher—via reducing the hydrodynamic radius of γS-crystallins. ATP undermined the hydrophobic effect by interacting strongly with water molecules in the protein hydration shell of γS-crystallins, preventing the hydrophobic collapse and overlap of hydration shells [73,399]. This effectively suppresses the phase separation and aggregation of γS-crystallin under crowding conditions [400–402].

Extensive evidence presented in experimental in vitro and in vivo studies indicate that the presence of ATP augments the ability of melatonin to prevent protein aggregation and enhance solubilization of condensates formed via phase separation [403–405]. The synergy between melatonin and ATP is facilitated primarily by the vdW π–π stacking of the indole and purine rings in melatonin and the ATP adenosine moiety, respectively (Figure 6). Experimental and theoretical studies revealed that the electronic coupling and mechanical stability of π–π stacking are significantly enhanced when the antiparallel alignment of the dipole moment is higher [406,407]. Depending on the different isomer conformations that are modulated by binding with water molecules, the calculated dipole moment for melatonin is high, often between 2.67 and 6.0 Debye (D), with an average of 4.08 D [354,408–410]. The aromatic purine ring of the adenosine moiety in ATP also engages in π–π, π–cation, and hydrogen bonding interactions [379]. The calculated dipole moment for the adenosine moiety in ATP can vary between 2.8 -- 5.6 D, depending on the conformation adopted [411].

Melatonin can stack comfortably with ATP to augment the adenosine moiety effect [403–405]. Assuming a dipole moment of 4.5 for melatonin, the stacking of melatonin's indole ring with ATP's adenosine moiety would likely increase their combined dipole moments. The net dipole would conceivably rise from ~5.6 D (adenosine) to approximately 6–7 D, depending on the stacking angle and local charge effects, due to partial vector addition of melatonin's 4.5 D and adenosine's 5.6 D [27,354,412]. A molecular dynamics study of melatonin in water showed that its hydrophobic indolyl ring favors interactions at the water-air interface, whereas its N-acetyl group group favors hydrogen bonding with water molecules, resulting in specific structural arrangements and enhanced molecular dynamics compared to bulk water [413]. Computational chemistry methods identified 52 unique

 doi:10.20944/preprints202510.0392.v1



conformers of melatonin, representing the possible spatial arrangements and conformational energies, enabled by its flexible side chain with rotatable bonds [414] (Figure 4). Hence, the combined effect of melatonin and adenosine π–π stacking can be further magnified by conformational changes in melatonin as a result of vdW interactions and hydrogen bonding [360,408,409,414].

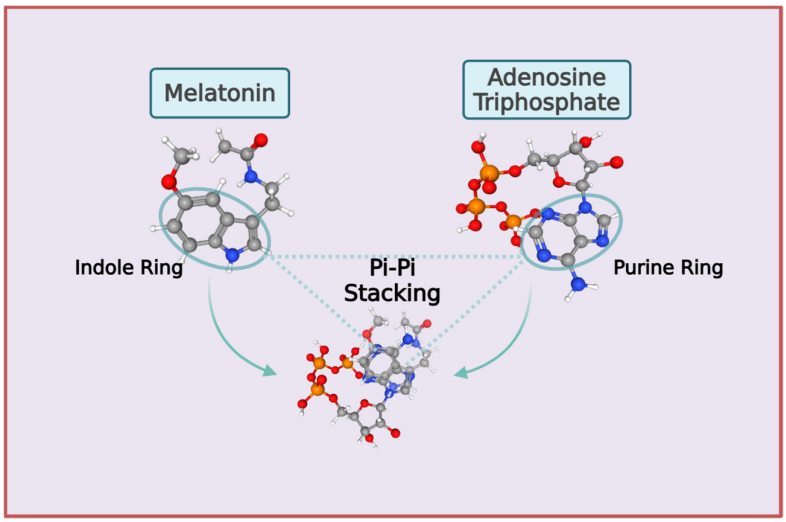


**Figure 6.** Visual Representation of vdW π–π stacking between melatonin's indole ring and the purine ring of the adenosine moiety of ATP.

*5.3. Melatonin Prevents Lipid Peroxidation-Induced α-Crystallin Membrane Aggregation by Enhancing Cholesterol Liquid-Ordered Domain Stability*

α-Crystallins are effective chaperones that help maintain lens transparency by binding to damaged crystallins, preventing pathological aggregation [195]. Entropically-driven hydrophobic contacts allow α-crystallins to access newly-exposed hydrophobic sites of unfolded crystallins in the outer regions of the younger lenses where intact α-crystallins are mainly located [[200,415]]. Age-related changes and molecular crowding can induce the phase separation of α-crystallins [416]. The insoluble, phase-separated, pathological aggregates of α-crystallin are reported to bind to lens membranes via hydrophobic interactions, contributing to cataract formation not only in the lens outer regions, but also the lens nucleus [417–419]. It is not a coincidence that the binding of α-crystallin aggregates to lens membranes is increased with age and/or cataractogenesis [420,421].

5.3.1. Increased Chol in Membranes Reduces Aggregation of α-Crystallins

Inadequate GSH during the aging process and/or cataractogenesis results in peroxidation of lipids in lens membranes. However, the binding of α-crystallin aggregates to lens membranes is decreased according to cholesterol (Chol) saturation. Increased Chol decreases membrane surface hydrophobicity, suppressing the hydrophobic binding of α-crystallins to lens membranes and increasing their content in lens cytoplasm. A complete inhibition of α-crystallin membrane binding was achieved by saturating Chol content in the membrane bilayer [422,423]. Chol phase separates into liquid-ordered ($L_O$) and liquid-disordered ($L_D$) domains. The co-existence of these distinct phases creates lateral heterogeneity within the membrane, allowing for the distinct organization of different lipid and protein components into functional domains [424–426]. Chol modulates the membrane hydrophobicity whereby its presence significantly decreases membrane surface hydrophobicity but increases hydrophobicity in the central regions of the membrane bilayer. Increased Chol content in membranes transitions $L_D$ domains into $L_O$ domains. Consequently, $L_O$ domains contain significantly higher levels of Chol [427]. The increased Chol in $L_O$ domains elevates hydrophobic thickness,

 doi:10.20944/preprints202510.0392.v1



thereby enhancing overall hydrophobicity of the central bilayer core while decreasing membrane surface hydrophobicity [428,429], leading to inhibition of binding by α-crystallins.

#### 5.3.2. Membrane Lipid Peroxidation Promotes Extensive Aggregation of α-Crystallins

During the aging process, increased ROS and decreased GSH in the lens elevate lipid peroxidation that induces phase separation of membranes into $L_O$ and $L_D$ domains, with increased abundance of the $L_D$, Chol-poor phase. The accumulation of peroxidized lipids and their chemically modified products in the $L_D$ phase disturbs lipid packing and lipid raft locations in lipid bilayers [430]. Lipid peroxidation that disturbs lens membrane orders is one of the primary reasons why aging and cataractogenesis is associated with increased binding of α-crystallin to membranes that inactivate their chaperone, protective features and exacerbating aggregation of crystallins. Imbalances in Cys redox chemistry can lead to the peroxidation of Chol and lipids in lens membranes [431]. Kadka and co-workers (2025) reported the photosensitized peroxidation of Chol and lipids in the bovine lens nuclear membrane (NM) promoted the extensive aggregation of αAc, αBc, and αABc crystallins in the nucleus. In addition, the use of atomic force microscopy (AFM) method revealed that Chol and lipid peroxidation in the NM of a 67-year-old male donor with grade 2 cortical and nuclear cataracts was 1.5-fold higher than those detected in bovine NM oxidized for 1 hour [432].

#### 5.3.3. Melatonin Increases Chol in Membranes and Prevents Lipid Peroxidation by Promoting Phase Separation of Lipid Domains and Dampening Dissipative Processes

Melatonin is a potent antioxidant known for its ability to inhibit peroxidation of lipids [433–440]. More importantly, melatonin stabilizes phase separation of Chol and lipids, preserving the coexistence of $L_O$ and $L_D$ phases over an extended range of temperatures in model phospholipid membranes. Starting at 25 °C, the lateral diffusion coefficient ($D_l$) of lipids increases. When the temperature reaches ~45 °C, bilayer lipids become highly disordered, promoting a single fluid $L_D$ phase [441,442]. This phenomenon is suppressed by the addition of 20 mol% melatonin, maintaining the coexistence of $L_O$ and $L_D$ phases even at 45 °C [442]. The features of melatonin in suppressing membrane lipids from peroxidation and maintaining Chol-rich $L_O$ domains are intimately related, with the former, surprisingly, dependent on the latter and not vice versa.

Bolmatov and co-workers (2020) probed the nanoscale dynamics of dimyristoylphosphatidylcholine (DMPC)-Chol model membranes with melatonin at 27 mol%, employing all-atom molecular dynamics (MD) simulations and inelastic X-ray scattering (IXS). The results of their investigations revealed that melatonin stabilizes $L_O$ domains by dampening dissipative processes. The insertion of melatonin into the membrane, anchoring near phospholipid heads and interacting with tails, modifies the viscoelastic properties, shifting the membrane toward a more elastic state with reduced viscosity. This curbs the rapid rattling and relaxation that drive raft transience, stabilizing the $L_O$ phase structurally by reinforcing the rigidity and packing of $L_O$ domains. Accordingly, melatonin inclusion in lipids promotes resistance to thermal disorder and lipid exchange, effectively prolonging their persistence against dissipation via self-diffusion. The increased rigidity, coupled with the reduced $D_l$, creates a protective barrier that hinders the lateral and transverse movement of lipids. More importantly, it limits the pathways available for small molecules like oxygen to permeate through the bilayer. The fact that the $D_l$ is reduced by 6.37-fold upon melatonin inclusion is directly correlated with the protective barrier function because lower lipid mobility restricts the dynamic fluctuations (e.g., pore formation or undulations) that small molecules exploit to cross membranes. Therefore, melatonin's suppressive feature on membrane lipid peroxidation is dependent upon its ability to maintain $L_O$ domains and by reducing dissipation via self-diffusion [443].

Lipid peroxidation is a chain reaction initiated by ROS molecules that abstract hydrogen atoms from polyunsaturated fatty acid chains in membrane phospholipids. The formation and propagation of lipid radicals results in membrane damage, altered fluidity, and cell dysfunction. Accordingly, the availability of oxygen and lipid mobility are critical for this process to proceed efficiently. Sodium

 doi:10.20944/preprints202510.0392.v1



selenite causes rapid opacification in the lens nucleus by oxidizing free thiol groups in GSH or Cys residues to form seleno-disulfide. In the lens nucleus where GSH availability is limited to begin with, depletion of GSH results not only in lipid peroxidation, but the formation of irreversible disulfides and S-glutathionylation. This chain of events quickly results in phase separation and pathological aggregation of crystallins—including $\alpha$-crystallins—via molecular crowding and the hydrophobic effect. Melatonin is able to quickly reduce nuclear membrane lipid peroxidation by stabilizing Chol Lo domains in sodium selenite treated rat pups. Compared to selenite-treated groups, melatonin treatment (10 mg/kg, intraperitoneal injection) was associated with significant reductions in oxidative stress biomarkers. The lipid peroxidation product malonaldehyde [444] was reduced by 48.9%. Additionally, the antioxidant enzyme catalase was increased by a staggering 71.3%. Rat pups that did not receive melatonin all developed dense nuclear cataracts from sodium selenite. Conversely, 71% of rat pups treated with melatonin exhibited slight nuclear opacity while the rest of the group had completely clear lenses [87] (Table 1).

*5.4. Melatonin Determines the Outcome of Ultraviolet Exposure in the Human Lens*

The cascading effects of lipid peroxidation caused by exposure to UV exposure are a major long-term causative factor for cataractogenesis [445]. The chronic and cumulative exposure to ultraviolet (UV) radiation is an established, significant risk factor in cataractogenesis [446–448]. UV-A exposure-induced deamidation of $\alpha$B-crystallins caused complete loss of chaperone activity due to structural alterations from increased oxidation [449]. Deleterious oxidative effects of chronic, low-level UVA light exposure in guinea pigs increased lipid peroxidation and protein aggregation, and decreased the already low levels of GSH in the lens nucleus at the same time [450]. $\alpha$:$\beta$:$\gamma$ crystallin protein mixtures exposed to UV-B radiation formed amyloid-like, cataractous fibrils [451]. Under UV-C light, human $\gamma$D-crystallin proteins formed intermediate and structurally different aggregate species [452], whereas under UV-B irradiation, the native $\beta$-sandwich in human $\gamma$D-crystallin Greek key motif formed amyloid fibril $\beta$-sheets [453]. Nevertheless, controversial evidence points to a dualistic role of UV radiation in eye lenses.

Experimental results report extensive PTMs and oxidation of Cys in human $\gamma$S-crystallins (H$\gamma$S) upon exposure to > 10.8 kGy of gamma radiation. Despite the formation of protein-protein crosslinks, (H$\gamma$S) remain stubbornly folded [454]. In vitro studies reported that upon exposure to low dose UVB, Trp residues in human $\gamma$D-crystallins served a protective function by absorbing UV radiation to minimize photooxidation damage, safeguarding the retina. Notwithstanding, UV exposure leads to the covalent scission and breakdown of the Trp indole rings, forming degradation products that accelerate aggregation and cataractogenesis [455–457]. Surprisingly, an in vitro study employing crystallographic structures demonstrated that UV illumination cleaved disulfide bonds formed in human $\gamma$D-crystallins as a result of UV oxidation. Specifically, the photolysis restored free thiols, preventing dimerization and aggregation [458]. Although this appears to be a "rescue pathway" for maintaining lens protein stability, its effects may be unsustainable over a longer timeframe. The UV irradiation-induced cleavage of disulfide bonds is dependent upon the availability of Trp and Tyr in the vicinity, acting as photosensitizers. $\gamma$D-crystallins have multiple Trp and Tyr residues near Cys that help support and enhance disulfide cleavage by transferring energy/electrons to oxidized cystine disulfide bonds [459]. Nonetheless, long-term UV exposure can easily exhaust the support pool, rendering the rescue pathway unsustainable. Accordingly, chronic UV photooxidizes Trp and Tyr, reducing their photosensitizing capacity while depleting lens antioxidants and promoting the re-oxidation of thiols or the formation of damaging sulfur species, leading to protein aggregation and cataract progression.

A cross-sectional analytical study based on data from the 5th Korean National Health and Nutrition Examination Survey (KNHANES V, conducted 2010–2012) with 952 participants examined the relationship between sunlight exposure time and the prevalence of cataracts. Results indicate that daily sunlight exposure time of ≥ 5 h is correlated with a higher prevalence of cataracts in both men and women. However, women with 2–5 h of sunlight exposure had a higher incidence of cataracts

 doi:10.20944/preprints202510.0392.v1



compared to men with the same exposure time. Individuals aged > 45 reported significantly higher incidence of cataracts regardless of gender and exposure time [460]. Experimental results demonstrated that melatonin can effectively prevent the formation of cataracts caused by exposure to UVB [89] and ionizing gamma irradiation [86]. It is perhaps not a coincidence that older women exhibited significantly lower overnight urinary 6-sulfatoxymelatonin excretion than men [461]. The higher melatonin in males could have delayed cataractogenesis in the Korean population study. However, the decline in endogenous melatonin production in both genders eventually results in the failure to counter the long-term effects of chronic, prolonged UV exposure.

## 6. Conclusions and Perspectives

The inherent nature of crystallins predisposes the lens to the formation of aggregates as a direct consequence of redox-mediated molecular interactions that promote irreversible phase separation. Melatonin can act as a potent free radical scavenger that reduces excess ROS and free radicals to maintain GSH:GSSG redox balance, and prevent lipid peroxidation in membranes to protect the chaperone function of $\alpha$-crystallins. Concurrently, melatonin can bind to exposed aromatic, hydrophobic residues in $\beta/\gamma$ crystallins, preventing phase separation and aggregation. Melatonin achieves these effects by employing vdW forces, hydrogen bonds, and other hydrophobic interactions to shield exposed hydrophobic residues from hydrophobic interactions that elevate molecular crowding and hydrophobic collapse. The effective application of melatonin in the prevention and attenuation of cataractogenesis may be dependent upon the redox environment of the lens. In older adults and younger individuals with chronic high sun exposure, a higher dose may be necessary to counterbalance lower antioxidants responses and higher oxidative stress status. Even though topical melatonin is viewed as a low-risk, affordable adjunctive therapy, at present, surgery remains the gold standard for advanced cataracts. Human clinical trials on ocular melatonin application remain scarce. There is an urgent need for large-scale, randomized controlled trials to establish efficacy, optimal dosing, safety, and formulations, specifically nanoparticle-enhanced drops for better solubility, bioavailability, and penetration.

**Author Contributions:** Conceptualization, data curation, writing—original draft preparation: DL; review and editing: DL and RJR; visualization, DL. All authors have read and agreed to the published version of the manuscript.

**Funding:** This research received no external funding.

**Institutional Review Board Statement:** Not applicable.

**Informed Consent Statement:** Not applicable.

**Acknowledgments:** Special thanks to Daniel Matrone for technical assistance. Figures 1-6 were created with BioRender.com.

**Conflicts of Interest:** The authors declare no conflicts of interest.

## Abbreviations

| | |
|---|---|
| ATP | Adenosine triphosphate |
| BC | Biomolecular condensate |
| Chol | Cholesterol |
| Cys | Cysteine |
| D, | Lateral diffusion coefficient |
| GSH | Glutathione |
| $L_O$ | Liquid-ordered |
| $L_D$ | Liquid-disordered |
| Met | Methionine |
| NADPH | Nicotinamide adenine dinucleotide phosphate |

 doi:10.20944/preprints202510.0392.v1



| | |
|---|---|
| Phe | Phenylalanine |
| ROS | Reactive oxygen species |
| $T_{ph}$ | Phase separation temperature |
| Trp | Tryptophan |
| Tyr | Tyrosine |
| UCST | Upper critical solution temperature |
| LCST | Lower critical solution temperature |
| UV | Ultraviolet |
| vdW | Van der Waals |
| WT | Wild-type |

## References


1. Roskamp, K.W.; Paulson, C.N.; Brubaker, W.D.; Martin, R.W. Function and Aggregation in Structural Eye Lens Crystallins. *Acc. Chem. Res.* **2020**, *53*, 863–874, doi:10.1021/acs.accounts.0c00014.
2. Zhao, H.; Magone, M.T.; Schuck, P. The Role of Macromolecular Crowding in the Evolution of Lens Crystallins with High Molecular Refractive Index. *Phys. Biol.* **2011**, *8*, 046004, doi:10.1088/1478-3975/8/4/046004.
3. Fernández, J.; Rodríguez-Vallejo, M.; Martínez, J.; Tauste, A.; Piñero, D.P. From Presbyopia to Cataracts: A Critical Review on Dysfunctional Lens Syndrome. *J. Ophthalmol.* **2018**, *2018*, 4318405, doi:10.1155/2018/4318405.
4. Pescosolido, N.; Barbato, A.; Giannotti, R.; Komaiha, C.; Lenarduzzi, F. Age-Related Changes in the Kinetics of Human Lenses: Prevention of the Cataract. *Int. J. Ophthalmol.* **2016**, *9*, 1506–1517, doi:10.18240/ijo.2016.10.23.
5. Vision Loss Expert Group of the Global Burden of Disease Study; GBD 2019 Blindness and Vision Impairment Collaborators Global Estimates on the Number of People Blind or Visually Impaired by Cataract: A Meta-Analysis from 2000 to 2020. *EYE* **2024**, *38*, 2156–2172, doi:10.1038/s41433-024-02961-1.
6. Lin, L.; Liang, Y.; Jiang, G.; Gan, Q.; Yang, T.; Liao, P.; Liang, H. Global, Regional, and National Burden of Cataract: A Comprehensive Analysis and Projections from 1990 to 2021. *PLoS One* **2025**, *20*, e0326263, doi:10.1371/journal.pone.0326263.
7. Wang, Z.; Friedrich, M.G.; Truscott, R.J.W.; Schey, K.L. Identification of Age- and Cataract-Related Changes in High-Density Lens Protein Aggregates. *Invest. Ophthalmol. Vis. Sci.* **2025**, *66*, 34, doi:10.1167/iovs.66.5.34.
8. Wang, Y.; Cao, K.; Guo, Z.-X.; Wan, X.-H. Effect of Lens Crystallins Aggregation on Cataract Formation. *Exp. Eye Res.* **2025**, *253*, 110288, doi:10.1016/j.exer.2025.110288.
9. Rao, P.V. The Pulling, Pushing and Fusing of Lens Fibers: A Role for Rho GTPases. *Cell Adh. Migr.* **2008**, *2*, 170–173, doi:10.4161/cam.2.3.6495.
10. Grosas, A.B.; Carver, J.A. Eye Lens Crystallins: Remarkable Long--lived Proteins. *Long--lived Proteins in Human Aging and Disease* 2021, 59–96.
11. Rodriguez, J.; Tan, Q.; Šikić, H.; Taber, L.A.; Bassnett, S. The Effect of Fibre Cell Remodelling on the Power and Optical Quality of the Lens. *J. R. Soc. Interface* **2023**, *20*, 20230316, doi:10.1098/rsif.2023.0316.
12. Zhao, H.; Brown, P.H.; Magone, M.T.; Schuck, P. The Molecular Refractive Function of Lens γ-Crystallins. *J. Mol. Biol.* **2011**, *411*, 680–699, doi:10.1016/j.jmb.2011.06.007.
13. Peschek, J.; Braun, N.; Franzmann, T.M.; Georgalis, Y.; Haslbeck, M.; Weinkauf, S.; Buchner, J. The Eye Lens Chaperone Alpha-Crystallin Forms Defined Globular Assemblies. *Proc. Natl. Acad. Sci. U. S. A.* **2009**, *106*, 13272–13277, doi:10.1073/pnas.0902651106.
14. Vendra, V.P.R.; Khan, I.; Chandani, S.; Muniyandi, A.; Balasubramanian, D. Gamma Crystallins of the Human Eye Lens. *Biochim. Biophys. Acta* **2016**, *1860*, 333–343, doi:10.1016/j.bbagen.2015.06.007.
15. Kröger, R.H.; Campbell, M.C.; Munger, R.; Fernald, R.D. Refractive Index Distribution and Spherical Aberration in the Crystalline Lens of the African Cichlid Fish Haplochromis Burtoni. *Vision Res.* **1994**, *34*, 1815–1822, doi:10.1016/0042-6989(94)90306-9.
16. Kiss, A.J.; Mirarefi, A.Y.; Ramakrishnan, S.; Zukoski, C.F.; Devries, A.L.; Cheng, C.-H.C. Cold-Stable Eye Lens Crystallins of the Antarctic Notothenioid Toothfish Dissostichus Mawsoni Norman. *J. Exp. Biol.* **2004**, *207*, 4633–4649, doi:10.1242/jeb.01312.

 doi:10.20944/preprints202510.0392.v1




17. Zhao, H.; Chen, Y.; Rezabkova, L.; Wu, Z.; Wistow, G.; Schuck, P. Solution Properties of γ-Crystallins: Hydration of Fish and Mammal γ-Crystallins: Hydration of Fish and Mammal γ-Crystallins. *Protein Sci.* **2014**, *23*, 88–99, doi:10.1002/pro.2394.
18. Delaye, M.; Tardieu, A. Short-Range Order of Crystallin Proteins Accounts for Eye Lens Transparency. *Nature* **1983**, *302*, 415–417, doi:10.1038/302415a0.
19. Lin, P.; Lin, Y.; Lu, Y.; Chen, X.; Zhou, Z.; Zhao, X.; Cui, L. Unveiling the Dynamic Drivers: Phase Separation's Pivotal Role in Stem Cell Biology and Therapeutic Potential. *Stem Cell Res. Ther.* **2025**, *16*, 266, doi:10.1186/s13287-025-04403-5.
20. Dasmeh, P.; Doronin, R.; Wagner, A. The Length Scale of Multivalent Interactions Is Evolutionarily Conserved in Fungal and Vertebrate Phase-Separating Proteins. *Genetics* **2022**, *220*, doi:10.1093/genetics/iyab184.
21. Uzorka, A.; Olaniyan, A.O.; Bawa, M. Biophysical Mechanisms of Liquid–Liquid Phase Separation in Biological Systems. *Biophys. Rev. Lett.* **2024**, *19*, 1–16, doi:10.1142/S1793048024300019.
22. Banani, S.F.; Lee, H.O.; Hyman, A.A.; Rosen, M.K. Biomolecular Condensates: Organizers of Cellular Biochemistry. *Nat. Rev. Mol. Cell Biol.* **2017**, *18*, 285–298, doi:10.1038/nrm.2017.7.
23. Pappu, R.V. Phase Separation-A Physical Mechanism for Organizing Information and Biochemical Reactions. *Dev. Cell* **2020**, *55*, 1–3, doi:10.1016/j.devcel.2020.09.023.
24. Gao, Y.; Li, X.; Li, P.; Lin, Y. A Brief Guideline for Studies of Phase-Separated Biomolecular Condensates. *Nat. Chem. Biol.* **2022**, *18*, 1307–1318, doi:10.1038/s41589-022-01204-2.
25. Borcherds, W.; Bremer, A.; Borgia, M.B.; Mittag, T. How Do Intrinsically Disordered Protein Regions Encode a Driving Force for Liquid-Liquid Phase Separation? *arXiv [q-bio.BM]* 2020.
26. Reza Masoodi, H.; Sadat Pourhosseini, R.; Bagheri, S. The Role of Nature of Aromatic Ring on Cooperativity between π–π Stacking and Ion–π Interactions: A Computational Study. *Comput. Theor. Chem.* **2023**, *1220*, 114022, doi:10.1016/j.comptc.2023.114022.
27. Doveiko, D.; Kubiak-Ossowska, K.; Chen, Y. Estimating Binding Energies of π-Stacked Aromatic Dimers Using Force Field-Driven Molecular Dynamics. *Int. J. Mol. Sci.* **2024**, *25*, 5783, doi:10.3390/ijms25115783.
28. Lee, J.; Cho, H.; Kwon, I. Phase Separation of Low-Complexity Domains in Cellular Function and Disease. *Exp. Mol. Med.* **2022**, *54*, 1412–1422, doi:10.1038/s12276-022-00857-2.
29. Dignon, G.L.; Zheng, W.; Kim, Y.C.; Mittal, J. Temperature-Controlled Liquid-Liquid Phase Separation of Disordered Proteins. *ACS Cent. Sci.* **2019**, *5*, 821–830, doi:10.1021/acscentsci.9b00102.
30. MacAinsh, M.; Dey, S.; Zhou, H.-X. Direct and Indirect Salt Effects on Homotypic Phase Separation. *eLife* 2024.
31. Nandy, M.; Ganar, K.A.; Ippel, H.; Dijkgraaf, I.; Deshpande, S. PH-Responsive Phase Separation Dynamics of Intrinsically Disordered Peptides. *bioRxiv* 2025, 2025.01.09.632076.
32. Zigman, S.; Lerman, S. Properties of a Cold-Precipitable Protein Fraction in the Lens. *Exp. Eye Res.* **1965**, *4*, 24–30, doi:10.1016/s0014-4835(65)80005-7.
33. Petitt, P.; Forciniti, D. Cold Cataracts: A Naturally Occurring Aqueous Two-Phase System. *J. Chromatogr. B Biomed. Sci. Appl.* **2000**, *743*, 431–441, doi:10.1016/s0378-4347(00)00220-6.
34. Blackburn, B.J.; McPheeters, M.T.; Jenkins, M.W.; Dupps, W.J., Jr; Rollins, A.M. Phase-Decorrelation Optical Coherence Tomography Measurement of Cold-Induced Nuclear Cataract. *Transl. Vis. Sci. Technol.* **2023**, *12*, 25, doi:10.1167/tvst.12.3.25.
35. Sivak, J.G.; Stuart, D.D.; Weerheim, J.A. Optical Performance of the Bovine Lens before and after Cold Cataract. *Appl. Opt.* **1992**, *31*, 3616–3620, doi:10.1364/AO.31.003616.
36. Li, Y.; Li, Y.; Liu, X.; He, Y.; Guan, T. Protein and Water Distribution Across Visual Axis in Mouse Lens: A Confocal Raman MicroSpectroscopic Study for Cold Cataract. *Front Chem* **2021**, *9*, 767696, doi:10.3389/fchem.2021.767696.
37. Yang, H.; Ping, X.; Zhou, J.; Ailifeire, H.; Wu, J.; Nadal-Nicolás, F.M.; Miyagishima, K.J.; Bao, J.; Huang, Y.; Cui, Y.; et al. Reversible Cold-Induced Lens Opacity in a Hibernator Reveals a Molecular Target for Treating Cataracts. *J. Clin. Invest.* **2024**, *134*, doi:10.1172/JCI169666.
38. Loewenstein, M.A.; Bettelheim, F.A. Cold Cataract Formation in Fish Lenses. *Exp. Eye Res.* **1979**, *28*, 651–663, doi:10.1016/0014-4835(79)90066-6.

 doi:10.20944/preprints202510.0392.v1




39. Bierma, J.C.; Roskamp, K.W.; Ledray, A.P.; Kiss, A.J.; Cheng, C.-H.C.; Martin, R.W. Controlling Liquid-Liquid Phase Separation of Cold-Adapted Crystallin Proteins from the Antarctic Toothfish. *J. Mol. Biol.* **2018**, *430*, 5151–5168, doi:10.1016/j.jmb.2018.10.023.
40. Liedtke, W.B. Deconstructing Mammalian Thermoregulation. *Proc. Natl. Acad. Sci. U. S. A.* **2017**, *114*, 1765–1767, doi:10.1073/pnas.1620579114.
41. Barnes, B.M. Freeze Avoidance in a Mammal: Body Temperatures below 0 Degree C in an Arctic Hibernator. *Science* **1989**, *244*, 1593–1595, doi:10.1126/science.2740905.
42. Zhang, H.; Wu, C.; Singh, M.; Nair, A.; Aglyamov, S.; Larin, K. Optical Coherence Elastography of Cold Cataract in Porcine Lens. *J. Biomed. Opt.* **2019**, *24*, 1–7, doi:10.1117/1.JBO.24.3.036004.
43. Thomson, J.A.; Schurtenberger, P.; Thurston, G.M.; Benedek, G.B. Binary Liquid Phase Separation and Critical Phenomena in a Protein/water Solution. *Proc. Natl. Acad. Sci. U. S. A.* **1987**, *84*, 7079–7083, doi:10.1073/pnas.84.20.7079.
44. Seuring, J.; Agarwal, S. Polymers with Upper Critical Solution Temperature in Aqueous Solution. *Macromol. Rapid Commun.* **2012**, *33*, 1898–1920, doi:10.1002/marc.201200433.
45. Wadsworth, G.M.; Zahurancik, W.J.; Zeng, X.; Pullara, P.; Lai, L.B.; Sidharthan, V.; Pappu, R.V.; Gopalan, V.; Banerjee, P.R. RNAs Undergo Phase Transitions with Lower Critical Solution Temperatures. *Nat. Chem.* **2023**, doi:10.1038/s41557-023-01353-4.
46. Kapnistos, M.; Hinrichs, A.; Vlassopoulos, D.; Anastasiadis, S.H.; Stammer, A.; Wolf, B.A. Rheology of a Lower Critical Solution Temperature Binary Polymer Blend in the Homogeneous, Phase-Separated, and Transitional Regimes. *Macromolecules* **1996**, *29*, 7155–7163, doi:10.1021/ma960835n.
47. Kingsley, C.N.; Bierma, J.C.; Pham, V.; Martin, R.W. γS-Crystallin Proteins from the Antarctic Nototheniid Toothfish: A Model System for Investigating Differential Resistance to Chemical and Thermal Denaturation. *J. Phys. Chem. B* **2014**, *118*, 13544–13553, doi:10.1021/jp509134d.
48. Wycherly, B.J.; Moak, M.A.; Christensen, M.J. High Dietary Intake of Sodium Selenite Induces Oxidative DNA Damage in Rat Liver. *Nutr. Cancer* **2004**, *48*, 78–83, doi:10.1207/s15327914nc4801_11.
49. Ammar, E.M.; Couri, D. Acute Toxicity of Sodium Selenite and Selenomethionine in Mice after ICV or IV Administration. *Neurotoxicology* **1981**, *2*, 383–386.
50. Ostádalová, I.; Babický, A.; Obenberger, J. Cataract Induced by Administration of a Single Dose of Sodium Selenite to Suckling Rats. *Experientia* **1978**, *34*, 222–223, doi:10.1007/bf01944690.
51. Padmanabha, S.; Vallikannan, B. Fatty Acids Influence the Efficacy of Lutein in the Modulation of α-Crystallin Chaperone Function: Evidence from Selenite Induced Cataract Rat Model. *Biochem. Biophys. Res. Commun.* **2020**, *529*, 425–431, doi:10.1016/j.bbrc.2020.06.021.
52. Liu, Y.; Sha, T.-T.; Sun, G.-L.; Liang, S.-Z.; Yu, F.-F. Endoplasmic Reticulum Stress Involved in Age-Related Nuclear Cataract Induced by Sodium Selenite. *Sci. Rep.* **2025**, *15*, 22227, doi:10.1038/s41598-025-07745-5.
53. Clark, J.I.; Steele, J.E. Phase-Separation Inhibitors and Prevention of Selenite Cataract. *Proc. Natl. Acad. Sci. U. S. A.* **1992**, *89*, 1720–1724, doi:10.1073/pnas.89.5.1720.
54. Shearer, T.R.; David, L.L.; Anderson, R.S. Selenite Decreases Phase Separation Temperature in Rat Lens. *Exp. Eye Res.* **1986**, *42*, 503–506, doi:10.1016/0014-4835(86)90010-2.
55. Mitton, K.P.; Hess, J.L.; Bunce, G.E. Causes of Decreased Phase Transition Temperature in Selenite Cataract Model. *Invest. Ophthalmol. Vis. Sci.* **1995**, *36*, 914–924.
56. Bloemendal, H.; de Jong, W.; Jaenicke, R.; Lubsen, N.H.; Slingsby, C.; Tardieu, A. Ageing and Vision: Structure, Stability and Function of Lens Crystallins. *Prog. Biophys. Mol. Biol.* **2004**, *86*, 407–485, doi:10.1016/j.pbiomolbio.2003.11.012.
57. Wang, X.; Garcia, C.M.; Shui, Y.-B.; Beebe, D.C. Expression and Regulation of Alpha-, Beta-, and Gamma-Crystallins in Mammalian Lens Epithelial Cells. *Invest. Ophthalmol. Vis. Sci.* **2004**, *45*, 3608–3619, doi:10.1167/iovs.04-0423.
58. Voorter, C.E.; De Haard-Hoekman, W.A.; Hermans, M.M.; Bloemendal, H.; De Jong, W.W. Differential Synthesis of Crystallins in the Developing Rat Eye Lens. *Exp. Eye Res.* **1990**, *50*, 429–437, doi:10.1016/0014-4835(90)90144-j.
59. Slingsby, C.; Wistow, G.J. Functions of Crystallins in and out of Lens: Roles in Elongated and Post-Mitotic Cells. *Prog. Biophys. Mol. Biol.* **2014**, *115*, 52–67, doi:10.1016/j.pbiomolbio.2014.02.006.

 doi:10.20944/preprints202510.0392.v1




60. Annunziata, O.; Ogun, O.; Benedek, G.B. Observation of Liquid-Liquid Phase Separation for Eye Lens gammaS-Crystallin. *Proc. Natl. Acad. Sci. U. S. A.* **2003**, *100*, 970–974, doi:10.1073/pnas.242746499.
61. Liu, C.; Asherie, N.; Lomakin, A.; Pande, J.; Ogun, O.; Benedek, G.B. Phase Separation in Aqueous Solutions of Lens Gamma-Crystallins: Special Role of Gamma S. *Proc. Natl. Acad. Sci. U. S. A.* **1996**, *93*, 377–382, doi:10.1073/pnas.93.1.377.
62. Clark, J.I.; Neuringer, J.R.; Benedek, G.B. Phase Separation and Lens Cell Age. *J. Gerontol.* **1983**, *38*, 287–292, doi:10.1093/geronj/38.3.287.
63. Pande, J.; Lomakin, A.; Fine, B.; Ogun, O.; Sokolinski, I.; Benedek, G. Oxidation of Gamma II-Crystallin Solutions Yields Dimers with a High Phase Separation Temperature. *Proc. Natl. Acad. Sci. U. S. A.* **1995**, *92*, 1067–1071, doi:10.1073/pnas.92.4.1067.
64. Komariah, C.; Nugraha, J.; Sujuti, H.; Others Mechanism of Sodium Selenite-Induced Cataract Through Autophagy in Wistar (Rattus Norvegicus) Rats. *Journal of Medicinal and Chemical Sciences* **2024**, *7*, 203–214, doi:10.26655/JMCHEMSCI.2024.1.19.
65. Lasmaini, O.; Hidayat, M.; Wati, R. The Effect of Topical Glutathione on Malondialdehyde Levels in Rat with Cataract-Induced Sodium Selenite. *BioSci. Med. J. Biomed. Transl. Res.* **2023**, *7*, 3356–3361, doi:10.37275/bsm.v7i6.829.
66. Fris, M.; Tessem, M.-B.; Saether, O.; Midelfart, A. Biochemical Changes in Selenite Cataract Model Measured by High-Resolution MAS H NMR Spectroscopy. *Acta Ophthalmol. Scand.* **2006**, *84*, 684–692, doi:10.1111/j.1600-0420.2006.00716.x.
67. Varma, S.D.; Hegde, K.R.; Kovtun, S. Inhibition of Selenite-Induced Cataract by Caffeine. *Acta Ophthalmol.* **2010**, *88*, e245–e249, doi:10.1111/j.1755-3768.2010.02014.x.
68. Serebryany, E.; Yu, S.; Trauger, S.A.; Budnik, B.; Shakhnovich, E.I. Dynamic Disulfide Exchange in a Crystallin Protein in the Human Eye Lens Promotes Cataract-Associated Aggregation. *J. Biol. Chem.* **2018**, *293*, 17997–18009, doi:10.1074/jbc.RA118.004551.
69. Halverson-Kolkind, K.; Thorn, D.C.; Tovar-Ramirez, M.; Shakhnovich, E.; David, L.; Lampi, K. The Eye Lens Protein, γS Crystallin, Undergoes Glutathionylation-Induced Disulfide Bonding between Cysteines 22 and 26. *Biomolecules* **2025**, *15*, 402, doi:10.3390/biom15030402.
70. Norton-Baker, B.; Mehrabi, P.; Kwok, A.O.; Roskamp, K.W.; Rocha, M.A.; Sprague-Piercy, M.A.; von Stetten, D.; Miller, R.J.D.; Martin, R.W. Deamidation of the Human Eye Lens Protein γS-Crystallin Accelerates Oxidative Aging. *Structure* **2022**, *30*, 763–776.e4, doi:10.1016/j.str.2022.03.002.
71. Park, S.; Barnes, R.; Lin, Y.; Jeon, B.-J.; Najafi, S.; Delaney, K.T.; Fredrickson, G.H.; Shea, J.-E.; Hwang, D.S.; Han, S. Dehydration Entropy Drives Liquid-Liquid Phase Separation by Molecular Crowding. *Communications Chemistry* **2020**, *3*, 83, doi:10.1038/s42004-020-0328-8.
72. Kaur, T.; Alshareedah, I.; Wang, W.; Ngo, J.; Moosa, M.M.; Banerjee, P.R. Molecular Crowding Tunes Material States of Ribonucleoprotein Condensates. *Biomolecules* **2019**, *9*, 71, doi:10.3390/biom9020071.
73. Li, J.; Hou, C.; Ma, X.; Guo, S.; Zhang, H.; Shi, L.; Liao, C.; Zheng, B.; Ye, L.; Yang, L.; et al. Entropy-Enthalpy Compensations Fold Proteins in Precise Ways. *Int. J. Mol. Sci.* **2021**, *22*, 9653, doi:10.3390/ijms22179653.
74. Kim, H.; Jeon, B.-J.; Kim, S.; Jho, Y.; Hwang, D.S. Upper Critical Solution Temperature (UCST) Behavior of Coacervate of Cationic Protamine and Multivalent Anions. *Polymers (Basel)* **2019**, *11*, 691, doi:10.3390/polym11040691.
75. Biswas, S.; Hecht, A.L.; Noble, S.A.; Huang, Q.; Gillilan, R.E.; Xu, A.Y. Understanding the Impacts of Molecular and Macromolecular Crowding Agents on Protein-Polymer Complex Coacervates. *Biomacromolecules* **2023**, *24*, 4771–4782, doi:10.1021/acs.biomac.3c00545.
76. Zhao, L.; Chen, X.-J.; Zhu, J.; Xi, Y.-B.; Yang, X.; Hu, L.-D.; Ouyang, H.; Patel, S.H.; Jin, X.; Lin, D.; et al. Lanosterol Reverses Protein Aggregation in Cataracts. *Nature* **2015**, *523*, 607–611, doi:10.1038/nature14650.
77. Yang, T.; Lin, X.; Li, H.; Zhou, X.; Fan, F.; Yang, J.; Luo, Y.; Liu, X. Acetyl-11-Keto-Beta Boswellic Acid (AKBA) Protects Lens Epithelial Cells against H2O2-Induced Oxidative Injury and Attenuates Cataract Progression by Activating Keap1/Nrf2/HO-1 Signaling. *Front. Pharmacol.* **2022**, *13*, 927871, doi:10.3389/fphar.2022.927871.
78. Maddirala, Y.; Tobwala, S.; Karacal, H.; Ercal, N. Prevention and Reversal of Selenite-Induced Cataracts by N-Acetylcysteine Amide in Wistar Rats. *BMC Ophthalmol.* **2017**, *17*, 54, doi:10.1186/s12886-017-0443-1.

 doi:10.20944/preprints202510.0392.v1




79. Turgut, B.; Ergen, İ.; İlhan, N. The Protective Effect of Sesamol in the Selenite-Induced Experimental Cataract Model. *Turkish Journal of Ophthalmology* **2017**, *47*, 309–314, doi:10.4274/tjo.42385.
80. Ishida, H.; Sasaki, Y.; Shibata, T.; Sasaki, H.; Chhunchha, B.; Singh, D.P.; Kubo, E. Topical Instillation of N-Acetylcysteine and N-Acetylcysteine Amide Impedes Age-Related Lens Opacity in Mice. *Biomolecules* **2025**, *15*, 442, doi:10.3390/biom15030442.
81. Serebryany, E.; Chowdhury, S.; Woods, C.N.; Thorn, D.C.; Watson, N.E.; McClelland, A.A.; Klevit, R.E.; Shakhnovich, E.I. A Native Chemical Chaperone in the Human Eye Lens. *Elife* **2022**, *11*, doi:10.7554/eLife.76923.
82. Goulet, D.R.; Knee, K.M.; King, J.A. Inhibition of Unfolding and Aggregation of Lens Protein Human Gamma D Crystallin by Sodium Citrate. *Exp. Eye Res.* **2011**, *93*, 371–381, doi:10.1016/j.exer.2011.04.011.
83. Hsueh, S.-S.; Lu, J.-H.; Wu, J.W.; Lin, T.-H.; Wang, S.S.-S. Protection of Human γD-Crystallin Protein from Ultraviolet C-Induced Aggregation by Ortho-Vanillin. *Spectrochim. Acta A Mol. Biomol. Spectrosc.* **2021**, *261*, 120023, doi:10.1016/j.saa.2021.120023.
84. Abe, M.; Reiter, R.J.; Orhii, P.B.; Hara, M.; Poeggeler, B. Inhibitory Effect of Melatonin on Cataract Formation in Newborn Rats: Evidence for an Antioxidative Role for Melatonin. *J. Pineal Res.* **1994**, *17*, 94–100, doi:10.1111/j.1600-079x.1994.tb00119.x.
85. Li, Z.R.; Reiter, R.J.; Fujimori, O.; Oh, C.S.; Duan, Y.P. Cataractogenesis and Lipid Peroxidation in Newborn Rats Treated with Buthionine Sulfoximine: Preventive Actions of Melatonin. *J. Pineal Res.* **1997**, *22*, 117–123, doi:10.1111/j.1600-079x.1997.tb00312.x.
86. Karslioglu, I.; Ertekin, M.V.; Taysi, S.; Koçer, I.; Sezen, O.; Gepdiremen, A.; Koç, M.; Bakan, N. Radioprotective Effects of Melatonin on Radiation-Induced Cataract. *J. Radiat. Res.* **2005**, *46*, 277–282, doi:10.1269/jrr.46.277.
87. Yağci, R.; Aydin, B.; Erdurmuş, M.; Karadağ, R.; Gürel, A.; Durmuş, M.; Yiğitoğlu, R. Use of Melatonin to Prevent Selenite-Induced Cataract Formation in Rat Eyes. *Curr. Eye Res.* **2006**, *31*, 845–850, doi:10.1080/02713680600899663.
88. Khorsand, M.; Akmali, M.; Sharzad, S.; Beheshtitabar, M. Melatonin Reduces Cataract Formation and Aldose Reductase Activity in Lenses of Streptozotocin-Induced Diabetic Rat. *Iran. J. Med. Sci.* **2016**, *41*, 305–313, doi:10.1385/ENDO:27:2:101.
89. Mi, Y.; Wei, C.; Sun, L.; Liu, H.; Zhang, J.; Luo, J.; Yu, X.; He, J.; Ge, H.; Liu, P. Melatonin Inhibits Ferroptosis and Delays Age-Related Cataract by Regulating SIRT6/p-Nrf2/GPX4 and SIRT6/NCOA4/FTH1 Pathways. *Biomed. Pharmacother.* **2023**, *157*, 114048, doi:10.1016/j.biopha.2022.114048.
90. Nourazaran, M.; Yousefi, R.; Moosavi-Movahedi, F.; Panahi, F.; Hong, J.; Moosavi-Movahedi, A.A. The Structural and Functional Consequences of Melatonin and Serotonin on Human αB-Crystallin and Their Dual Role in the Eye Lens Transparency. *Biochim. Biophys. Acta: Proteins Proteomics* **2023**, *1871*, 140928, doi:10.1016/j.bbapap.2023.140928.
91. Xie, X.; Ding, D.; Bai, D.; Zhu, Y.; Sun, W.; Sun, Y.; Zhang, D. Melatonin Biosynthesis Pathways in Nature and Its Production in Engineered Microorganisms. *Synth Syst Biotechnol* **2022**, *7*, 544–553, doi:10.1016/j.synbio.2021.12.011.
92. Lee, K.; Choi, G.-H.; Back, K. Functional Characterization of Serotonin N-Acetyltransferase in Archaeon Thermoplasma Volcanium. *Antioxidants (Basel)* **2022**, *11*, doi:10.3390/antiox11030596.
93. Hardeland, R.; Cardinali, D.P.; Srinivasan, V.; Spence, D.W.; Brown, G.M.; Pandi-Perumal, S.R. Melatonin—A Pleiotropic, Orchestrating Regulator Molecule. *Prog. Neurobiol.* **2011**, *93*, 350–384, doi:10.1016/j.pneurobio.2010.12.004.
94. Pino-Rios, R.; Solà, M. The Relative Stability of Indole Isomers Is a Consequence of the Glidewell-Lloyd Rule. *J. Phys. Chem. A* **2021**, *125*, 230–234, doi:10.1021/acs.jpca.0c09549.
95. Sravanthi, T.V.; Manju, S.L. Indoles—A Promising Scaffold for Drug Development. *Eur. J. Pharm. Sci.* **2016**, *91*, 1–10, doi:10.1016/j.ejps.2016.05.025.
96. Debnath, B.; Nandi, B.; Paul, S.; Manna, S.; Maity, A.; Bandyopadhyay, K.; Panda, S.; Khan, S.A.; Nath, R.; Akhtar, M.J. Novel Indole-Based Synthetic Molecules in Cancer Treatment: Synthetic Strategies and Structure-Activity Relationship. *Med. Drug Discov.* **2025**, *27*, 100208, doi:10.1016/j.medidd.2025.100208.

 doi:10.20944/preprints202510.0392.v1




97. Zeng, W.; Han, C.; Mohammed, S.; Li, S.; Song, Y.; Sun, F.; Du, Y. Indole-Containing Pharmaceuticals: Targets, Pharmacological Activities, and SAR Studies. *RSC Med. Chem.* **2024**, *15*, 788–808, doi:10.1039/d3md00677h.
98. Reiter, R.J.; Mayo, J.C.; Tan, D.-X.; Sainz, R.M.; Alatorre-Jimenez, M.; Qin, L. Melatonin as an Antioxidant: Under Promises but over Delivers. *J. Pineal Res.* **2016**, *61*, 253–278, doi:10.1111/jpi.12360.
99. Korkmaz, A.; Reiter, R.J.; Topal, T.; Manchester, L.C.; Oter, S.; Tan, D.-X. Melatonin: An Established Antioxidant Worthy of Use in Clinical Trials. *Mol. Med.* **2009**, *15*, 43–50, doi:10.2119/molmed.2008.00117.
100. Manda, K.; Ohkubo, K.; Shoji, Y.; Zoardar, A.K.M.R.K.; Kamibayashi, M.; Ozawa, T.; Anzai, K.; Nakanishi, I. In Vitro Radical-Scavenging Mechanism of Melatonin and Its in Vivo Protective Effect against Radiation-Induced Lipid Peroxidation. *Redox Biochem. Chem.* **2023**, *3-4*, 100003, doi:10.1016/j.rbc.2023.100003.
101. Tan, D.-X.; Reiter, R.J.; Manchester, L.C.; Yan, M.-T.; El-Sawi, M.; Sainz, R.M.; Mayo, J.C.; Kohen, R.; Allegra, M.; Hardeland, R. Chemical and Physical Properties and Potential Mechanisms: Melatonin as a Broad Spectrum Antioxidant and Free Radical Scavenger. *Curr. Top. Med. Chem.* **2002**, *2*, 181–197, doi:10.2174/1568026023394443.
102. National Center for Biotechnology Information (2023) PubChem Compound Summary for CID 896, Melatonin Available online: https://pubchem.ncbi.nlm.nih.gov/compound/Melatonin (accessed on 7 January 2023).
103. Tan, D.-X.; Manchester, L.C.; Esteban-Zubero, E.; Zhou, Z.; Reiter, R.J. Melatonin as a Potent and Inducible Endogenous Antioxidant: Synthesis and Metabolism. *Molecules* **2015**, *20*, 18886–18906, doi:10.3390/molecules201018886.
104. de Sá Alves, F.R.; Barreiro, E.J.; Fraga, C.A.M. From Nature to Drug Discovery: The Indole Scaffold as a "Privileged Structure." *Mini Rev. Med. Chem.* **2009**, *9*, 782–793, doi:10.2174/138955709788452649.
105. Van Lommel, R.; Bettens, T.; Barlow, T.M.A.; Bertouille, J.; Ballet, S.; De Proft, F. A Quantum Chemical Deep-Dive into the π-π Interactions of 3-Methylindole and Its Halogenated Derivatives-towards an Improved Ligand Design and Tryptophan Stacking. *Pharmaceuticals (Basel)* **2022**, *15*, 935, doi:10.3390/ph15080935.
106. Watanabe, K.; Hattori, A. Aging-Induced Memory Loss due to Decreased N1-Acetyl-5-Methoxykynuramine, a Melatonin Metabolite, in the Hippocampus: A Potential Prophylactic Agent for Dementia. *Neural Regeneration Res.* 10.4103/NRR.NRR, doi:10.4103/NRR.NRR-D-24-00379.
107. Slominski, A.T.; Kim, T.-K.; Janjetovic, Z.; Slominski, R.M.; Ganguli-Indra, G.; Athar, M.; Indra, A.K.; Reiter, R.J.; Kleszczyński, K. Melatonin and the Skin: Current Progress and Perspectives for Human Health. *J. Invest. Dermatol.* **2025**, doi:10.1016/j.jid.2024.11.012.
108. Bocheva, G.; Bakalov, D.; Iliev, P.; Tafradjiiska-Hadjiolova, R. The Vital Role of Melatonin and Its Metabolites in the Neuroprotection and Retardation of Brain Aging. *Int. J. Mol. Sci.* **2024**, *25*, doi:10.3390/ijms25105122.
109. Zhao, Y.; Wang, Q.; Gu, D.; Huang, F.; Liu, J.; Yu, L.; Yu, X. Melatonin, a Phytohormone for Enhancing the Accumulation of High-Value Metabolites and Stress Tolerance in Microalgae: Applications, Mechanisms, and Challenges. *Bioresour. Technol.* **2024**, *393*, 130093, doi:10.1016/j.biortech.2023.130093.
110. Galano, A.; Reiter, R.J. Melatonin and Its Metabolites vs Oxidative Stress: From Individual Actions to Collective Protection. *J. Pineal Res.* **2018**, *65*, e12514, doi:10.1111/jpi.12514.
111. Tan, D.-X.; Manchester, L.C.; Terron, M.P.; Flores, L.J.; Reiter, R.J. One Molecule, Many Derivatives: A Never-Ending Interaction of Melatonin with Reactive Oxygen and Nitrogen Species? *J. Pineal Res.* **2007**, *42*, 28–42, doi:10.1111/j.1600-079X.2006.00407.x.
112. Hardeland, R.; Pandi-Perumal, S.R. Melatonin, a Potent Agent in Antioxidative Defense: Actions as a Natural Food Constituent, Gastrointestinal Factor, Drug and Prodrug. *Nutr. Metab. (Lond.)* **2005**, *2*, 22, doi:10.1186/1743-7075-2-22.
113. Tan, D.X.; Manchester, L.C.; Burkhardt, S.; Sainz, R.M.; Mayo, J.C.; Kohen, R.; Shohami, E.; Huo, Y.S.; Hardeland, R.; Reiter, R.J. N1-Acetyl-N2-Formyl-5-Methoxykynuramine, a Biogenic Amine and Melatonin Metabolite, Functions as a Potent Antioxidant. *FASEB J.* **2001**, *15*, 2294–2296, doi:10.1096/fj.01-0309fje.

 doi:10.20944/preprints202510.0392.v1




114. Hardeland, R.; Poeggeler, B.; Niebergall, R.; Zelosko, V. Oxidation of Melatonin by Carbonate Radicals and Chemiluminescence Emitted during Pyrrole Ring Cleavage: Carbonate Radicals and Melatonin. *J. Pineal Res.* **2003**, *34*, 17–25, doi:10.1034/j.1600-079x.2003.02941.x.
115. Galano, A.; Tan, D.X.; Reiter, R.J. On the Free Radical Scavenging Activities of Melatonin's Metabolites, AFMK and AMK. *J. Pineal Res.* **2013**, *54*, 245–257, doi:10.1111/jpi.12010.
116. Hardeland, R. Melatonin, Its Metabolites and Their Interference with Reactive Nitrogen Compounds. *Molecules* **2021**, *26*, doi:10.3390/molecules26134105.
117. Ma, X.; Idle, J.R.; Krausz, K.W.; Tan, D.-X.; Ceraulo, L.; Gonzalez, F.J. Urinary Metabolites and Antioxidant Products of Exogenous Melatonin in the Mouse. *J. Pineal Res.* **2006**, *40*, 343–349, doi:10.1111/j.1600-079X.2006.00321.x.
118. Ma, X.; Chen, C.; Krausz, K.W.; Idle, J.R.; Gonzalez, F.J. A Metabolomic Perspective of Melatonin Metabolism in the Mouse. *Endocrinology* **2008**, *149*, 1869–1879, doi:10.1210/en.2007-1412.
119. Böhm, E.W.; Buonfiglio, F.; Voigt, A.M.; Bachmann, P.; Safi, T.; Pfeiffer, N.; Gericke, A. Oxidative Stress in the Eye and Its Role in the Pathophysiology of Ocular Diseases. *Redox Biol.* **2023**, *68*, 102967, doi:10.1016/j.redox.2023.102967.
120. Rozov, S.V.; Filatova, E.V.; Orlov, A.A.; Volkova, A.V.; Zhloba, A.R.A.; Blashko, E.L.; Pozdeyev, N.V. N1-Acetyl-N2-Formyl-5-Methoxykynuramine Is a Product of Melatonin Oxidation in Rats. *J. Pineal Res.* **2003**, *35*, 245–250, doi:10.1034/j.1600-079x.2003.00081.x.
121. Bai, J.; Dong, L.; Song, Z.; Ge, H.; Cai, X.; Wang, G.; Liu, P. The Role of Melatonin as an Antioxidant in Human Lens Epithelial Cells. *Free Radic. Res.* **2013**, *47*, 635–642, doi:10.3109/10715762.2013.808743.
122. Li, C.; Li, Z.; Wu, Z.; Lu, H. Phase Separation in Gene Transcription Control. *Acta Biochim. Biophys. Sin.* **2023**, *55*, 1052–1063, doi:10.3724/abbs.2023099.
123. Ding, K.; Wang, H.; Xu, J.; Li, T.; Zhang, L.; Ding, Y.; Zhu, L.; He, J.; Zhou, M. Melatonin Stimulates Antioxidant Enzymes and Reduces Oxidative Stress in Experimental Traumatic Brain Injury: The Nrf2-ARE Signaling Pathway as a Potential Mechanism. *Free Radic. Biol. Med.* **2014**, *73*, 1–11, doi:10.1016/j.freeradbiomed.2014.04.031.
124. Fischer, T.W.; Kleszczyński, K.; Hardkop, L.H.; Kruse, N.; Zillikens, D. Melatonin Enhances Antioxidative Enzyme Gene Expression (CAT, GPx, SOD), Prevents Their UVR-Induced Depletion, and Protects against the Formation of DNA Damage (8-Hydroxy-2′-Deoxyguanosine) in Ex Vivo Human Skin. *J. Pineal Res.* **2013**, *54*, 303–312, doi:10.1111/jpi.12018.
125. Rodriguez, C.; Mayo, J.C.; Sainz, R.M.; Antolín, I.; Herrera, F.; Martín, V.; Reiter, R.J. Regulation of Antioxidant Enzymes: A Significant Role for Melatonin. *J. Pineal Res.* **2004**, *36*, 1–9, doi:10.1046/j.1600-079x.2003.00092.x.
126. Mayo, J.C.; Sainz, R.M.; Antoli, I.; Herrera, F.; Martin, V.; Rodriguez, C. Melatonin Regulation of Antioxidant Enzyme Gene Expression. *Cell. Mol. Life Sci.* **2002**, *59*, 1706–1713, doi:10.1007/pl00012498.
127. Urata, Y.; Honma, S.; Goto, S.; Todoroki, S.; Iida, T.; Cho, S.; Honma, K.; Kondo, T. Melatonin Induces γ-Glutamylcysteine Synthetase Mediated by Activator Protein-1 in Human Vascular Endothelial Cells. *Free Radical Biology and Medicine* **1999**, *27*, 838–847, doi:10.1016/S0891-5849(99)00131-8.
128. Kotler, M.; Rodríguez, C.; Sáinz, R.M.; Antolín, I.; Menéndez-Peláez, A. Melatonin Increases Gene Expression for Antioxidant Enzymes in Rat Brain Cortex. *J. Pineal Res.* **1998**, *24*, 83–89, doi:10.1111/j.1600-079x.1998.tb00371.x.
129. Oloumi, H.; Maleki, M. Melatonin Modulates the Phytochelatin Synthase and Glutathione Synthase Gene Expression and the Antioxidant Performance of Soybean Plants Under Cadmium Stress. *International Journal of Agronomy* **2025**, *2025*, doi:10.1155/ioa/4586748.
130. Tan, D.-X.; Hardeland, R.; Manchester, L.C.; Galano, A.; Reiter, R.J. Cyclic-3-Hydroxymelatonin (C3HOM), a Potent Antioxidant, Scavenges Free Radicals and Suppresses Oxidative Reactions. *Curr. Med. Chem.* **2014**, *21*, 1557–1565, doi:10.2174/0929867321666131129113146.
131. Ressmeyer, A.-R.; Mayo, J.C.; Zelosko, V.; Sáinz, R.M.; Tan, D.-X.; Poeggeler, B.; Antolín, I.; Zsizsik, B.K.; Reiter, R.J.; Hardeland, R. Antioxidant Properties of the Melatonin Metabolite N1-Acetyl-5-Methoxykynuramine (AMK): Scavenging of Free Radicals and Prevention of Protein Destruction. *Redox Rep.* **2003**, *8*, 205–213, doi:10.1179/135100003225002709.

 doi:10.20944/preprints202510.0392.v1




132. Purushothaman, A.; Sheeja, A.A.; Janardanan, D. Hydroxyl Radical Scavenging Activity of Melatonin and Its Related Indolamines. *Free Radic. Res.* **2020**, *54*, 373–383, doi:10.1080/10715762.2020.1774575.
133. Reiter, R.J.; Tan, D.-X.; Terron, M.P.; Flores, L.J.; Czarnocki, Z. Melatonin and Its Metabolites: New Findings Regarding Their Production and Their Radical Scavenging Actions. *Acta Biochim. Pol.* **2007**, *54*, 1–9.
134. Ma, J.; Han, Y.; Yang, H.; Liu, L.; Wei, Z.; Wang, F.; Wan, Y. Melatonin Protects Leydig Cells from HT-2 Toxin-Induced Ferroptosis and Apoptosis via Glucose-6-Phosphate Dehydrogenase/glutathione - Dependent Pathway. *Int. J. Biochem. Cell Biol.* **2023**, *159*, 106410, doi:10.1016/j.biocel.2023.106410.
135. Kushnir, O.Y.; Yaremii, I.M.; Pantsiuk, K.A.; Kushnir, O.O.; Yaremii, K.M.; Vlasova, K.V.; Vlasova, O.V. Carbohydrate Metabolism in the Rats' Liver under Conditions of Light and Dark Deprivation and Correction by Melatonin. *Wiad. Lek.* **2025**, *78*, 1361–1366, doi:10.36740/wlek/205592.
136. Hu, L.; Zhang, S.; Wen, H.; Liu, T.; Cai, J.; Du, D.; Zhu, D.; Chen, F.; Xia, C. Melatonin Decreases M1 Polarization via Attenuating Mitochondrial Oxidative Damage Depending on UCP2 Pathway in Prorenin-Treated Microglia. *PLoS One* **2019**, *14*, e0212138, doi:10.1371/journal.pone.0212138.
137. Garcia, A.; Eljack, N.D.; Sani, M.-A.; Separovic, F.; Rasmussen, H.H.; Kopec, W.; Khandelia, H.; Cornelius, F.; Clarke, R.J. Membrane Accessibility of Glutathione. *Biochim. Biophys. Acta* **2015**, *1848*, 2430–2436, doi:10.1016/j.bbamem.2015.07.016.
138. Reiter, R.J.; Sharma, R.; Tan, D.-X.; Chuffa, L.G. de A.; da Silva, D.G.H.; Slominski, A.T.; Steinbrink, K.; Kleszczynski, K. Dual Sources of Melatonin and Evidence for Different Primary Functions. *Front. Endocrinol.* **2024**, *15*, doi:10.3389/fendo.2024.1414463.
139. Alkozi, H.A.; Wang, X.; Perez de Lara, M.J.; Pintor, J. Presence of Melanopsin in Human Crystalline Lens Epithelial Cells and Its Role in Melatonin Synthesis. *Exp. Eye Res.* **2017**, *154*, 168–176, doi:10.1016/j.exer.2016.11.019.
140. Itoh, M.T.; Takahashi, N.; Abe, M.; Shimizu, K. Expression and Cellular Localization of Melatonin-Synthesizing Enzymes in the Rat Lens. *J. Pineal Res.* **2007**, *42*, 92–96, doi:10.1111/j.1600-079X.2006.00389.x.
141. Abe, M.; Itoh, M.T.; Miyata, M.; Ishikawa, S.; Sumi, Y. Detection of Melatonin, Its Precursors and Related Enzyme Activities in Rabbit Lens. *Exp. Eye Res.* **1999**, *68*, 255–262, doi:10.1006/exer.1998.0601.
142. Felder-Schmittbuhl, M.P.; Hicks, D.; Ribelayaga, C.P.; Tosini, G. Melatonin in the Mammalian Retina: Synthesis, Mechanisms of Action and Neuroprotection. *J. Pineal Res.* **2024**, *76*, e12951, doi:10.1111/jpi.12951.
143. Zmijewski, M.A.; Sweatman, T.W.; Slominski, A.T. The Melatonin-Producing System Is Fully Functional in Retinal Pigment Epithelium (ARPE-19). *Mol. Cell. Endocrinol.* **2009**, *307*, 211–216, doi:10.1016/j.mce.2009.04.010.
144. Yu, H.; Dickson, E.J.; Jung, S.-R.; Koh, D.-S.; Hille, B. High Membrane Permeability for Melatonin. *J. Gen. Physiol.* **2016**, *147*, 63–76, doi:10.1085/jgp.201511526.
145. Costa, E.J.; Lopes, R.H.; Lamy-Freund, M.T. Permeability of Pure Lipid Bilayers to Melatonin. *J. Pineal Res.* **1995**, *19*, 123–126, doi:10.1111/j.1600-079x.1995.tb00180.x.
146. Rehan, M.; Alsohim, A.S.; El-Fadly, G.; Tisa, L.S. Detoxification and Reduction of Selenite to Elemental Red Selenium by Frankia. *Antonie Van Leeuwenhoek* **2019**, *112*, 127–139, doi:10.1007/s10482-018-1196-4.
147. Kieliszek, M.; Serrano Sandoval, S.N. The Importance of Selenium in Food Enrichment Processes. A Comprehensive Review. *J. Trace Elem. Med. Biol.* **2023**, *79*, 127260, doi:10.1016/j.jtemb.2023.127260.
148. Wang, Z.; Hou, X.; Guo, Z.; Lei, X.; Peng, M. Biodegradation of Sodium Selenite by a Highly Tolerant Strain Rhodococcus Qingshengii PM1: Biochemical Characterization and Comparative Genome Analysis. *Curr. Res. Microb. Sci.* **2025**, *9*, 100426, doi:10.1016/j.crmicr.2025.100426.
149. Sies, H.; Jones, D.P. Reactive Oxygen Species (ROS) as Pleiotropic Physiological Signalling Agents. *Nat. Rev. Mol. Cell Biol.* **2020**, *21*, 363–383, doi:10.1038/s41580-020-0230-3.
150. Brieger, K.; Schiavone, S.; Miller, F.J., Jr; Krause, K.-H. Reactive Oxygen Species: From Health to Disease. *Swiss Med. Wkly* **2012**, *142*, w13659, doi:10.4414/smw.2012.13659.
151. Lu, J.; Berndt, C.; Holmgren, A. Metabolism of Selenium Compounds Catalyzed by the Mammalian Selenoprotein Thioredoxin Reductase. *Biochim. Biophys. Acta* **2009**, *1790*, 1513–1519, doi:10.1016/j.bbagen.2009.04.013.

 doi:10.20944/preprints202510.0392.v1




152. Wajner, S.M.; Rohenkohl, H.C.; Serrano, T.; Maia, A.L. Sodium Selenite Supplementation Does Not Fully Restore Oxidative Stress-Induced Deiodinase Dysfunction: Implications for the Nonthyroidal Illness Syndrome. *Redox Biol.* **2015**, *6*, 436–445, doi:10.1016/j.redox.2015.09.002.
153. Misra, S.; Boylan, M.; Selvam, A.; Spallholz, J.E.; Björnstedt, M. Redox-Active Selenium Compounds--from Toxicity and Cell Death to Cancer Treatment. *Nutrients* **2015**, *7*, 3536–3556, doi:10.3390/nu7053536.
154. Guan, L.; Han, B.; Li, Z.; Hua, F.; Huang, F.; Wei, W.; Yang, Y.; Xu, C. Sodium Selenite Induces Apoptosis by ROS-Mediated Endoplasmic Reticulum Stress and Mitochondrial Dysfunction in Human Acute Promyelocytic Leukemia NB4 Cells. *Apoptosis* **2009**, *14*, 218–225, doi:10.1007/s10495-008-0295-5.
155. Selvaraj, V.; Tomblin, J.; Yeager Armistead, M.; Murray, E. Selenium (sodium Selenite) Causes Cytotoxicity and Apoptotic Mediated Cell Death in PLHC-1 Fish Cell Line through DNA and Mitochondrial Membrane Potential Damage. *Ecotoxicol. Environ. Saf.* **2013**, *87*, 80–88, doi:10.1016/j.ecoenv.2012.09.028.
156. Palsamy, P.; Bidasee, K.R.; Shinohara, T. Selenite Cataracts: Activation of Endoplasmic Reticulum Stress and Loss of Nrf2/Keap1-Dependent Stress Protection. *Biochim. Biophys. Acta* **2014**, *1842*, 1794–1805, doi:10.1016/j.bbadis.2014.06.028.
157. Mitton, K.P.; Hess, J.L.; Bunce, G.E. Free Amino Acids Reflect Impact of Selenite-Dependent Stress on Primary Metabolism in Rat Lens. *Curr. Eye Res.* **1997**, *16*, 997–1005, doi:10.1076/ceyr.16.10.997.9016.
158. Algieri, C.; Oppedisano, F.; Trombetti, F.; Fabbri, M.; Palma, E.; Nesci, S. Selenite Ameliorates the ATP Hydrolysis of Mitochondrial F1FO-ATPase by Changing the Redox State of Thiol Groups and Impairs the ADP Phosphorylation. *Free Radic. Biol. Med.* **2024**, *210*, 333–343, doi:10.1016/j.freeradbiomed.2023.11.041.
159. Poole, L.B. The Basics of Thiols and Cysteines in Redox Biology and Chemistry. *Free Radic. Biol. Med.* **2015**, *80*, 148–157, doi:10.1016/j.freeradbiomed.2014.11.013.
160. Averill-Bates, D.A. The Antioxidant Glutathione. *Vitam. Horm.* **2023**, *121*, 109–141, doi:10.1016/bs.vh.2022.09.002.
161. Pastore, A.; Federici, G.; Bertini, E.; Piemonte, F. Analysis of Glutathione: Implication in Redox and Detoxification. *Clin. Chim. Acta* **2003**, *333*, 19–39, doi:10.1016/s0009-8981(03)00200-6.
162. Millis, K.K.; Weaver, K.H.; Rabenstein, D.L. Oxidation/reduction Potential of Glutathione. *J. Org. Chem.* **1993**, *58*, 4144–4146, doi:10.1021/jo00067a060.
163. Meyer, A.J.; Hell, R. Glutathione Homeostasis and Redox-Regulation by Sulfhydryl Groups. *Photosynth. Res.* **2005**, *86*, 435–457, doi:10.1007/s11120-005-8425-1.
164. Aoyama, K.; Nakaki, T. Glutathione in Cellular Redox Homeostasis: Association with the Excitatory Amino Acid Carrier 1 (EAAC1). *Molecules* **2015**, *20*, 8742–8758, doi:10.3390/molecules20058742.
165. Filomeni, G.; Rotilio, G.; Ciriolo, M.R. Cell Signalling and the Glutathione Redox System. *Biochem. Pharmacol.* **2002**, *64*, 1057–1064, doi:10.1016/s0006-2952(02)01176-0.
166. Aquilano, K.; Baldelli, S.; Ciriolo, M.R. Glutathione: New Roles in Redox Signaling for an Old Antioxidant. *Front. Pharmacol.* **2014**, *5*, 196, doi:10.3389/fphar.2014.00196.
167. Taylor, E.R.; Hurrell, F.; Shannon, R.J.; Lin, T.-K.; Hirst, J.; Murphy, M.P. Reversible Glutathionylation of Complex I Increases Mitochondrial Superoxide Formation. *J. Biol. Chem.* **2003**, *278*, 19603–19610, doi:10.1074/jbc.M209359200.
168. Beer, S.M.; Taylor, E.R.; Brown, S.E.; Dahm, C.C.; Costa, N.J.; Runswick, M.J.; Murphy, M.P. Glutaredoxin 2 Catalyzes the Reversible Oxidation and Glutathionylation of Mitochondrial Membrane Thiol Proteins: Implications for Mitochondrial Redox Regulation and Antioxidant DEFENSE: Implications for Mitochondrial Redox Regulation and Antioxidant Defense. *J. Biol. Chem.* **2004**, *279*, 47939–47951, doi:10.1074/jbc.M408011200.
169. Passarelli, C.; Tozzi, G.; Pastore, A.; Bertini, E.; Piemonte, F. GSSG-Mediated Complex I Defect in Isolated Cardiac Mitochondria. *Int. J. Mol. Med.* **2010**, *26*, 95–99, doi:10.3892/ijmm_00000439.
170. Dereven'kov, I.A.; Molodtsov, P.A.; Makarov, S.V. Kinetic and Mechanistic Studies of the First Step of the Reaction between Thiols and Selenite. *React. Kinet. Mech. Catal.* **2020**, *131*, 555–566, doi:10.1007/s11144-020-01877-7.
171. Chen, H.; Tian, W.; Huang, K. Effect of Blood-Retinal Barrier Development on Formation of Selenite Nuclear Cataract in Rat. *Toxicol. Lett.* **2013**, *216*, 181–188, doi:10.1016/j.toxlet.2012.11.016.

 doi:10.20944/preprints202510.0392.v1




172. Kyselova, Z. Different Experimental Approaches in Modelling Cataractogenesis: An Overview of Selenite-Induced Nuclear Cataract in Rats. *Interdiscip. Toxicol.* **2010**, *3*, 3–14, doi:10.2478/v10102-010-0005-3.
173. Kulbay, M.; Wu, K.Y.; Nirwal, G.K.; Bélanger, P.; Tran, S.D. Oxidative Stress and Cataract Formation: Evaluating the Efficacy of Antioxidant Therapies. *Biomolecules* **2024**, *14*, 1055, doi:10.3390/biom14091055.
174. Garner, B.; Davies, M.J.; Truscott, R.J. Formation of Hydroxyl Radicals in the Human Lens Is Related to the Severity of Nuclear Cataract. *Exp. Eye Res.* **2000**, *70*, 81–88, doi:10.1006/exer.1999.0754.
175. Gennari, F.; Sharma, V.K.; Pettine, M.; Campanella, L.; Millero, F.J. Reduction of Selenite by Cysteine in Ionic Media. *Geochim. Cosmochim. Acta* **2014**, *124*, 98–108, doi:10.1016/j.gca.2013.09.019.
176. Lou, M.F.; Augusteyn, R.C. Oxidation-Induced Mixed Disulfide and Cataract Formation: A Review. *Antioxidants (Basel)* **2025**, *14*, 425, doi:10.3390/antiox14040425.
177. Wiedemann, C.; Kumar, A.; Lang, A.; Ohlenschläger, O. Cysteines and Disulfide Bonds as Structure-Forming Units: Insights from Different Domains of Life and the Potential for Characterization by NMR. *Front. Chem.* **2020**, *8*, 280, doi:10.3389/fchem.2020.00280.
178. Mondal, M.; Jankoski, P.E.; Lee, L.D.; Dinakarapandian, D.M.; Chiu, T.-Y.; Swetman, W.S.; Wu, H.; Paravastu, A.K.; Clemons, T.D.; Rangachari, V. Reversible Disulfide Bond Cross-Links as Tunable Levers of Phase Separation in Designer Biomolecular Condensates. *J. Am. Chem. Soc.* **2024**, *146*, 25299–25311, doi:10.1021/jacs.4c09557.
179. Wang, B.; Wang, Y.; Pan, T.; Zhou, L.; Ran, Y.; Zou, J.; Yan, X.; Wen, Z.; Lin, S.; Ren, A.; et al. Targeting a Key Disulfide Linkage to Regulate RIG-I Condensation and Cytosolic RNA-Sensing. *Nat. Cell Biol.* **2025**, *27*, 817–834, doi:10.1038/s41556-025-01646-5.
180. Manteca, A.; Alonso-Caballero, Á.; Fertin, M.; Poly, S.; De Sancho, D.; Perez-Jimenez, R. The Influence of Disulfide Bonds on the Mechanical Stability of Proteins Is Context Dependent. *J. Biol. Chem.* **2017**, *292*, 13374–13380, doi:10.1074/jbc.M117.784934.
181. Mandal, K.; Bose, S.K.; Chakrabarti, B.; Siezen, R.J. Structure and Stability of Gamma-Crystallins. II. Differences in Microenvironments and Spatial Arrangements of Cysteine Residues. *Biochim. Biophys. Acta* **1987**, *911*, 277–284, doi:10.1016/0167-4838(87)90068-9.
182. Anderson, R.S.; Trune, D.R.; Shearer, T.R. Histologic Changes in Selenite Cortical Cataract. *Invest. Ophthalmol. Vis. Sci.* **1988**, *29*, 1418–1427.
183. Pau, H.; Graf, P.; Sies, H. Glutathione Levels in Human Lens: Regional Distribution in Different Forms of Cataract. *Exp. Eye Res.* **1990**, *50*, 17–20, doi:10.1016/0014-4835(90)90005-f.
184. Kamei, A. Glutathione Levels of the Human Crystalline Lens in Aging and Its Antioxidant Effect against the Oxidation of Lens Proteins. *Biol. Pharm. Bull.* **1993**, *16*, 870–875, doi:10.1248/bpb.16.870.
185. Mackic, J.B.; Kannan, R.; Kaplowitz, N.; Zlokovic, B.V. Low de Novo Glutathione Synthesis from Circulating Sulfur Amino Acids in the Lens Epithelium. *Exp. Eye Res.* **1997**, *64*, 615–626, doi:10.1006/exer.1996.0260.
186. Lim, J.C.; Grey, A.C.; Zahraei, A.; Donaldson, P.J. Age-Dependent Changes in Glutathione Metabolism Pathways in the Lens: New Insights into Therapeutic Strategies to Prevent Cataract Formation-A Review. *Clin. Experiment. Ophthalmol.* **2020**, *48*, 1031–1042, doi:10.1111/ceo.13801.
187. Whitson, J.A.; Sell, D.R.; Goodman, M.C.; Monnier, V.M.; Fan, X. Evidence of Dual Mechanisms of Glutathione Uptake in the Rodent Lens: A Novel Role for Vitreous Humor in Lens Glutathione Homeostasis. *Invest. Ophthalmol. Vis. Sci.* **2016**, *57*, 3914–3925, doi:10.1167/iovs.16-19592.
188. Wang, G.; Quan, Y.; Ma, B.; Gu, S.; Jiang, J.X. Mechano-Activated Connexin Hemichannels Mediate Intercellular Glutathione Transport and Support Lens Redox Homeostasis. *Redox Biol.* **2025**, *85*, 103767, doi:10.1016/j.redox.2025.103767.
189. Fan, X.; Monnier, V.M.; Whitson, J. Lens Glutathione Homeostasis: Discrepancies and Gaps in Knowledge Standing in the Way of Novel Therapeutic Approaches. *Exp. Eye Res.* **2017**, *156*, 103–111, doi:10.1016/j.exer.2016.06.018.
190. Giblin, F.J. Glutathione: A Vital Lens Antioxidant. *J. Ocul. Pharmacol. Ther.* **2000**, *16*, 121–135, doi:10.1089/jop.2000.16.121.

 doi:10.20944/preprints202510.0392.v1




191. Li, B.; Suzuki-Kerr, H.; Lim, C.J.J.; Martis, R.M.; Yang, F.O.; Carlos, E.; Donaldson, P.J.; Poulsen, R.C.; Lim, J.C. Light Influences Time-of-Day Differences in the Expression of Clock Genes and Redox Genes Involved in Glutathione Homeostasis in the Lens. *Invest. Ophthalmol. Vis. Sci.* **2025**, *66*, 24, doi:10.1167/iovs.66.6.24.
192. Grey, A.C.; Demarais, N.J.; West, B.J.; Donaldson, P.J. A Quantitative Map of Glutathione in the Aging Human Lens. *Int. J. Mass Spectrom.* **2019**, *437*, 58–68, doi:10.1016/j.ijms.2017.10.008.
193. Ferrer, J.V.; Gascó, E.; Sastre, J.; Pallardó, F.V.; Asensi, M.; Viña, J. Age-Related Changes in Glutathione Synthesis in the Eye Lens. *Biochem. J.* **1990**, *269*, 531–534, doi:10.1042/bj2690531.
194. Slingsby, C.; Wistow, G.J.; Clark, A.R. Evolution of Crystallins for a Role in the Vertebrate Eye Lens. *Protein Sci.* **2013**, *22*, 367–380, doi:10.1002/pro.2229.
195. Horwitz, J.; Bova, M.P.; Ding, L.-L.; Haley, D.A.; Stewart, P.L. Lens α-Crystallin: Function and Structure. *Eye* **1999**, *13*, 403–408, doi:10.1038/eye.1999.114.
196. Horwitz, J. Alpha-Crystallin. *Exp. Eye Res.* **2003**, *76*, 145–153, doi:10.1016/s0014-4835(02)00278-6.
197. Raman, B.; Rao, C.M. Chaperone-like Activity and Temperature-Induced Structural Changes of α-Crystallin *. *J. Biol. Chem.* **1997**, *272*, 23559–23564, doi:10.1074/jbc.272.38.23559.
198. Raman, B.; Ramakrishna, T.; Rao, C.M. Temperature Dependent Chaperone-like Activity of Alpha-Crystallin. *FEBS Lett.* **1995**, *365*, 133–136, doi:10.1016/0014-5793(95)00440-k.
199. Xiao, F.; Chen, Z.; Wei, Z.; Tian, L. Hydrophobic Interaction: A Promising Driving Force for the Biomedical Applications of Nucleic Acids. *Adv. Sci. (Weinh.)* **2020**, *7*, 2001048, doi:10.1002/advs.202001048.
200. Reddy, G.B.; Kumar, P.A.; Kumar, M.S. Chaperone-like Activity and Hydrophobicity of Alpha-Crystallin. *IUBMB Life* **2006**, *58*, 632–641, doi:10.1080/15216540601010096.
201. Roy, D.; Spector, A. Absence of Low-Molecular-Weight Alpha Crystallin in Nuclear Region of Old Human Lenses. *Proc. Natl. Acad. Sci. U. S. A.* **1976**, *73*, 3484–3487, doi:10.1073/pnas.73.10.3484.
202. Lynnerup, N.; Kjeldsen, H.; Heegaard, S.; Jacobsen, C.; Heinemeier, J. Radiocarbon Dating of the Human Eye Lens Crystallines Reveal Proteins without Carbon Turnover throughout Life. *PLoS One* **2008**, *3*, e1529, doi:10.1371/journal.pone.0001529.
203. Hughes, J.R.; Levchenko, V.A.; Blanksby, S.J.; Mitchell, T.W.; Williams, A.; Truscott, R.J.W. No Turnover in Lens Lipids for the Entire Human Lifespan. *Elife* **2015**, *4*, doi:10.7554/eLife.06003.
204. Kappé, G.; Purkiss, A.G.; van Genesen, S.T.; Slingsby, C.; Lubsen, N.H. Explosive Expansion of Betagamma-Crystallin Genes in the Ancestral Vertebrate. *J. Mol. Evol.* **2010**, *71*, 219–230, doi:10.1007/s00239-010-9379-2.
205. Barnwal, R.P.; Jobby, M.K.; Devi, K.M.; Sharma, Y.; Chary, K.V.R. Solution Structure and Calcium-Binding Properties of M-Crystallin, a Primordial Betagamma-Crystallin from Archaea. *J. Mol. Biol.* **2009**, *386*, 675–689, doi:10.1016/j.jmb.2008.12.058.
206. Vendra, V.; Thangapandian, M. The Importance of the Fourth Greek Key Motif of Human γD-Crystallin in Maintaining Lens Transparency-the Tale Told by the Tail. *Mol. Vis.* **2024**, *30*, 37–48.
207. Hutchinson, E.G.; Thornton, J.M. The Greek Key Motif: Extraction, Classification and Analysis. *Protein Eng. Des. Sel.* **1993**, *6*, 233–245, doi:10.1093/protein/6.3.233.
208. Vendra, V.P.R.; Agarwal, G.; Chandani, S.; Talla, V.; Srinivasan, N.; Balasubramanian, D. Structural Integrity of the Greek Key Motif in βγ-Crystallins Is Vital for Central Eye Lens Transparency. *PLoS One* **2013**, *8*, e70336, doi:10.1371/journal.pone.0070336.
209. Mills, I.A.; Flaugh, S.L.; Kosinski-Collins, M.S.; King, J.A. Folding and Stability of the Isolated Greek Key Domains of the Long-Lived Human Lens Proteins gammaD-Crystallin and gammaS-Crystallin. *Protein Sci.* **2007**, *16*, 2427–2444, doi:10.1110/ps.072970207.
210. Yashchuk, V.M.; Kudrya, V.Y.; Levchenko, S.M.; Tkachuk, Z.Y.; Hovorun, D.M.; Mel'nik, V.I.; Vorob'yov, V.P.; Klishevich, G.V. Optical Response of the Polynucleotides-Proteins Interaction. *Mol. Cryst. Liq. Cryst.* **2011**, *535*, 93–110, doi:10.1080/15421406.2011.537953.
211. Sagar, V.; Wistow, G. Acquired Disorder and Asymmetry in a Domain-Swapped Model for γ-Crystallin Aggregation. *J. Mol. Biol.* **2022**, *434*, 167559, doi:10.1016/j.jmb.2022.167559.
212. Chatterjee, K.S.; Tripathi, V.; Das, R. A Conserved and Buried Edge-to-Face Aromatic Interaction in Small Ubiquitin-like Modifier (SUMO) Has a Role in SUMO Stability and Function. *J. Biol. Chem.* **2019**, *294*, 6772–6784, doi:10.1074/jbc.RA118.006642.

 doi:10.20944/preprints202510.0392.v1




213. Pal, S.; Udgaonkar, J.B. Mutations of Evolutionarily Conserved Aromatic Residues Suggest That Misfolding of the Mouse Prion Protein May Commence in Multiple Ways. *J. Neurochem.* **2023**, *167*, 696–710, doi:10.1111/jnc.16007.
214. Zhou, H.-X.; Pang, X. Electrostatic Interactions in Protein Structure, Folding, Binding, and Condensation. *Chem. Rev.* **2018**, *118*, 1691–1741, doi:10.1021/acs.chemrev.7b00305.
215. Pace, C.N.; Treviño, S.; Prabhakaran, E.; Scholtz, J.M. Protein Structure, Stability and Solubility in Water and Other Solvents. *Philos. Trans. R. Soc. Lond. B Biol. Sci.* **2004**, *359*, 1225–1234; discussion 1234–1235, doi:10.1098/rstb.2004.1500.
216. Taricska, N.; Bokor, M.; Menyhárd, D.K.; Tompa, K.; Perczel, A. Hydration Shell Differentiates Folded and Disordered States of a Trp-Cage Miniprotein, Allowing Characterization of Structural Heterogeneity by Wide-Line NMR Measurements. *Sci. Rep.* **2019**, *9*, 2947, doi:10.1038/s41598-019-39121-5.
217. Hemmingsen, J.M.; Gernert, K.M.; Richardson, J.S.; Richardson, D.C. The Tyrosine Corner: A Feature of Most Greek Key Beta-Barrel Proteins. *Protein Sci.* **1994**, *3*, 1927–1937, doi:10.1002/pro.5560031104.
218. Marazzi, M.; Navizet, I.; Lindh, R.; Frutos, L.M. Photostability Mechanisms in Human γB-Crystallin: Role of the Tyrosine Corner Unveiled by Quantum Mechanics and Hybrid Quantum Mechanics/molecular Mechanics Methodologies. *J. Chem. Theory Comput.* **2012**, *8*, 1351–1359, doi:10.1021/ct300114w.
219. Kong, F.; King, J. Contributions of Aromatic Pairs to the Folding and Stability of Long-Lived Human γD-Crystallin. *Protein Sci.* **2011**, *20*, 513–528, doi:10.1002/pro.583.
220. Burley, S.K.; Petsko, G.A. Aromatic-Aromatic Interaction: A Mechanism of Protein Structure Stabilization. *Science* **1985**, *229*, 23–28, doi:10.1126/science.3892686.
221. Gibbs, C.A.; Weber, D.S.; Warren, J.J. Clustering of Aromatic Amino Acid Residues around Methionine in Proteins. *Biomolecules* **2021**, *12*, 6, doi:10.3390/biom12010006.
222. Weber, D.S.; Warren, J.J. The Interaction between Methionine and Two Aromatic Amino Acids Is an Abundant and Multifunctional Motif in Proteins. *Arch. Biochem. Biophys.* **2019**, *672*, 108053, doi:10.1016/j.abb.2019.07.018.
223. Valley, C.C.; Cembran, A.; Perlmutter, J.D.; Lewis, A.K.; Labello, N.P.; Gao, J.; Sachs, J.N. The Methionine-Aromatic Motif Plays a Unique Role in Stabilizing Protein Structure. *J. Biol. Chem.* **2012**, *287*, 34979–34991, doi:10.1074/jbc.M112.374504.
224. Serebryany, E.; Martin, R.W.; Takahashi, G.R. The Functional Significance of High Cysteine Content in Eye Lens γ-Crystallins. *Biomolecules* **2024**, *14*, doi:10.3390/biom14050594.
225. Levine, R.L.; Mosoni, L.; Berlett, B.S.; Stadtman, E.R. Methionine Residues as Endogenous Antioxidants in Proteins. *Proc. Natl. Acad. Sci. U. S. A.* **1996**, *93*, 15036–15040, doi:10.1073/pnas.93.26.15036.
226. Rosenfeld, M.A.; Yurina, L.V.; Vasilyeva, A.D. Antioxidant Role of Methionine-Containing Intra- and Extracellular Proteins. *Biophys. Rev.* **2023**, *15*, 367–383, doi:10.1007/s12551-023-01056-7.
227. Bechtel, T.J.; Weerapana, E. From Structure to Redox: The Diverse Functional Roles of Disulfides and Implications in Disease. *Proteomics* **2017**, *17*, 1600391, doi:10.1002/pmic.201600391.
228. Kilgore, H.R.; Raines, R.T. N→π* Interactions Modulate the Properties of Cysteine Residues and Disulfide Bonds in Proteins. *J. Am. Chem. Soc.* **2018**, *140*, 17606–17611, doi:10.1021/jacs.8b09701.
229. Roos, G.; Foloppe, N.; Messens, J. Understanding the pK(a) of Redox Cysteines: The Key Role of Hydrogen Bonding. *Antioxid. Redox Signal.* **2013**, *18*, 94–127, doi:10.1089/ars.2012.4521.
230. MacDonald, J.T.; Purkiss, A.G.; Smith, M.A.; Evans, P.; Goodfellow, J.M.; Slingsby, C. Unfolding Crystallins: The Destabilizing Role of a Beta-Hairpin Cysteine in betaB2-Crystallin by Simulation and Experiment. *Protein Sci.* **2005**, *14*, 1282–1292, doi:10.1110/ps.041227805.
231. Wieligmann, K.; Mayr, E.M.; Jaenicke, R. Folding and Self-Assembly of the Domains of betaB2-Crystallin from Rat Eye Lens. *J. Mol. Biol.* **1999**, *286*, 989–994, doi:10.1006/jmbi.1999.2554.
232. Mills-Henry, I.A.; Thol, S.L.; Kosinski-Collins, M.S.; Serebryany, E.; King, J.A. Kinetic Stability of Long-Lived Human Lens γ-Crystallins and Their Isolated Double Greek Key Domains. *Biophys. J.* **2019**, *117*, 269–280, doi:10.1016/j.bpj.2019.06.006.
233. Serebryany, E.; King, J.A. The βγ-Crystallins: Native State Stability and Pathways to Aggregation. *Prog. Biophys. Mol. Biol.* **2014**, *115*, 32–41, doi:10.1016/j.pbiomolbio.2014.05.002.

 doi:10.20944/preprints202510.0392.v1




234. Das, P.; King, J.A.; Zhou, R. Aggregation of γ-Crystallins Associated with Human Cataracts via Domain Swapping at the C-Terminal β-Strands. *Proc. Natl. Acad. Sci. U. S. A.* **2011**, *108*, 10514–10519, doi:10.1073/pnas.1019152108.
235. Trinkl, S.; Glockshuber, R.; Jaenicke, R. Dimerization of Beta B2-Crystallin: The Role of the Linker Peptide and the N- and C-Terminal Extensions. *Protein Sci.* **1994**, *3*, 1392–1400, doi:10.1002/pro.5560030905.
236. D'Alessio, G. The Evolution of Monomeric and Oligomeric Betagamma-Type Crystallins. Facts and Hypotheses. *Eur. J. Biochem.* **2002**, *269*, 3122–3130, doi:10.1046/j.1432-1033.2002.03004.x.
237. Bax, B.; Lapatto, R.; Nalini, V.; Driessen, H.; Lindley, P.F.; Mahadevan, D.; Blundell, T.L.; Slingsby, C. X-Ray Analysis of Beta B2-Crystallin and Evolution of Oligomeric Lens Proteins. *Nature* **1990**, *347*, 776–780, doi:10.1038/347776a0.
238. Rolland, A.D.; Takata, T.; Donor, M.T.; Lampi, K.J.; Prell, J.S. Eye Lens β-Crystallins Are Predicted by Native Ion Mobility-Mass Spectrometry and Computations to Form Compact Higher-Ordered Heterooligomers. *Structure* **2023**, *31*, 1052–1064.e3, doi:10.1016/j.str.2023.06.013.
239. Basak, A.K.; Kroone, R.C.; Lubsen, N.H.; Naylor, C.E.; Jaenicke, R.; Slingsby, C. The C-Terminal Domains of gammaS-Crystallin Pair about a Distorted Twofold Axis. *Protein Eng.* **1998**, *11*, 337–344, doi:10.1093/protein/11.5.337.
240. Wu, Z.; Delaglio, F.; Wyatt, K.; Wistow, G.; Bax, A. Solution Structure of (gamma)S-Crystallin by Molecular Fragment Replacement NMR. *Protein Sci.* **2005**, *14*, 3101–3114, doi:10.1110/ps.051635205.
241. Gronenborn, A.M. Protein Acrobatics in Pairs--Dimerization via Domain Swapping. *Curr. Opin. Struct. Biol.* **2009**, *19*, 39–49, doi:10.1016/j.sbi.2008.12.002.
242. Bennett, M.J.; Schlunegger, M.P.; Eisenberg, D. 3D Domain Swapping: A Mechanism for Oligomer Assembly. *Protein Sci.* **1995**, *4*, 2455–2468, doi:10.1002/pro.5560041202.
243. Murray, C.W.; Verdonk, M.L. The Consequences of Translational and Rotational Entropy Lost by Small Molecules on Binding to Proteins. *J. Comput. Aided Mol. Des.* **2002**, *16*, 741–753, doi:10.1023/a:1022446720849.
244. Kshirsagar, M.; Meller, A.; Humphreys, I.R.; Sledzieski, S.; Xu, Y.; Dodhia, R.; Horvitz, E.; Berger, B.; Bowman, G.R.; Ferres, J.L.; et al. Rapid and Accurate Prediction of Protein Homo-Oligomer Symmetry Using Seq2Symm. *Nat. Commun.* **2025**, *16*, 2017, doi:10.1038/s41467-025-57148-3.
245. Schlunegger, M.P.; Bennett, M.J.; Eisenberg, D. Oligomer Formation by 3D Domain Swapping: A Model for Protein Assembly and Misassembly. *Adv. Protein Chem.* **1997**, *50*, 61–122, doi:10.1016/s0065-3233(08)60319-8.
246. Marcus, Y. Thermodynamics of Solvation of Ions. Part 5.—Gibbs Free Energy of Hydration at 298.15 K. *J. Chem. Soc., Faraday Trans.* **1991**, *87*, 2995–2999, doi:10.1039/FT9918702995.
247. Lee, B. Enthalpy-Entropy Compensation in the Thermodynamics of Hydrophobicity. *Biophys. Chem.* **1994**, *51*, 271–277; discussion 277–278, doi:10.1016/0301-4622(94)00048-4.
248. Yang, S.; Cho, S.S.; Levy, Y.; Cheung, M.S.; Levine, H.; Wolynes, P.G.; Onuchic, J.N. Domain Swapping Is a Consequence of Minimal Frustration. *Proc. Natl. Acad. Sci. U. S. A.* **2004**, *101*, 13786–13791, doi:10.1073/pnas.0403724101.
249. Serebryany, E.; Woodard, J.C.; Adkar, B.V.; Shabab, M.; King, J.A.; Shakhnovich, E.I. An Internal Disulfide Locks a Misfolded Aggregation-Prone Intermediate in Cataract-Linked Mutants of Human γD-Crystallin. *J. Biol. Chem.* **2016**, *291*, 19172–19183, doi:10.1074/jbc.M116.735977.
250. Georgelin, R.; Jackson, C.J. Entropy, Enthalpy, and Evolution: Adaptive Trade-Offs in Protein Binding Thermodynamics. *Curr. Opin. Struct. Biol.* **2025**, *94*, 103080, doi:10.1016/j.sbi.2025.103080.
251. Roterman, I.; Stapor, K.; Dułak, D.; Konieczny, L. Domain Swapping: A Mathematical Model for Quantitative Assessment of Structural Effects. *FEBS Open Bio* **2024**, *14*, 2006–2025, doi:10.1002/2211-5463.13911.
252. Rousseau, F.; Schymkowitz, J.W.H.; Itzhaki, L.S. The Unfolding Story of Three-Dimensional Domain Swapping. *Structure* **2003**, *11*, 243–251, doi:10.1016/s0969-2126(03)00029-7.
253. Garcia-Manyes, S.; Giganti, D.; Badilla, C.L.; Lezamiz, A.; Perales-Calvo, J.; Beedle, A.E.M.; Fernández, J.M. Single-Molecule Force Spectroscopy Predicts a Misfolded, Domain-Swapped Conformation in Human γD-Crystallin Protein. *J. Biol. Chem.* **2016**, *291*, 4226–4235, doi:10.1074/jbc.M115.673871.

 doi:10.20944/preprints202510.0392.v1




254. Jaskólski, M. 3D Domain Swapping, Protein Oligomerization, and Amyloid Formation. *Acta Biochim. Pol.* **2001**, *48*, 807–827, doi:10.18388/abp.2001_3849.
255. Mondal, B.; Nagesh, J.; Reddy, G. Double Domain Swapping in Human γC and γD Crystallin Drives Early Stages of Aggregation. *J. Phys. Chem. B* **2021**, *125*, 1705–1715, doi:10.1021/acs.jpcb.0c07833.
256. Thorn, D.; Serebryany, E.; Birrane, G.; Grosas, A.; Kaya, A.; Kraay, C.; Bitran, A.; Carver, J.; Shakhnovich, E. The Thermodynamic Cost of Domain-Swapping in Long-Lived γ-Crystallins and the Evolution of Durable Transparency in the Human Eye Lens. *Invest. Ophthalmol. Vis. Sci.* **2025**, *66*, 3269–3269.
257. Zhao, H.; Brown, P.H.; Schuck, P. On the Distribution of Protein Refractive Index Increments. *Biophys. J.* **2011**, *100*, 2309–2317, doi:10.1016/j.bpj.2011.03.004.
258. Wible, R.S.; Sutter, T.R. Soft Cysteine Signaling Network: The Functional Significance of Cysteine in Protein Function and the Soft Acids/bases Thiol Chemistry That Facilitates Cysteine Modification. *Chem. Res. Toxicol.* **2017**, *30*, 729–762, doi:10.1021/acs.chemrestox.6b00428.
259. Marino, S.M.; Gladyshev, V.N. Analysis and Functional Prediction of Reactive Cysteine Residues. *J. Biol. Chem.* **2012**, *287*, 4419–4425, doi:10.1074/jbc.R111.275578.
260. Mora, M.; Board, S.; Languin-Cattoën, O.; Masino, L.; Stirnemann, G.; Garcia-Manyes, S. A Single-Molecule Strategy to Capture Non-Native Intramolecular and Intermolecular Protein Disulfide Bridges. *Nano Lett.* **2022**, *22*, 3922–3930, doi:10.1021/acs.nanolett.2c00043.
261. Fan, X.; Zhou, S.; Wang, B.; Hom, G.; Guo, M.; Li, B.; Yang, J.; Vaysburg, D.; Monnier, V.M. Evidence of Highly Conserved β-Crystallin Disulfidome That Can Be Mimicked by in Vitro Oxidation in Age-Related Human Cataract and Glutathione Depleted Mouse Lens. *Mol. Cell. Proteomics* **2015**, *14*, 3211–3223, doi:10.1074/mcp.M115.050948.
262. Serebryany, E.; Thorn, D.C.; Quintanar, L. Redox Chemistry of Lens Crystallins: A System of Cysteines. *Exp. Eye Res.* **2021**, *211*, 108707, doi:10.1016/j.exer.2021.108707.
263. Ramkumar, S.; Fan, X.; Wang, B.; Yang, S.; Monnier, V.M. Reactive Cysteine Residues in the Oxidative Dimerization and Cu2+ Induced Aggregation of Human γD-Crystallin: Implications for Age-Related Cataract. *Biochim. Biophys. Acta Mol. Basis Dis.* **2018**, *1864*, 3595–3604, doi:10.1016/j.bbadis.2018.08.021.
264. Strofaldi, A.; Khan, A.R.; McManus, J.J. Surface Exposed Free Cysteine Suppresses Crystallization of Human γD-Crystallin. *J. Mol. Biol.* **2021**, *433*, 167252, doi:10.1016/j.jmb.2021.167252.
265. Derewenda, Z.S.; Vekilov, P.G. Entropy and Surface Engineering in Protein Crystallization. *Acta Crystallogr. D Biol. Crystallogr.* **2006**, *62*, 116–124, doi:10.1107/S0907444905035237.
266. Hentschel, L.; Hansen, J.; Egelhaaf, S.U.; Platten, F. The Crystallization Enthalpy and Entropy of Protein Solutions: Microcalorimetry, Van't Hoff Determination and Linearized Poisson-Boltzmann Model of Tetragonal Lysozyme Crystals. *Phys. Chem. Chem. Phys.* **2021**, *23*, 2686–2696, doi:10.1039/d0cp06113a.
267. Hanson, S.R.; Smith, D.L.; Smith, J.B. Deamidation and Disulfide Bonding in Human Lens Gamma-Crystallins. *Exp. Eye Res.* **1998**, *67*, 301–312, doi:10.1006/exer.1998.0530.
268. Anderson, D.M.; Nye-Wood, M.G.; Rose, K.L.; Donaldson, P.J.; Grey, A.C.; Schey, K.L. MALDI Imaging Mass Spectrometry of β- and γ-Crystallins in the Ocular Lens. *J. Mass Spectrom.* **2020**, *55*, e4473, doi:10.1002/jms.4473.
269. Purkiss, A.G.; Bateman, O.A.; Goodfellow, J.M.; Lubsen, N.H.; Slingsby, C. The X-Ray Crystal Structure of Human Gamma S-Crystallin C-Terminal Domain. *J. Biol. Chem.* **2002**, *277*, 4199–4205, doi:10.1074/jbc.M110083200.
270. Thorn, D.C.; Serebryany, E.; Birrane, G.; Kaya, A.I.; Shakhnovich, E.I. Domain-Swapped Dimeric γ-Crystallin: The Missing Link in the Evolution of Oligomeric β-Crystallins. *FASEB J.* **2022**, *36 Suppl 1*, doi:10.1096/fasebj.2022.36.S1.R3926.
271. Wang, Y.; Lomakin, A.; McManus, J.J.; Ogun, O.; Benedek, G.B. Phase Behavior of Mixtures of Human Lens Proteins Gamma D and Beta B1. *Proc. Natl. Acad. Sci. U. S. A.* **2010**, *107*, 13282–13287, doi:10.1073/pnas.1008353107.
272. Feller, G.; d'Amico, D.; Gerday, C. Thermodynamic Stability of a Cold-Active Alpha-Amylase from the Antarctic Bacterium Alteromonas Haloplanctis. *Biochemistry* **1999**, *38*, 4613–4619, doi:10.1021/bi982650+.

 doi:10.20944/preprints202510.0392.v1




273. García-Arribas, O.; Mateo, R.; Tomczak, M.M.; Davies, P.L.; Mateu, M.G. Thermodynamic Stability of a Cold-Adapted Protein, Type III Antifreeze Protein, and Energetic Contribution of Salt Bridges. *Protein Sci.* **2007**, *16*, 227–238, doi:10.1110/ps.062448907.
274. Brubaker, W.D.; Freites, J.A.; Golchert, K.J.; Shapiro, R.A.; Morikis, V.; Tobias, D.J.; Martin, R.W. Separating Instability from Aggregation Propensity in γS-Crystallin Variants. *Biophys. J.* **2011**, *100*, 498–506, doi:10.1016/j.bpj.2010.12.3691.
275. Qin, S.; Zhou, H.-X. Atomistic Modeling of Liquid-Liquid Phase Equilibrium Explains Dependence of Critical Temperature on γ-Crystallin Sequence. *Commun. Biol.* **2023**, *6*, 886, doi:10.1038/s42003-023-05270-7.
276. Rocha, M.A.; Sprague-Piercy, M.A.; Kwok, A.O.; Roskamp, K.W.; Martin, R.W. Chemical Properties Determine Solubility and Stability in βγ-Crystallins of the Eye Lens. *Chembiochem* **2021**, *22*, 1329–1346, doi:10.1002/cbic.202000739.
277. Cooper, A.J.; Pinto, J.T.; Callery, P.S. Reversible and Irreversible Protein Glutathionylation: Biological and Clinical Aspects. *Expert Opin. Drug Metab. Toxicol.* **2011**, *7*, 891–910, doi:10.1517/17425255.2011.577738.
278. Cremers, C.M.; Jakob, U. Oxidant Sensing by Reversible Disulfide Bond Formation. *J. Biol. Chem.* **2013**, *288*, 26489–26496, doi:10.1074/jbc.R113.462929.
279. Betz, S.F. Disulfide Bonds and the Stability of Globular Proteins. *Protein Sci.* **1993**, *2*, 1551–1558, doi:10.1002/pro.5560021002.
280. Xiong, Y.; Uys, J.D.; Tew, K.D.; Townsend, D.M. S-Glutathionylation: From Molecular Mechanisms to Health Outcomes. *Antioxid. Redox Signal.* **2011**, *15*, 233–270, doi:10.1089/ars.2010.3540.
281. Lushchak, V.I. Glutathione Homeostasis and Functions: Potential Targets for Medical Interventions. *J. Amino Acids* **2012**, *2012*, 736837, doi:10.1155/2012/736837.
282. Musaogullari, A.; Chai, Y.-C. Redox Regulation by Protein S-Glutathionylation: From Molecular Mechanisms to Implications in Health and Disease. *Int. J. Mol. Sci.* **2020**, *21*, 8113, doi:10.3390/ijms21218113.
283. Kalinina, E.; Novichkova, M. Glutathione in Protein Redox Modulation through S-Glutathionylation and S-Nitrosylation. *Molecules* **2021**, *26*, 435, doi:10.3390/molecules26020435.
284. Liang, J.N.; Pelletier, M.R. Destabilization of Lens Protein Conformation by Glutathione Mixed Disulfide. *Exp. Eye Res.* **1988**, *47*, 17–25, doi:10.1016/0014-4835(88)90020-6.
285. Dalle-Donne, I.; Rossi, R.; Colombo, G.; Giustarini, D.; Milzani, A. Protein S-Glutathionylation: A Regulatory Device from Bacteria to Humans. *Trends Biochem. Sci.* **2009**, *34*, 85–96, doi:10.1016/j.tibs.2008.11.002.
286. Lampi, K.J.; Thorn, D.; Halverson-Kolkind, K.; David, L. Mechanism of Glutathionylation-Induced Heat Precipitation of γS-Crystallin. *Invest. Ophthalmol. Vis. Sci.* **2025**, *66*, 1277–1277.
287. Thorn, D.C.; Grosas, A.B.; Mabbitt, P.D.; Ray, N.J.; Jackson, C.J.; Carver, J.A. The Structure and Stability of the Disulfide-Linked γS-Crystallin Dimer Provide Insight into Oxidation Products Associated with Lens Cataract Formation. *J. Mol. Biol.* **2019**, *431*, 483–497, doi:10.1016/j.jmb.2018.12.005.
288. Harding, J.J. Free and Protein-Bound Glutathione in Normal and Cataractous Human Lenses. *Biochem. J.* **1970**, *117*, 957–960, doi:10.1042/bj1170957.
289. Craghill, J.; Cronshaw, A.D.; Harding, J.J. The Identification of a Reaction Site of Glutathione Mixed-Disulphide Formation on gammaS-Crystallin in Human Lens. *Biochem. J.* **2004**, *379*, 595–600, doi:10.1042/BJ20031367.
290. Khago, D.; Wong, E.K.; Kingsley, C.N.; Freites, J.A.; Tobias, D.J.; Martin, R.W. Increased Hydrophobic Surface Exposure in the Cataract-Related G18V Variant of Human γS-Crystallin. *Biochim. Biophys. Acta* **2016**, *1860*, 325–332, doi:10.1016/j.bbagen.2015.09.022.
291. Lampi, K.; Kraay, C.; Halverson-Kolkind, K.; Thorn, D.; Shakhnovich, E.; David, L. BPS2025—Pursuit of the Elusive Disulfide Crosslink in Oxidized γS-Crystallin from the Eye Lens. *Biophys. J.* **2025**, *124*, 213a, doi:10.1016/j.bpj.2024.11.1179.
292. Wang, Z.; Schey, K.L. Quantification of Thioether-Linked Glutathione Modifications in Human Lens Proteins. *Exp. Eye Res.* **2018**, *175*, 83–89, doi:10.1016/j.exer.2018.06.002.
293. Townsend, D.M.; Lushchak, V.I.; Cooper, A.J.L. A Comparison of Reversible versus Irreversible Protein Glutathionylation. *Adv. Cancer Res.* **2014**, *122*, 177–198, doi:10.1016/B978-0-12-420117-0.00005-0.

 doi:10.20944/preprints202510.0392.v1




294. Kim, K.T.; Chiba, Y.; Arai, H.; Ishii, M. Discovery of an Intermolecular Disulfide Bond Required for the Thermostability of a Heterodimeric Protein from the Thermophile Hydrogenobacter Thermophilus. *Biosci. Biotechnol. Biochem.* **2016**, *80*, 232–240, doi:10.1080/09168451.2015.1079476.
295. Troussicot, L.; Vallet, A.; Molin, M.; Burmann, B.M.; Schanda, P. Disulfide-Bond-Induced Structural Frustration and Dynamic Disorder in a Peroxiredoxin from MAS NMR. *J. Am. Chem. Soc.* **2023**, *145*, 10700–10711, doi:10.1021/jacs.3c01200.
296. Wankowicz, S.A.; Fraser, J.S. Advances in Uncovering the Mechanisms of Macromolecular Conformational Entropy. *Nat. Chem. Biol.* **2025**, *21*, 623–634, doi:10.1038/s41589-025-01879-3.
297. Martin, E.W.; Mittag, T. Relationship of Sequence and Phase Separation in Protein Low-Complexity Regions. *Biochemistry* **2018**, *57*, 2478–2487, doi:10.1021/acs.biochem.8b00008.
298. Cho, S.S.; Levy, Y.; Onuchic, J.N.; Wolynes, P.G. Overcoming Residual Frustration in Domain-Swapping: The Roles of Disulfide Bonds in Dimerization and Aggregation. *Phys. Biol.* **2005**, *2*, S44–S55, doi:10.1088/1478-3975/2/2/S05.
299. Zheng, W.; Schafer, N.P.; Wolynes, P.G. Frustration in the Energy Landscapes of Multidomain Protein Misfolding. *Proc. Natl. Acad. Sci. U. S. A.* **2013**, *110*, 1680–1685, doi:10.1073/pnas.1222130110.
300. Lou, M.F. Glutathione and Glutaredoxin in Redox Regulation and Cell Signaling of the Lens. *Antioxidants (Basel)* **2022**, *11*, doi:10.3390/antiox11101973.
301. Serebryany, E.; King, J.A. Wild-Type Human γD-Crystallin Promotes Aggregation of Its Oxidation-Mimicking, Misfolding-Prone W42Q Mutant. *J. Biol. Chem.* **2015**, *290*, 11491–11503, doi:10.1074/jbc.M114.621581.
302. Thorn, D.; Serebryany, E.; David, L.L.; Lampi, K.J.; Shakhnovich, E. Playing "redox Hot Potato": Disulfide Transfer between γ-Crystallins in the Aging, Pre-Cataractous Lens. *Invest. Ophthalmol. Vis. Sci.* **2023**, *64*, 1230–1230.
303. Adav, S.S. Advances in the Study of Protein Deamidation: Unveiling Its Influence on Aging, Disease Progression, Forensics and Therapeutic Efficacy. *Proteomes* **2025**, *13*, 24, doi:10.3390/proteomes13020024.
304. Lapko, V.N.; Purkiss, A.G.; Smith, D.L.; Smith, J.B. Deamidation in Human Gamma S-Crystallin from Cataractous Lenses Is Influenced by Surface Exposure. *Biochemistry* **2002**, *41*, 8638–8648, doi:10.1021/bi015924t.
305. Guseman, A.J.; Whitley, M.J.; González, J.J.; Rathi, N.; Ambarian, M.; Gronenborn, A.M. Assessing the Structures and Interactions of γD-Crystallin Deamidation Variants. *Structure* **2021**, *29*, 284–291.e3, doi:10.1016/j.str.2020.11.006.
306. Kato, K.; Nakayoshi, T.; Kitamura, Y.; Kurimoto, E.; Oda, A.; Ishikawa, Y. Identification of the Most Impactful Asparagine Residues for γS-Crystallin Aggregation by Deamidation. *Biochemistry* **2023**, *62*, 1679–1688, doi:10.1021/acs.biochem.3c00097.
307. Ray, N.J.; Hall, D.; Carver, J.A. Deamidation of N76 in Human γS-Crystallin Promotes Dimer Formation. *Biochim. Biophys. Acta* **2016**, *1860*, 315–324, doi:10.1016/j.bbagen.2015.08.015.
308. Pande, A.; Mokhor, N.; Pande, J. Deamidation of Human γS-Crystallin Increases Attractive Protein Interactions: Implications for Cataract. *Biochemistry* **2015**, *54*, 4890–4899, doi:10.1021/acs.biochem.5b00185.
309. Vetter, C.J.; Thorn, D.C.; Wheeler, S.G.; Mundorff, C.C.; Halverson, K.A.; Wales, T.E.; Shinde, U.P.; Engen, J.R.; David, L.L.; Carver, J.A.; et al. Cumulative Deamidations of the Major Lens Protein γS-Crystallin Increase Its Aggregation during Unfolding and Oxidation. *Protein Sci.* **2020**, *29*, 1945–1963, doi:10.1002/pro.3915.
310. Forsythe, H.M.; Vetter, C.J.; Jara, K.A.; Reardon, P.N.; David, L.L.; Barbar, E.J.; Lampi, K.J. Altered Protein Dynamics and Increased Aggregation of Human γS-Crystallin due to Cataract-Associated Deamidations. *Biochemistry* **2019**, *58*, 4112–4124, doi:10.1021/acs.biochem.9b00593.
311. Lampi, K.J.; Wilmarth, P.A.; Murray, M.R.; David, L.L. Lens β-Crystallins: The Role of Deamidation and Related Modifications in Aging and Cataract. *Prog. Biophys. Mol. Biol.* **2014**, *115*, 21–31, doi:10.1016/j.pbiomolbio.2014.02.004.
312. Michiel, M.; Duprat, E.; Skouri-Panet, F.; Lampi, J.A.; Tardieu, A.; Lampi, K.J.; Finet, S. Aggregation of Deamidated Human betaB2-Crystallin and Incomplete Rescue by Alpha-Crystallin Chaperone. *Exp. Eye Res.* **2010**, *90*, 688–698, doi:10.1016/j.exer.2010.02.007.

 doi:10.20944/preprints202510.0392.v1




313. Takata, T.; Oxford, J.T.; Demeler, B.; Lampi, K.J. Deamidation Destabilizes and Triggers Aggregation of a Lens Protein, betaA3-Crystallin. *Protein Sci.* **2008**, *17*, 1565–1575, doi:10.1110/ps.035410.108.
314. Lampi, K.J.; Amyx, K.K.; Ahmann, P.; Steel, E.A. Deamidation in Human Lens betaB2-Crystallin Destabilizes the Dimer. *Biochemistry* **2006**, *45*, 3146–3153, doi:10.1021/bi052051k.
315. Lampi, K.J.; Fox, C.B.; David, L.L. Changes in Solvent Accessibility of Wild-Type and Deamidated βB2-Crystallin Following Complex Formation with αA-Crystallin. *Exp. Eye Res.* **2012**, *104*, 48–58, doi:10.1016/j.exer.2012.09.001.
316. Budnar, P.; Tangirala, R.; Bakthisaran, R.; Rao, C.M. Protein Aggregation and Cataract: Role of Age-Related Modifications and Mutations in α-Crystallins. *Biochemistry* **2022**, *87*, 225–241, doi:10.1134/S000629792203004X.
317. Takata, T.; Oxford, J.T.; Brandon, T.R.; Lampi, K.J. Deamidation Alters the Structure and Decreases the Stability of Human Lens betaA3-Crystallin. *Biochemistry* **2007**, *46*, 8861–8871, doi:10.1021/bi700487q.
318. Flaugh, S.L.; Mills, I.A.; King, J. Glutamine Deamidation Destabilizes Human gammaD-Crystallin and Lowers the Kinetic Barrier to Unfolding. *J. Biol. Chem.* **2006**, *281*, 30782–30793, doi:10.1074/jbc.M603882200.
319. Lampi, K.J.; Kim, Y.H.; Bächinger, H.P.; Boswell, B.A.; Lindner, R.A.; Carver, J.A.; Shearer, T.R.; David, L.L.; Kapfer, D.M. Decreased Heat Stability and Increased Chaperone Requirement of Modified Human betaB1-Crystallins. *Mol. Vis.* **2002**, *8*, 359–366.
320. Strub, C.; Alies, C.; Lougarre, A.; Ladurantie, C.; Czaplicki, J.; Fournier, D. Mutation of Exposed Hydrophobic Amino Acids to Arginine to Increase Protein Stability. *BMC Biochem.* **2004**, *5*, 9, doi:10.1186/1471-2091-5-9.
321. Antifeeva, I.A.; Fonin, A.V.; Fefilova, A.S.; Stepanenko, O.V.; Povarova, O.I.; Silonov, S.A.; Kuznetsova, I.M.; Uversky, V.N.; Turoverov, K.K. Liquid-Liquid Phase Separation as an Organizing Principle of Intracellular Space: Overview of the Evolution of the Cell Compartmentalization Concept. *Cell. Mol. Life Sci.* **2022**, *79*, 251, doi:10.1007/s00018-022-04276-4.
322. Tanford, C. The Hydrophobic Effect and the Organization of Living Matter. *Science* **1978**, *200*, 1012–1018, doi:10.1126/science.653353.
323. van Gils, J.H.M.; Gogishvili, D.; van Eck, J.; Bouwmeester, R.; van Dijk, E.; Abeln, S. How Sticky Are Our Proteins? Quantifying Hydrophobicity of the Human Proteome. *Bioinform. Adv.* **2022**, *2*, vbac002, doi:10.1093/bioadv/vbac002.
324. Mahalakshmi, R. Aromatic Interactions in β-Hairpin Scaffold Stability: A Historical Perspective. *Arch. Biochem. Biophys.* **2019**, *661*, 39–49, doi:10.1016/j.abb.2018.11.001.
325. De Sancho, D.; López, X. Crossover in Aromatic Amino Acid Interaction Strength: Tyrosine vs. Phenylalanine in Biomolecular Condensates. *eLife* 2025.
326. De Sancho, D. Phase Separation in Amino Acid Mixtures Is Governed by Composition. *Biophys. J.* **2022**, *121*, 4119–4127, doi:10.1016/j.bpj.2022.09.031.
327. Vendruscolo, M.; Fuxreiter, M. Towards Sequence-Based Principles for Protein Phase Separation Predictions. *Curr. Opin. Chem. Biol.* **2023**, *75*, 102317, doi:10.1016/j.cbpa.2023.102317.
328. Gupta, R.; Srivastava, O.P. Deamidation Affects Structural and Functional Properties of Human alphaA-Crystallin and Its Oligomerization with alphaB-Crystallin. *J. Biol. Chem.* **2004**, *279*, 44258–44269, doi:10.1074/jbc.M405648200.
329. Das, K.P.; Petrash, J.M.; Surewicz, W.K. Conformational Properties of Substrate Proteins Bound to a Molecular Chaperone Alpha-Crystallin. *J. Biol. Chem.* **1996**, *271*, 10449–10452, doi:10.1074/jbc.271.18.10449.
330. Dougherty, D.A. Cation-Pi Interactions Involving Aromatic Amino Acids. *J. Nutr.* **2007**, *137*, 1504S–1508S; discussion 1516S–1517S, doi:10.1093/jn/137.6.1504S.
331. Sivasakthi, V.; Anitha, P.; Kumar, K.M.; Bag, S.; Senthilvel, P.; Lavanya, P.; Swetha, R.; Anbarasu, A.; Ramaiah, S. Aromatic-Aromatic Interactions: Analysis of π-π Interactions in Interleukins and TNF Proteins. *Bioinformation* **2013**, *9*, 432–439, doi:10.6026/97320630009432.
332. Wheeler, S.E. Understanding Substituent Effects in Noncovalent Interactions Involving Aromatic Rings. *Acc. Chem. Res.* **2013**, *46*, 1029–1038, doi:10.1021/ar300109n.
333. Calinsky, R.; Levy, Y. Aromatic Residues in Proteins: Re-Evaluating the Geometry and Energetics of π-π, Cation-π, and CH-π Interactions. *J. Phys. Chem. B* **2024**, *128*, 8687–8700, doi:10.1021/acs.jpcb.4c04774.

 doi:10.20944/preprints202510.0392.v1




334. Carter-Fenk, K.; Liu, M.; Pujal, L.; Loipersberger, M.; Tsanai, M.; Vernon, R.M.; Forman-Kay, J.D.; Head-Gordon, M.; Heidar-Zadeh, F.; Head-Gordon, T. The Energetic Origins of Pi-Pi Contacts in Proteins. *J. Am. Chem. Soc.* **2023**, doi:10.1021/jacs.3c09198.
335. Ribas, J.; Cubero, E.; Luque, F.J.; Orozco, M. Theoretical Study of Alkyl-Pi and Aryl-Pi Interactions. Reconciling Theory and Experiment. *J. Org. Chem.* **2002**, *67*, 7057–7065, doi:10.1021/jo0201225.
336. Boeynaems, S.; Alberti, S.; Fawzi, N.L.; Mittag, T.; Polymenidou, M.; Rousseau, F.; Schymkowitz, J.; Shorter, J.; Wolozin, B.; Van Den Bosch, L.; et al. Protein Phase Separation: A New Phase in Cell Biology. *Trends Cell Biol.* **2018**, *28*, 420–435, doi:10.1016/j.tcb.2018.02.004.
337. Das, S.; Lin, Y.-H.; Vernon, R.M.; Forman-Kay, J.D.; Chan, H.S. Comparative Roles of Charge, $\pi$, and Hydrophobic Interactions in Sequence-Dependent Phase Separation of Intrinsically Disordered Proteins. *Proc. Natl. Acad. Sci. U. S. A.* **2020**, *117*, 28795–28805, doi:10.1073/pnas.2008122117.
338. Vernon, R.M.; Chong, P.A.; Tsang, B.; Kim, T.H.; Bah, A.; Farber, P.; Lin, H.; Forman-Kay, J.D. Pi-Pi Contacts Are an Overlooked Protein Feature Relevant to Phase Separation. *Elife* **2018**, *7*, doi:10.7554/eLife.31486.
339. Southall, N.T.; Dill, K.A.; Haymet, A.D.J. A View of the Hydrophobic Effect. *J. Phys. Chem. B* **2002**, *106*, 521–533, doi:10.1021/jp015514e.
340. Garde, S.; Patel, A.J. Unraveling the Hydrophobic Effect, One Molecule at a Time. *Proc. Natl. Acad. Sci. U. S. A.* **2011**, *108*, 16491–16492, doi:10.1073/pnas.1113256108.
341. Baldwin, R.L. Dynamic Hydration Shell Restores Kauzmann's 1959 Explanation of How the Hydrophobic Factor Drives Protein Folding. *Proc. Natl. Acad. Sci. U. S. A.* **2014**, *111*, 13052–13056, doi:10.1073/pnas.1414556111.
342. Benítez, M.J.; Jiménez, J.S. Gibbs Free Energy and Enthalpy–entropy Compensation in Protein Folding. *Biophysica* **2025**, *5*, 2, doi:10.3390/biophysica5010002.
343. Hazra, M.K.; Levy, Y. Affinity of Disordered Protein Complexes Is Modulated by Entropy-Energy Reinforcement. *Proc. Natl. Acad. Sci. U. S. A.* **2022**, *119*, e2120456119, doi:10.1073/pnas.2120456119.
344. Dannenhoffer-Lafage, T.; Best, R.B. A Data-Driven Hydrophobicity Scale for Predicting Liquid-Liquid Phase Separation of Proteins. *J. Phys. Chem. B* **2021**, *125*, 4046–4056, doi:10.1021/acs.jpcb.0c11479.
345. Uyaver, S. Tyrosine, Phenylalanine, and Tryptophan Undergo Self-Aggregation in Similar and Different Manners. *Atmosphere (Basel)* **2022**, *13*, 1448, doi:10.3390/atmos13091448.
346. Pham, D.Q.H.; Chwastyk, M.; Cieplak, M. The Coexistence Region in the Van Der Waals Fluid and the Liquid-Liquid Phase Transitions. *Front. Chem.* **2022**, *10*, 1106599, doi:10.3389/fchem.2022.1106599.
347. Moss, J.H.; Doblhoff-Dier, K. If It Fits, It Sits: Solvation Shell Geometry and Water Structure Constrain Ion Positions at the Interface. *ChemRxiv* 2025.
348. Cyran, J.D.; Donovan, M.A.; Vollmer, D.; Siro Brigiano, F.; Pezzotti, S.; Galimberti, D.R.; Gaigeot, M.-P.; Bonn, M.; Backus, E.H.G. Molecular Hydrophobicity at a Macroscopically Hydrophilic Surface. *Proc. Natl. Acad. Sci. U. S. A.* **2019**, *116*, 1520–1525, doi:10.1073/pnas.1819000116.
349. Dignon, G.L.; Best, R.B.; Mittal, J. Biomolecular Phase Separation: From Molecular Driving Forces to Macroscopic Properties. *Annu. Rev. Phys. Chem.* **2020**, *71*, 53–75, doi:10.1146/annurev-physchem-071819-113553.
350. Zheng, J.; Zhao, L.; Zhang, Y.; He, W.; Guo, X.; Wang, J. Melatonin Alleviates High Glucose-Induced Cardiomyocyte Injury through Suppressing Mitochondrial FUNDC1-DRP1 Axis. *J. Pharm. Pharmacol.* **2024**, *76*, 1431–1448, doi:10.1093/jpp/rgae114.
351. Zhu, L.; Gong, Y.; Lju, H.; Sun, G.; Zhang, Q.; Qian, Z. Mechanisms of Melatonin Binding and Destabilizing the Protofilament and Filament of Tau R3-R4 Domains Revealed by Molecular Dynamics Simulation. *Phys. Chem. Chem. Phys.* **2021**, *23*, 20615–20626, doi:10.1039/d1cp03142b.
352. Martí, J.; Lu, H. Microscopic Interactions of Melatonin, Serotonin and Tryptophan with Zwitterionic Phospholipid Membranes. *Int. J. Mol. Sci.* **2021**, *22*, 2842, doi:10.3390/ijms22062842.
353. Gong, Y.; Zhan, C.; Zou, Y.; Qian, Z.; Wei, G.; Zhang, Q. Serotonin and Melatonin Show Different Modes of Action on Aβ42 Protofibril Destabilization. *ACS Chem. Neurosci.* **2021**, *12*, 799–809, doi:10.1021/acschemneuro.1c00038.

 doi:10.20944/preprints202510.0392.v1




354. Al-Zaqri, N.; Pooventhiran, T.; Alsalme, A.; Warad, I.; John, A.M.; Thomas, R. Structural and Physico-Chemical Evaluation of Melatonin and Its Solution-State Excited Properties, with Emphasis on Its Binding with Novel Coronavirus Proteins. *J. Mol. Liq.* **2020**, *318*, 114082, doi:10.1016/j.molliq.2020.114082.
355. Lu, H.; Martí, J. Binding and Dynamics of Melatonin at the Interface of Phosphatidylcholine-Cholesterol Membranes. *PLoS One* **2019**, *14*, e0224624, doi:10.1371/journal.pone.0224624.
356. Li, X.; Wang, S. Binding of Glutathione and Melatonin to Human Serum Albumin: A Comparative Study. *Colloids Surf. B Biointerfaces* **2015**, *125*, 96–103, doi:10.1016/j.colsurfb.2014.11.023.
357. Calamini, B.; Santarsiero, B.D.; Boutin, J.A.; Mesecar, A.D. Kinetic, Thermodynamic and X-Ray Structural Insights into the Interaction of Melatonin and Analogues with Quinone Reductase 2. *Biochem. J* **2008**, *413*, 81–91, doi:10.1042/BJ20071373.
358. Ten, G.N.; Yakovleva, A.A.; Baranov, V.I. Theoretical Study of Hydrophobicity and Hydrophilicity of Indole, Skatole, and Ethanole. *Journal of Structural Chemistry* **2014**, *54*, 1018–1028, doi:10.1134/S0022476613060048.
359. Norman, K.E.; Nymeyer, H. Indole Localization in Lipid Membranes Revealed by Molecular Simulation. *Biophys. J.* **2006**, *91*, 2046–2054, doi:10.1529/biophysj.105.080275.
360. Rodrigues, A.C.C.; de M. Camargo, L.T.F.; Francisco Lopes, Y.; Sallum, L.O.; Napolitano, H.B.; Camargo, A.J. Aqueous Solvation Study of Melatonin Using Ab Initio Molecular Dynamics. *J. Mol. Liq.* **2021**, *343*, 117451, doi:10.1016/j.molliq.2021.117451.
361. Camilloni, C.; Sutto, L.; Provasi, D.; Tiana, G.; Broglia, R.A. Early Events in Protein Folding: Is There Something More than Hydrophobic Burst? *Protein Sci.* **2008**, *17*, 1424–1433, doi:10.1110/ps.035105.108.
362. Ng, T.L.C.; Hoare, M.P.; Maristany, M.J.; Wilde, E.J.; Sneideris, T.; Huertas, J.; Agbetiameh, B.K.; Furukawa, M.; Joseph, J.A.; Knowles, T.P.J.; et al. Tandem-Repeat Proteins Introduce Tuneable Properties to Engineered Biomolecular Condensates. *Chem. Sci.* **2025**, *16*, 10532–10548, doi:10.1039/d5sc00903k.
363. Li, G.; Li, J.; Shao, R.; Zhao, J.; Chen, M. FUNDC1: A Promising Mitophagy Regulator at the Mitochondria-Associated Membrane for Cardiovascular Diseases. *Front. Cell Dev. Biol.* **2021**, *9*, 788634, doi:10.3389/fcell.2021.788634.
364. Twig, G.; Shirihai, O.S. The Interplay between Mitochondrial Dynamics and Mitophagy. *Antioxid. Redox Signal.* **2011**, *14*, 1939–1951, doi:10.1089/ars.2010.3779.
365. Lin, Y.; Fichou, Y.; Longhini, A.P.; Llanes, L.C.; Yin, P.; Bazan, G.C.; Kosik, K.S.; Han, S. Liquid-Liquid Phase Separation of Tau Driven by Hydrophobic Interaction Facilitates Fibrillization of Tau. *J. Mol. Biol.* **2021**, *433*, 166731, doi:10.1016/j.jmb.2020.166731.
366. Boyko, S.; Surewicz, K.; Surewicz, W.K. Regulatory Mechanisms of Tau Protein Fibrillation under the Conditions of Liquid-Liquid Phase Separation. *Proc. Natl. Acad. Sci. U. S. A.* **2020**, *117*, 31882–31890, doi:10.1073/pnas.2012460117.
367. Boyko, S.; Surewicz, W.K. Tau Liquid-Liquid Phase Separation in Neurodegenerative Diseases. *Trends Cell Biol.* **2022**, *32*, 611–623, doi:10.1016/j.tcb.2022.01.011.
368. Najafi, S.; Lin, Y.; Longhini, A.P.; Zhang, X.; Delaney, K.T.; Kosik, K.S.; Fredrickson, G.H.; Shea, J.-E.; Han, S. Liquid-Liquid Phase Separation of Tau by Self and Complex Coacervation. *Protein Sci.* **2021**, *30*, 1393–1407, doi:10.1002/pro.4101.
369. Wegmann, S.; Eftekharzadeh, B.; Tepper, K.; Zoltowska, K.M.; Bennett, R.E.; Dujardin, S.; Laskowski, P.R.; MacKenzie, D.; Kamath, T.; Commins, C.; et al. Tau Protein Liquid-Liquid Phase Separation Can Initiate Tau Aggregation. *EMBO J.* **2018**, *37*, doi:10.15252/embj.201798049.
370. Gui, X.; Feng, S.; Li, Z.; Li, Y.; Reif, B.; Shi, B.; Niu, Z. Liquid-Liquid Phase Separation of Amyloid-β Oligomers Modulates Amyloid Fibrils Formation. *J. Biol. Chem.* **2023**, *299*, 102926, doi:10.1016/j.jbc.2023.102926.
371. Morris, O.M.; Toprakcioglu, Z.; Röntgen, A.; Cali, M.; Knowles, T.P.J.; Vendruscolo, M. Aggregation of the Amyloid-β Peptide (Aβ40) within Condensates Generated through Liquid-Liquid Phase Separation. *Sci. Rep.* **2024**, *14*, 22633, doi:10.1038/s41598-024-72265-7.
372. Fu, Q.; Zhang, B.; Chen, X.; Chu, L. Liquid-Liquid Phase Separation in Alzheimer's Disease. *J. Mol. Med.* **2024**, *102*, 167–181, doi:10.1007/s00109-023-02407-3.

 doi:10.20944/preprints202510.0392.v1




373. Lin, P.; Xu, J.; Yang, F.; Li, D.; Zhang, R.; Jiang, Y.; Zheng, T. Elevated Concentrations of Amyloid-β Oligomers and Their Proapoptotic Effects on Age-Related Cataract. *FASEB J.* **2024**, *38*, e23861, doi:10.1096/fj.202301281RR.
374. Abu-Hussien, M.; Viswanathan, G.K.; Haj, E.; Paul, A.; Gazit, E.; Segal, D. An Amyloidogenic Hexapeptide from the Cataract-Associated γD-Crystallin Is a Model for the Full-Length Protein and Is Inhibited by Naphthoquinone-Tryptophan Hybrids. *Int. J. Biol. Macromol.* **2020**, *157*, 424–433, doi:10.1016/j.ijbiomac.2020.04.079.
375. Alperstein, A.M.; Ostrander, J.S.; Zhang, T.O.; Zanni, M.T. Amyloid Found in Human Cataracts with Two-Dimensional Infrared Spectroscopy. *Proc. Natl. Acad. Sci. U. S. A.* **2019**, *116*, 6602–6607, doi:10.1073/pnas.1821534116.
376. Zhang, T.O.; Alperstein, A.M.; Zanni, M.T. Amyloid β-Sheet Secondary Structure Identified in UV-Induced Cataracts of Porcine Lenses Using 2D IR Spectroscopy. *J. Mol. Biol.* **2017**, *429*, 1705–1721, doi:10.1016/j.jmb.2017.04.014.
377. Attanasio, F.; Cataldo, S.; Fisichella, S.; Nicoletti, S.; Nicoletti, V.G.; Pignataro, B.; Savarino, A.; Rizzarelli, E. Protective Effects of L- and D-Carnosine on Alpha-Crystallin Amyloid Fibril Formation: Implications for Cataract Disease. *Biochemistry* **2009**, *48*, 6522–6531, doi:10.1021/bi900343n.
378. Meehan, S.; Berry, Y.; Luisi, B.; Dobson, C.M.; Carver, J.A.; MacPhee, C.E. Amyloid Fibril Formation by Lens Crystallin Proteins and Its Implications for Cataract Formation. *J. Biol. Chem.* **2004**, *279*, 3413–3419, doi:10.1074/jbc.M308203200.
379. Mao, L.; Wang, Y.; Liu, Y.; Hu, X. Molecular Determinants for ATP-Binding in Proteins: A Data Mining and Quantum Chemical Analysis. *J. Mol. Biol.* **2004**, *336*, 787–807, doi:10.1016/j.jmb.2003.12.056.
380. Mogami, G.; Wazawa, T.; Morimoto, N.; Kodama, T.; Suzuki, M. Hydration Properties of Adenosine Phosphate Series as Studied by Microwave Dielectric Spectroscopy. *Biophys. Chem.* **2011**, *154*, 1–7, doi:10.1016/j.bpc.2010.11.006.
381. Hautke, A.; Ebbinghaus, S. The Emerging Role of ATP as a Cosolute for Biomolecular Processes. *Biol. Chem.* **2023**, *404*, 897–908, doi:10.1515/hsz-2023-0202.
382. Mehringer, J.; Do, T.-M.; Touraud, D.; Hohenschutz, M.; Khoshsima, A.; Horinek, D.; Kunz, W. Hofmeister versus Neuberg: Is ATP Really a Biological Hydrotrope? *Cell Reports Physical Science* **2021**, *2*, 100343, doi:10.1016/j.xcrp.2021.100343.
383. Kamski-Hennekam, E.R.; Huang, J.; Ahmed, R.; Melacini, G. Toward a Molecular Mechanism for the Interaction of ATP with Alpha-Synuclein. *Chem. Sci.* **2023**, *14*, 9933–9942, doi:10.1039/d3sc03612j.
384. Dec, R.; Dzwolak, W.; Winter, R. From a Droplet to a Fibril and from a Fibril to a Droplet: Intertwined Transition Pathways in Highly Dynamic Enzyme-Modulated Peptide-Adenosine Triphosphate Systems. *J. Am. Chem. Soc.* **2024**, *146*, 6045–6052, doi:10.1021/jacs.3c13152.
385. Dang, M.; Li, Y.; Song, J. ATP Biphasically Modulates LLPS of SARS-CoV-2 Nucleocapsid Protein and Specifically Binds Its RNA-Binding Domain. *Biochem. Biophys. Res. Commun.* **2021**, *541*, 50–55, doi:10.1016/j.bbrc.2021.01.018.
386. Hayes, M.H.; Peuchen, E.H.; Dovichi, N.J.; Weeks, D.L. Dual Roles for ATP in the Regulation of Phase Separated Protein Aggregates in Xenopus Oocyte Nucleoli. *Elife* **2018**, *7*, doi:10.7554/eLife.35224.
387. Nishizawa, M.; Walinda, E.; Morimoto, D.; Kohn, B.; Scheler, U.; Shirakawa, M.; Sugase, K. Effects of Weak Nonspecific Interactions with ATP on Proteins. *J. Am. Chem. Soc.* **2021**, *143*, 11982–11993, doi:10.1021/jacs.0c13118.
388. Kuramochi, M.; Nakamura, M.; Takahashi, H.; Komoriya, T.; Takita, T.; Pham, N.T.K.; Yasukawa, K.; Yoshimune, K. Adenosine Triphosphate Induces Amorphous Aggregation of Amyloid β by Increasing Aβ Dynamics. *Sci. Rep.* **2024**, *14*, 8134, doi:10.1038/s41598-024-58773-6.
389. Heo, C.E.; Han, J.Y.; Lim, S.; Lee, J.; Im, D.; Lee, M.J.; Kim, Y.K.; Kim, H.I. ATP Kinetically Modulates Pathogenic Tau Fibrillations. *ACS Chem. Neurosci.* **2020**, *11*, 3144–3152, doi:10.1021/acschemneuro.0c00479.
390. Dec, R.; Puławski, W.; Dzwolak, W. Selective and Stoichiometric Incorporation of ATP by Self-Assembling Amyloid Fibrils. *J. Mater. Chem. B Mater. Biol. Med.* **2021**, doi:10.1039/d1tb01976g.
391. Zhu, Y.; Lin, S.; Meng, L.; Sun, M.; Liu, M.; Li, J.; Tang, C.; Gong, Z. ATP Promotes Protein Coacervation through Conformational Compaction. *J. Mol. Cell Biol.* **2024**, mjae038, doi:10.1093/jmcb/mjae038.

 doi:10.20944/preprints202510.0392.v1




392. Sarkar, S.; Gupta, S.; Mahato, C.; Das, D.; Mondal, J. Elucidating ATP's Role as Solubilizer of Biomolecular Aggregate. *eLife* 2024.
393. Do, T.M.; Horinek, D.; Matubayasi, N. How ATP Suppresses the Fibrillation of Amyloid Peptides: Analysis of the Free-Energy Contributions. *Phys. Chem. Chem. Phys.* **2024**, *26*, 11880–11892, doi:10.1039/d4cp00179f.
394. Liu, F.; Wang, J. ATP Acts as a Hydrotrope to Regulate the Phase Separation of NBDY Clusters. *JACS Au* **2023**, *3*, 2578–2585, doi:10.1021/jacsau.3c00391.
395. Patel, A.; Malinovska, L.; Saha, S.; Wang, J.; Alberti, S.; Krishnan, Y.; Hyman, A.A. ATP as a Biological Hydrotrope. *Science* **2017**, *356*, 753–756, doi:10.1126/science.aaf6846.
396. Winkler, B.S.; Riley, M.V. Relative Contributions of Epithelial Cells and Fibers to Rabbit Lens ATP Content and Glycolysis. *Invest. Ophthalmol. Vis. Sci.* **1991**, *32*, 2593–2598.
397. Greiner, J.V.; Glonek, T. Hydrotropic Function of ATP in the Crystalline Lens. *Exp. Eye Res.* **2020**, *190*, 107862, doi:10.1016/j.exer.2019.107862.
398. Michael, R.; Bron, A.J. The Ageing Lens and Cataract: A Model of Normal and Pathological Ageing. *Philos. Trans. R. Soc. Lond. B Biol. Sci.* **2011**, *366*, 1278–1292, doi:10.1098/rstb.2010.0300.
399. He, Y.; Kang, J.; Song, J. ATP Differentially Antagonizes the Crowding-Induced Destabilization of Human γS-Crystallin and Its Four Cataract-Causing Mutants. *Biochem. Biophys. Res. Commun.* **2020**, *533*, 913–918, doi:10.1016/j.bbrc.2020.09.090.
400. Markossian, K.A.; Yudin, I.K.; Kurganov, B.I. Mechanism of Suppression of Protein Aggregation by α-Crystallin. *Int. J. Mol. Sci.* **2009**, *10*, 1314–1345, doi:10.3390/ijms10031314.
401. Armstrong, J.K.; Wenby, R.B.; Meiselman, H.J.; Fisher, T.C. The Hydrodynamic Radii of Macromolecules and Their Effect on Red Blood Cell Aggregation. *Biophys. J.* **2004**, *87*, 4259–4270, doi:10.1529/biophysj.104.047746.
402. Matsarskaia, O.; Braun, M.K.; Roosen-Runge, F.; Wolf, M.; Zhang, F.; Roth, R.; Schreiber, F. Cation-Induced Hydration Effects Cause Lower Critical Solution Temperature Behavior in Protein Solutions. *J. Phys. Chem. B* **2016**, *120*, 7731–7736, doi:10.1021/acs.jpcb.6b04506.
403. Loh, D.; Reiter, R.J. Light, Water, and Melatonin: The Synergistic Regulation of Phase Separation in Dementia. *Int. J. Mol. Sci.* **2023**, *24*, doi:10.3390/ijms24065835.
404. Loh, D.; Reiter, R.J. The Mitochondria Chronicles of Melatonin and ATP: Guardians of Phase Separation. *Mitochondrial Communications* **2024**, *2*, 67–84, doi:10.1016/j.mitoco.2024.07.002.
405. Loh, D.; Reiter, R.J. Melatonin Regulation of Phase Separation in Neuro-PASC: Out-Maneuvering Janus-Faced Amyloids. *Explor Neurosci* **2025**, *4*, 100678, doi:10.37349/en.2025.100678.
406. Zhang, C.; Cheng, J.; Wu, Q.; Hou, S.; Feng, S.; Jiang, B.; Lambert, C.J.; Gao, X.; Li, Y.; Li, J. Enhanced π-π Stacking between Dipole-Bearing Single Molecules Revealed by Conductance Measurement. *J. Am. Chem. Soc.* **2023**, *145*, 1617–1630, doi:10.1021/jacs.2c09656.
407. Singh, S.; Hsu, P.-J.; Kuo, J.-L.; Patwari, G.N. Dipole Moment Enhanced π-π Stacking in Fluorophenylacetylenes Is Carried over from Gas-Phase Dimers to Crystal Structures Propagated through Liquid like Clusters. *Phys. Chem. Chem. Phys.* **2021**, *23*, 9938–9947, doi:10.1039/d1cp00279a.
408. Singh, V.B.; Srivas, S.K. Spectroscopic Signatures and Conformational Preferences in Isolated Melatonin: A Computational Study. *Research Square* 2023.
409. Florio, G.M.; Zwier, T.S. Solvation of a Flexible Biomolecule in the Gas Phase: The Ultraviolet and Infrared Spectroscopy of Melatonin−Water Clusters. *J. Phys. Chem. A* **2003**, *107*, 974–983, doi:10.1021/jp027053i.
410. Kang, C.; Korter, T.M.; Pratt, D.W. Experimental Measurement of the Induced Dipole Moment of an Isolated Molecule in Its Ground and Electronically Excited States: Indole and Indole-H2O. *J. Chem. Phys.* **2005**, *122*, 174301, doi:10.1063/1.1883635.
411. Berthod, H.; Pullman, B. A Molecular Orbital Investigation of the Dipole Moments of the Syn and Anti Conformers of Purine and Pyrimidine Nucleosides. *Biochem. Biophys. Res. Commun.* **1972**, *46*, 125–129, doi:10.1016/0006-291x(72)90639-0.
412. Hunter, C.A.; Sanders, J.K.M. The Nature of .pi.-.pi. Interactions. *J. Am. Chem. Soc.* **1990**, *112*, 5525–5534, doi:10.1021/ja00170a016.

 doi:10.20944/preprints202510.0392.v1




413. Ritwiset, A.; Khajonrit, J.; Krongsuk, S.; Maensiri, S. Molecular Insight on the Formation Structure and Dynamics of Melatonin in an Aqueous Solution and at the Water-Air Interface: A Molecular Dynamics Study. *J. Mol. Graph. Model.* **2021**, *108*, 107983, doi:10.1016/j.jmgm.2021.107983.
414. Fogueri, U.R.; Kozuch, S.; Karton, A.; Martin, J.M.L. The Melatonin Conformer Space: Benchmark and Assessment of Wave Function and DFT Methods for a Paradigmatic Biological and Pharmacological Molecule. *J. Phys. Chem. A* **2013**, *117*, 2269–2277, doi:10.1021/jp312644t.
415. Grey, A.C.; Schey, K.L. Age-Related Changes in the Spatial Distribution of Human Lens Alpha-Crystallin Products by MALDI Imaging Mass Spectrometry. *Invest. Ophthalmol. Vis. Sci.* **2009**, *50*, 4319–4329, doi:10.1167/iovs.09-3522.
416. Shi, J.; Zhu, Y.-X.; Huang, R.-Y.; Bai, S.-M.; Zheng, Y.-X.; Zheng, J.; Xia, Z.-X.; Wang, Y.-L. Phase Separation of α-Crystallin-GFP Protein and Its Implication in Cataract Disease. *Sci. Rep.* **2023**, *13*, 4832, doi:10.1038/s41598-023-31845-9.
417. Ifeanyi, F.; Takemoto, L. Specificity of Alpha Crystallin Binding to the Lens Membrane. *Curr. Eye Res.* **1990**, *9*, 259–265, doi:10.3109/02713689009044521.
418. Su, S.-P.; McArthur, J.D.; Friedrich, M.G.; Truscott, R.J.W.; Aquilina, J.A. Understanding the α-Crystallin Cell Membrane Conjunction. *Mol. Vis.* **2011**, *17*, 2798–2807.
419. Cobb, B.A.; Petrash, J.M. Characterization of Alpha-Crystallin-Plasma Membrane Binding. *J. Biol. Chem.* **2000**, *275*, 6664–6672, doi:10.1074/jbc.275.9.6664.
420. Boyle, D.L.; Takemoto, L. EM Immunolocalization of Alpha-Crystallins: Association with the Plasma Membrane from Normal and Cataractous Human Lenses. *Curr. Eye Res.* **1996**, *15*, 577–582, doi:10.3109/02713689609000769.
421. Cenedella, R.J.; Fleschner, C.R. Selective Association of Crystallins with Lens "Native" Membrane during Dynamic Cataractogenesis. *Curr. Eye Res.* **1992**, *11*, 801–815, doi:10.3109/02713689209000753.
422. Timsina, R.; Trossi-Torres, G.; Thieme, J.; O'Dell, M.; Khadka, N.K.; Mainali, L. Alpha-Crystallin Association with the Model of Human and Animal Eye Lens-Lipid Membranes Is Modulated by Surface Hydrophobicity of Membranes. *Curr. Eye Res.* **2022**, *47*, 843–853, doi:10.1080/02713683.2022.2040539.
423. Timsina, R.; Trossi-Torres, G.; O'Dell, M.; Khadka, N.K.; Mainali, L. Cholesterol and Cholesterol Bilayer Domains Inhibit Binding of Alpha-Crystallin to the Membranes Made of the Major Phospholipids of Eye Lens Fiber Cell Plasma Membranes. *Exp. Eye Res.* **2021**, *206*, 108544, doi:10.1016/j.exer.2021.108544.
424. Schachter, I.; Paananen, R.O.; Fábián, B.; Jurkiewicz, P.; Javanainen, M. The Two Faces of the Liquid Ordered Phase. *J. Phys. Chem. Lett.* **2022**, *13*, 1307–1313, doi:10.1021/acs.jpclett.1c03712.
425. Heberle, F.A.; Feigenson, G.W. Phase Separation in Lipid Membranes. *Cold Spring Harb. Perspect. Biol.* **2011**, *3*, a004630–a004630, doi:10.1101/cshperspect.a004630.
426. de Santis, A.; Scoppola, E.; Ottaviani, M.F.; Koutsioubas, A.; Barnsley, L.C.; Paduano, L.; D'Errico, G.; Russo Krauss, I. Order vs. Disorder: Cholesterol and Omega-3 Phospholipids Determine Biomembrane Organization. *Int. J. Mol. Sci.* **2022**, *23*, 5322, doi:10.3390/ijms23105322.
427. Stetter, F.W.S.; Cwiklik, L.; Jungwirth, P.; Hugel, T. Single Lipid Extraction: The Anchoring Strength of Cholesterol in Liquid-Ordered and Liquid-Disordered Phases. *Biophys. J.* **2014**, *107*, 1167–1175, doi:10.1016/j.bpj.2014.07.018.
428. Subczynski, W.K.; Pasenkiewicz-Gierula, M.; Widomska, J.; Mainali, L.; Raguz, M. High Cholesterol/low Cholesterol: Effects in Biological Membranes: A Review. *Cell Biochem. Biophys.* **2017**, *75*, 369–385, doi:10.1007/s12013-017-0792-7.
429. Subczynski, W.K.; Wisniewska, A.; Yin, J.J.; Hyde, J.S.; Kusumi, A. Hydrophobic Barriers of Lipid Bilayer Membranes Formed by Reduction of Water Penetration by Alkyl Chain Unsaturation and Cholesterol. *Biochemistry* **1994**, *33*, 7670–7681, doi:10.1021/bi00190a022.
430. Balakrishnan, M.; Kenworthy, A.K. Lipid Peroxidation Drives Liquid–Liquid Phase Separation and Disrupts Raft Protein Partitioning in Biological Membranes. *J. Am. Chem. Soc.* **2024**, *146*, 1374–1387, doi:10.1021/jacs.3c10132.
431. Takemoto, L.J. Oxidation of Cysteine Residues from Alpha-A Crystallin during Cataractogenesis of the Human Lens. *Biochem. Biophys. Res. Commun.* **1996**, *223*, 216–220, doi:10.1006/bbrc.1996.0873.

 doi:10.20944/preprints202510.0392.v1




432. Khadka, N.K.; Hazen, P.; Akinola, O.; Pu, X.; Mainali, L. Lipid and Cholesterol Peroxidation Leads to α-Crystallin Membrane Aggregation and Cataract Formation. *Invest. Ophthalmol. Vis. Sci.* **2025**, *66*, 8, doi:10.1167/iovs.66.12.8.
433. Ortega-Arellano, H.F.; Jimenez-Del-Rio, M.; Velez-Pardo, C. Melatonin Increases Life Span, Restores the Locomotor Activity, and Reduces Lipid Peroxidation (LPO) in Transgenic Knockdown Parkin Drosophila Melanogaster Exposed to Paraquat or Paraquat/iron. *Neurotox. Res.* **2021**, *39*, 1551–1563, doi:10.1007/s12640-021-00397-z.
434. Iwan, P.; Stepniak, J.; Karbownik-Lewinska, M. Cumulative Protective Effect of Melatonin and Indole-3-Propionic Acid against KIO3-Induced Lipid Peroxidation in Porcine Thyroid. *Toxics* **2021**, *9*, 89, doi:10.3390/toxics9050089.
435. Malmir, M.; Naderi Noreini, S.; Ghafarizadeh, A.; Faraji, T.; Asali, Z. Ameliorative Effect of Melatonin on Apoptosis, DNA Fragmentation, Membrane Integrity and Lipid Peroxidation of Spermatozoa in the Idiopathic Asthenoteratospermic Men: In Vitro. *Andrologia* **2021**, *53*, e13944, doi:10.1111/and.13944.
436. Deng, W.-S.; Xu, Q.; Liu, Y.E.; Jiang, C.-H.; Zhou, H.; Gu, L. Effects of Melatonin on Liver Function and Lipid Peroxidation in a Rat Model of Hepatic Ischemia/reperfusion Injury. *Exp. Ther. Med.* **2016**, *11*, 1955–1960, doi:10.3892/etm.2016.3160.
437. García, J.J.; López-Pingarrón, L.; Almeida-Souza, P.; Tres, A.; Escudero, P.; García-Gil, F.A.; Tan, D.-X.; Reiter, R.J.; Ramírez, J.M.; Bernal-Pérez, M. Protective Effects of Melatonin in Reducing Oxidative Stress and in Preserving the Fluidity of Biological Membranes: A Review. *J. Pineal Res.* **2014**, *56*, 225–237, doi:10.1111/jpi.12128.
438. Reiter, R.J.; Tan, D.-X.; Galano, A. Melatonin Reduces Lipid Peroxidation and Membrane Viscosity. *Front. Physiol.* **2014**, *5*, 377, doi:10.3389/fphys.2014.00377.
439. Teixeira, A.; Morfim, M.P.; de Cordova, C.A.S.; Charão, C.C.T.; de Lima, V.R.; Creczynski-Pasa, T.B. Melatonin Protects against pro-Oxidant Enzymes and Reduces Lipid Peroxidation in Distinct Membranes Induced by the Hydroxyl and Ascorbyl Radicals and by Peroxynitrite. *J. Pineal Res.* **2003**, *35*, 262–268, doi:10.1034/j.1600-079x.2003.00085.x.
440. Longoni, B.; Salgo, M.G.; Pryor, W.A.; Marchiafava, P.L. Effects of Melatonin on Lipid Peroxidation Induced by Oxygen Radicals. *Life Sci.* **1998**, *62*, 853–859, doi:10.1016/s0024-3205(98)00002-2.
441. Wiemann, J.T.; Nguyen, D.; Li, Y.; Yu, Y. Domain-Selective Disruption and Compression of Phase-Separated Lipid Vesicles by Amphiphilic Janus Nanoparticles. *iScience* **2022**, *25*, 105525, doi:10.1016/j.isci.2022.105525.
442. Bolmatov, D.; McClintic, W.T.; Taylor, G.; Stanley, C.B.; Do, C.; Collier, C.P.; Leonenko, Z.; Lavrentovich, M.O.; Katsaras, J. Deciphering Melatonin-Stabilized Phase Separation in Phospholipid Bilayers. *Langmuir* **2019**, *35*, 12236–12245, doi:10.1021/acs.langmuir.9b01534.
443. Bolmatov, D.; Soloviov, D.; Zhernenkov, M.; Zav'yalov, D.; Mamontov, E.; Suvorov, A.; Cai, Y.Q.; Katsaras, J. Molecular Picture of the Transient Nature of Lipid Rafts. *Langmuir* **2020**, *36*, 4887–4896, doi:10.1021/acs.langmuir.0c00125.
444. Niedernhofer, L.J.; Daniels, J.S.; Rouzer, C.A.; Greene, R.E.; Marnett, L.J. Malondialdehyde, a Product of Lipid Peroxidation, Is Mutagenic in Human Cells. *J. Biol. Chem.* **2003**, *278*, 31426–31433, doi:10.1074/jbc.M212549200.
445. Hammond, B.R.; Johnson, B.A.; George, E.R. Oxidative Photodegradation of Ocular Tissues: Beneficial Effects of Filtering and Exogenous Antioxidants. *Exp. Eye Res.* **2014**, *129*, 135–150, doi:10.1016/j.exer.2014.09.005.
446. MacFarlane, E.R.; Donaldson, P.J.; Grey, A.C. UV Light and the Ocular Lens: A Review of Exposure Models and Resulting Biomolecular Changes. *Front. Ophthalmol. (Lausanne)* **2024**, *4*, 1414483, doi:10.3389/fopht.2024.1414483.
447. Li, X.; Cao, X.; Yu, Y.; Bao, Y. Correlation of Sunlight Exposure and Different Morphological Types of Age-Related Cataract. *Biomed Res. Int.* **2021**, *2021*, 8748463, doi:10.1155/2021/8748463.
448. Haag, R.; Sieber, N.; Heßling, M. Cataract Development by Exposure to Ultraviolet and Blue Visible Light in Porcine Lenses. *Medicina (Kaunas)* **2021**, *57*, 535, doi:10.3390/medicina57060535.

 doi:10.20944/preprints202510.0392.v1




449. Mafia, K.; Gupta, R.; Kirk, M.; Wilson, L.; Srivastava, O.P.; Barnes, S. UV-A-Induced Structural and Functional Changes in Human Lens Deamidated alphaB-Crystallin. *Mol. Vis.* **2008**, *14*, 234–248.
450. Giblin, F.J.; Leverenz, V.R.; Padgaonkar, V.A.; Unakar, N.J.; Dang, L.; Lin, L.R.; Lou, M.F.; Reddy, V.N.; Borchman, D.; Dillon, J.P. UVA Light in Vivo Reaches the Nucleus of the Guinea Pig Lens and Produces Deleterious, Oxidative Effects. *Exp. Eye Res.* **2002**, *75*, 445–458, doi:10.1016/s0014-4835(02)92039-7.
451. Cetinel, S.; Semenchenko, V.; Cho, J.-Y.; Sharaf, M.G.; Damji, K.F.; Unsworth, L.D.; Montemagno, C. UV-B Induced Fibrillization of Crystallin Protein Mixtures. *PLoS One* **2017**, *12*, e0177991, doi:10.1371/journal.pone.0177991.
452. Bawankar, M.; Thakur, A.K. Mechanism of Human γD-Crystallin Protein Aggregation in UV-C Light. *Mol. Vis.* **2021**, *27*, 415–428.
453. Moran, S.D.; Zhang, T.O.; Decatur, S.M.; Zanni, M.T. Amyloid Fiber Formation in Human γD-Crystallin Induced by UV-B Photodamage. *Biochemistry* **2013**, *52*, 6169–6181, doi:10.1021/bi4008353.
454. Norton-Baker, B.; Rocha, M.A.; Granger-Jones, J.; Fishman, D.A.; Martin, R.W. Human γS-Crystallin Resists Unfolding despite Extensive Chemical Modification from Exposure to Ionizing Radiation. *J. Phys. Chem. B* **2022**, *126*, 679–690, doi:10.1021/acs.jpcb.1c08157.
455. Borges-Rodríguez, Y.; Mata-Salgado, F.; Morales-Cueto, R.; Millan-Pacheco, C.; Muñoz-Garay, C.; Rivillas-Acevedo, L. Role of Human γD-Crystallin Tryptophans in the Ultraviolet Radiation Response. *Spectrochim. Acta A Mol. Biomol. Spectrosc.* **2025**, *338*, 126197, doi:10.1016/j.saa.2025.126197.
456. Schafheimer, N.; King, J. Tryptophan Cluster Protects Human γD-Crystallin from Ultraviolet Radiation-Induced Photoaggregation in Vitro. *Photochem. Photobiol.* **2013**, *89*, 1106–1115, doi:10.1111/php.12096.
457. Chen, J.; Callis, P.R.; King, J. Mechanism of the Very Efficient Quenching of Tryptophan Fluorescence in Human Gamma D- and Gamma S-Crystallins: The Gamma-Crystallin Fold May Have Evolved to Protect Tryptophan Residues from Ultraviolet Photodamage. *Biochemistry* **2009**, *48*, 3708–3716, doi:10.1021/bi802177g.
458. Hill, J.A.; Nyathi, Y.; Horrell, S.; von Stetten, D.; Axford, D.; Owen, R.L.; Beddard, G.S.; Pearson, A.R.; Ginn, H.M.; Yorke, B.A. An Ultraviolet-Driven Rescue Pathway for Oxidative Stress to Eye Lens Protein Human Gamma-D Crystallin. *Commun Chem* **2024**, *7*, 81, doi:10.1038/s42004-024-01163-w.
459. Zhao, Z.; Poojary, M.M.; Skibsted, L.H.; Lund, M.N. Cleavage of Disulfide Bonds in Cystine by UV-B Illumination Mediated by Tryptophan or Tyrosine as Photosensitizers. *J. Agric. Food Chem.* **2020**, *68*, 6900–6909, doi:10.1021/acs.jafc.0c01760.
460. Jang, H.-J.; Kang, J.-G. Correlation between Sunlight Exposure Time and Cataract Prevalence in Korean Adults. *Appl. Sci. (Basel)* **2024**, *14*, 10707, doi:10.3390/app142210707.
461. Obayashi, K.; Saeki, K.; Tone, N.; Iwamoto, J.; Miyata, K.; Ikada, Y.; Kurumatani, N. Lower Melatonin Secretion in Older Females: Gender Differences Independent of Light Exposure Profiles. *J. Epidemiol.* **2015**, *25*, 38–43, doi:10.2188/jea.JE20140035.